AFRL-HE-WP-TR-2001-0093

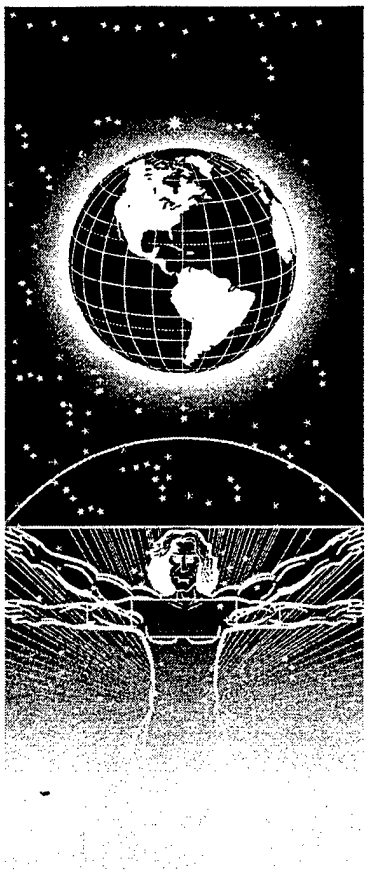

UNITED STATES AIR FORCE RESEARCH LABORATORY

Cumulative Damage to Window Panes

Jerold M. Haber

ACTA, Incorporated
24430 Hawthorne Street
Torrence CA 90505

July 1995

Interim Report for the Period February 1991 to July 1995

Human Effectiveness Directorate
Crew System Interface Division
2610 Seventh Street
Wright-Patterson AFB OH 45433-7901

NOTICES

When US Government drawings, specifications, or other data are used for any purpose other than a definitely related Government procurement operation, the Government thereby incurs no responsibility nor any obligation whatsoever, and the fact that the Government may have formulated, furnished, or in any way supplied the said drawings, specifications, or other data, is not to be regarded by implication or otherwise, as in any manner licensing the holder or any other person or corporation, or conveying any rights or permission to manufacture, use, or sell any patented invention that may in any way be related thereto.

Please do not request copies of this report from the Air Force Research Laboratory. Additional copies may be purchased from:

National Technical Information Service
5285 Port Royal Road
Springfield, Virginia 22161

Federal Government agencies and their contractors registered with the Defense Technical Information Center should direct requests for copies of this report to:

Defense Technical Information Center
8725 John J. Kingman Road, Suite 0944
Ft. Belvoir, Virginia 22060-6218

DISCLAIMER

This Technical Report is published as received and has not been edited by the Air Force Research Laboratory, Human Effectiveness Directorate.

TECHNICAL REVIEW AND APPROVAL

AFRL-HE-WP-TR-2001-0093

This report has been reviewed by the Office of Public Affairs (PA) and is releasable to the National Technical Information Service (NTIS). At NTIS, it will be available to the general public.

This technical report has been reviewed and is approved for publication.

FOR THE COMMANDER

MARIS M. VIKMANIS
Chief, Crew System Interface Division
Air Force Research Laboratory

REPORT DOCUMENTATION PAGE

Form Approved
OMB No. 0704-0188

1. AGENCY USE ONLY *(Leave blank)*	2. REPORT DATE	3. REPORT TYPE AND DATES COVERED
	July 1995	Interim - February 1991 to July 1995

4. TITLE AND SUBTITLE

Cumulative Damage to Window Panes

5. FUNDING NUMBERS

C - F33615-90-D-0653
PE - 62202F
PR -7757
TA - 7757C2
WU - 7757C201

6. AUTHOR(S)

Jerold M. Haber

7. PERFORMING ORGANIZATION NAME(S) AND ADDRESS(ES)

BBN Acoustic Technologies
A Division of Bolt Beranek and Newman Inc.
21120 Vanowen Street
Canoga Park CA 91303-2853

ACTA, Incorporated
24430 Hawthorne St
Torrence CA 90505

8. PERFORMING ORGANIZATION REPORT NUMBER

BBN Report No. 8087

9. SPONSORING/MONITORING AGENCY NAME(S) AND ADDRESS(ES)

Air Force Research Laboratory, Human Effectiveness Directorate
Crew System Interface Division
Aural Displays and Bioacoustics Branch
Air Force Materiel Command
Wright-Patterson AFB OH 45433-7901

10. SPONSORING/MONITORING AGENCY REPORT NUMBER

AFRL-HE-WP-TR-2001-0093

11. SUPPLEMENTARY NOTES

12a. DISTRIBUTION AVAILABILITY STATEMENT

Approved for public release; distribution is unlimited.

12b. DISTRIBUTION CODE

13. ABSTRACT *(Maximum 200 words)*

Three types of tests were employed: static tests, fatigue tests, and tests inside the Sonic Boom Test Facility (SBTF). Uniform loads across the glass surface were applied to glass panes in all tests. In the static tests, the panes were subjected to increasing pressure until they failed (typically between 30 and 90 sec loading). Fatigue tests sinusoidally loaded the panes at 3 Hz frequency until they failed or 24 hrs had elapsed (259,200 cycles). SBTF tests involved exposing the panes to up to 5000 sonic booms or until failure. Static tests were used to establish the strength of panes under a variety of conditions and to assess the variation of the glass strength for any particular condition. This included assessing the strength of new glass, after aging, with different edge conditions, flawed glass, and after other tests. Fatigue tests allowed testing at a significant fraction of the anticipated breaking strength and loading the panes more slowly than in the SBTF. These two factors increased the chance of breaking and, thus, of detecting glass fatigue behavior. The SBTF provided the most realistic simulation of repetitive sonic booms and, thus, the most credible demonstration of the importance of cumulative damage to the assessment of sonic boom damage to glass.

14. SUBJECT TERMS

sonic boom, windows, cumulative damage

15. NUMBER OF PAGES

106

16. PRICE CODE

17. SECURITY CLASSIFICATION OF REPORT	18. SECURITY CLASSIFICATION OF THIS PAGE	19. SECURITY CLASSIFICATION OF ABSTRACT	20. LIMITATION OF ABSTRACT
UNCLASSIFIED	UNCLASSIFIED	UNCLASSIFIED	UL

This page intentionally left blank.

PREFACE

This report was prepared under Contract F33615-90-D-0653 of the Noise and Sonic Boom Impact Technology (NSBIT) program. The NSBIT program is conducted by the United States Air Force under the direction of Major Jeffrey Fordon, Program Manager. Dr. Micah Downing served as the technical monitor for this effort.

The BBN team effort was directed by Mr. B. Andrew Kugler, BBN Program Manager. Mr. Matthew Sneddon was responsible for the design and construction of the Sonic Boom Testing Facility, and for the performance of the testing program.

This page intentionally left blank.

TABLE OF CONTENTS

LIST OF ILLUSTRATIONS

This page intentionally left blank.

LIST OF TABLES

This page intentionally left blank.

1 INTRODUCTION

Public law 96-588, the National Environmental Policy Act (NEPA) of 1969, requires the United States Air Force (USAF) and the U.S. Navy to perform environmental assessments of their flight activities. NEPA requires assessments not only of flight operations near air bases, but also of operations in about 350 Military Operations Areas (MOAs) and Restricted Areas (RAs), and along about 400 Military Training Routes (MTRs). Such regulated areas encompass roughly a half million square miles of domestic airspace. Compliance with the statutory and regulatory environmental requirements of these operations is not a simple task for the USAF. Assessment of the potential consequences of these operations and responses to public concerns about possible consequences generate significant technical and practical challenges.

The potential for cumulative damage from ongoing sonic boom exposures is a continuing public concern, frequently expressed during the environmental impact analysis process. Cumulative damage is defined as reduced structural capacity caused by multiple sonic booms. Previous investigations of sonic boom structural damage have not ruled out the possibility that cumulative damage may occur. Evaluation of the damage that may result from supersonic operations is an important component of the environmental assessments that USAF must perform whenever it needs to establish or modify Supersonic Operating Areas (SOAs) for pilot training and maintenance of pilots' skills.

This document describes a series of tests whose objective was to determine whether cumulative damage to glass is statistically significant and must therefore be addressed in environmental assessments. These tests are based upon the test plan published in:

> Haber, Jerold, and Alex See (1991), "*Noise and Sonic Boom Impact Technology* Test Plan for Glass and Plaster Tests," Report by ACTA Incorporated, and BBN Systems and Technologies for the USAF Noise and Sonic Boom Impact Technology Program, BBN Report No. 7643.

Deviations from the original test plan are noted in applicable sections of this report.

1.1 BACKGROUND

Glass failure is characterized by the activation of edge flaws and the growth of cracks associated with surface imperfections. Moisture, corrosive chemicals in the atmosphere, and temperature extremes are known to be associated with the growth of microscopic surface imperfections. These topic have been the focus of much of the literature regarding conditions under which glass fails. While repeated loading may be responsible for the growth of flaws, no sonic boom or blast field tests have been found to support the theory of cumulative damage to glass. Previous laboratory simulations of sonic boom loads on glass (White, 1972; Kao, 1970) have produced weak, equivocal relationships between final breaking pressures and the number of repetitive loads. White performed regression analyses of the data he and Kao collected

in an effort to relate breaking pressure to the number of exposures to sonic booms. His computed correlation coefficients were never larger than 0.17. Based on previous investigations, there is little reason to believe that fatigue increases damage from repetitive loads at sonic boom overpressures.

The primary objective of this study is to establish in a reasonably conclusive manner whether or not sonic boom loads can, as a result of a fatigue mechanism, produce cumulative damage.

1.2 OVERVIEW OF EXPERIMENTS

Three types of tests were employed in this study: static tests, fatigue tests, and tests inside the Sonic Boom Test Facility (SBTF). Uniform loads across the glass surface were applied to the glass panes in all three sets of tests. In the static tests, the glass panes were subjected to increasing pressure until the panes failed (typically between 30 and 90 seconds loading). Fatigue tests sinusoidally loaded the panes at a frequency of 3 Hz until the panes failed or until 24 hours had elapsed (259,200 cycles). Tests inside the SBTF involved exposing the panes to up to 5,000 sonic booms or until pane failure.

The static tests were used to establish the strength of glass panes under a variety of conditions and to assess the variation of the glass strength for any particular condition. This included establishing the strength of new glass, assessing the strength of glass after it had aged, assessing the strength of glass with different edge conditions, assessing the strength of glass that had been flawed to weaken it, and assessing the residual strength of glass after other tests. The fatigue tests allowed glass to be tested at a significant fraction of the anticipated breaking strength and to load the panes more slowly than in the SBTF. These two factors increased the chance of breaking the panes and, thus, of detecting glass fatigue behavior. The SBTF provided the most realistic simulation of repetitive sonic booms and thus, the most credible demonstration of the importance of cumulative damage to the assessment of sonic boom damage to glass.

Toward the end of this study, the SBTF was used to investigate the response of double-glazed windows to sonic booms. These tests were used to verify results of a highly simplified analysis of expected response. In addition, a fracture mechanics approach was combined with a finite element analysis to evaluate the effect of single sonic booms and repetitive sonic booms on precracked glass.

1.3 SUMMARY

The following are the major findings of this study:

- Aged glass is weaker than new glass. The reduction in strength depends upon the length of aging, the physical treatment of the pane surfaces during aging and the chemicals to which the glass is exposed as it is aging. This is consistent with previous investigations.

- Other investigators have compared the overpressures required to break glass windows with different edge conditions. A 1962 Canadian study using shock tubes (Murihead *et al.*, 1962) reports that "loosely mounted" glass required substantially higher overpressures to break than was required for windows with clamped edges. This contrasts with the earlier, more comprehensive study by Arde Associates (1959) that correctly argued that the sensitivity to shock waves depended on the dynamic response to the particular waveform and the stresses generated by the pane response. As a result, the required failure pressure to break identical panes with different edge conditions depends on the particular waveform and the pane dimensions. In some instances, a pane will require larger applied pressures to break with simply supported edges. Under other conditions, clamped edge conditions require larger applied pressures.

  This study evaluated failure of simply supported and clamped panes under quasi-static (ramp) loading. Calculated sixty-second static equivalent stress failure was greater for panes with clamped edges than for simply supported panes. (The maximum stress in a pane with clamped edge conditions occurs in the middle of the pane edges. The maximum stress in a pane with simply supported edges is initially in the center of the pane. When the pane undergoes large deflections, the maximum stress is in the corners of the panes.) The sixty-second static equivalent pressure at failure is also smaller for simply supported panes than for panes with clamped edges.

- No statistically significant differences were observed between the baseline strength of the glass panes and that of the panes surviving either the fatigue tests or the SBTF tests. These tests seem to have culled out weaker panes leaving a slightly stronger (not statistically significant) population of survivors.

- Cumulative damage from repetitive sonic booms or other cyclic loading such as in the fatigue tests is significant only for load levels that are a significant fraction of the level required to break a pane from a single application of the load. This means that cumulative damage is not a significant factor for ordinary window glass. By contrast, it may be an important factor for panes that have been previously severely damaged.

- Current ASAN models for sonic boom window damage in both conventional and unconventional structures are based on simplified models that have been superseded by more recent analyses.

- Damage predictions are dominated by the modeled capacity of precracked glass. This study has shown that the statistics employed in the glass strength model for precracked glass are inadequate.

1.4 DOCUMENT ORGANIZATION

The balance of this report is presented in two primary sections. Section 2 describes the test facilities, test articles, and test procedures, and characterizes the performance of the facility and test articles compared with design objectives. The preparation and execution of glass pane testing are documented. Section 3 summarizes the results of previous investigations and presents the results of the cumulative damage tests. Results of experiment findings are analyzed and discussed. An explanation of selected terms and a list of cited reference are provided in Sections 4 and 5, respectively. The Appendices provide supplemental information related to the test program. Appendix A presents significant characteristics of window glass. Appendix B lists suggestions for enhancing the ASAN glass damage model and presents an outline of a model for damage to glass panes from repetitive sonic booms.

2 CUMULATIVE DAMAGE TESTS

This section characterizes the tests performed during the investigation of cumulative damage to glass. It is organized in three primary subsections. The first two subsections describe the facilities, instrumentation and test procedures employed with the Static and Fatigue Test Facility and the SBTF respectively. The third subsection documents the preparation of the glass panes for testing.

2.1 STATIC AND FATIGUE TEST FACILITY

The static and fatigue test facility is a dual purpose fixture designed to augment the tests performed in the SBTF. As a static test facility, it is used to measure the strength of glass panes with specified edge conditions. As a fatigue test facility, it provides the ability to cyclically load the glass at a frequency of 3 Hz and to produce peak pressures within the range of approximately 15 to 55 psf. Use of the fatigue test facility greatly enhanced the ability to detect cumulative damage in glass over what would have been available with the SBTF alone. This facility allowed the glass to be tested at a significant fraction of the anticipated breaking strength in contrast to the SBTF, which was limited to a peak overpressure of no more than 16 psf. Tests conducted in the fatigue facility loaded the panes more slowly, thus, further increasing the probability of breaking the panes. In addition, the fatigue facility was operated to apply up to 259,200 load cycles to the panes, while the SBTF experiment was limited to simulating the effects of no more than 5,000 sonic booms.

2.1.1 Facility Description

The test facility (see Figure 2-1 and Figure 2-2) consists of a shallow chamber (approximately 3 inches in depth), closed on five sides. The glass pane (35 by 41-1/8 inches) to be tested is supported between two large metal frames in a vertical position across the open side of the chamber. Attached to the chamber are two valves, a pressure relief valve and a valve leading to cylinders of pressurized nitrogen. A pressure regulator is used to control the pressure level of the nitrogen gas introduced into the chamber.

A static test is performed by mounting a pane between the metal frames with suitable inserts between the glass and the frame to generate the desired edge condition, closing the relief valve, and opening the valve to the pressurized gas. Pressure is then allowed to increase gradually in the chamber until the glass fails.

The back of the test chamber consists of a metal plate connected to the sides of the chamber by heavy rubber gasketing. The metal plate is attached to an eccentric cam (see Figure 2-3).

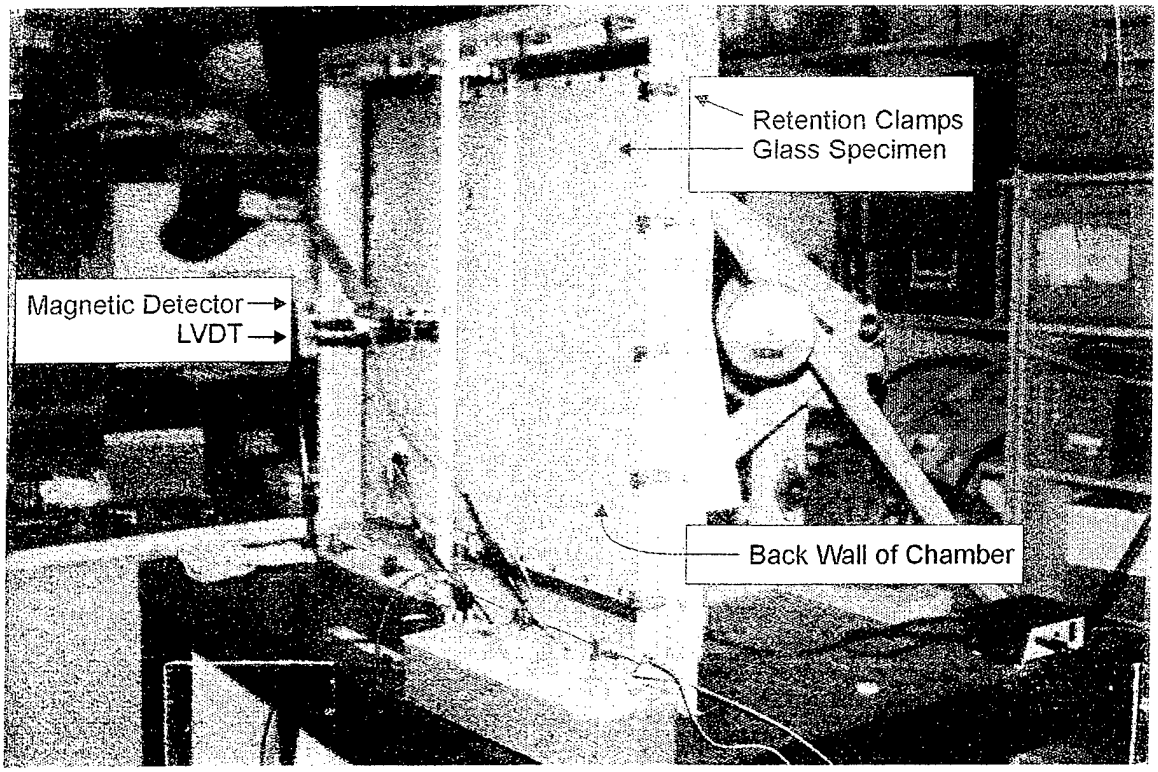

Figure 2-1. Static and Fatigue Test Facility (Front View).

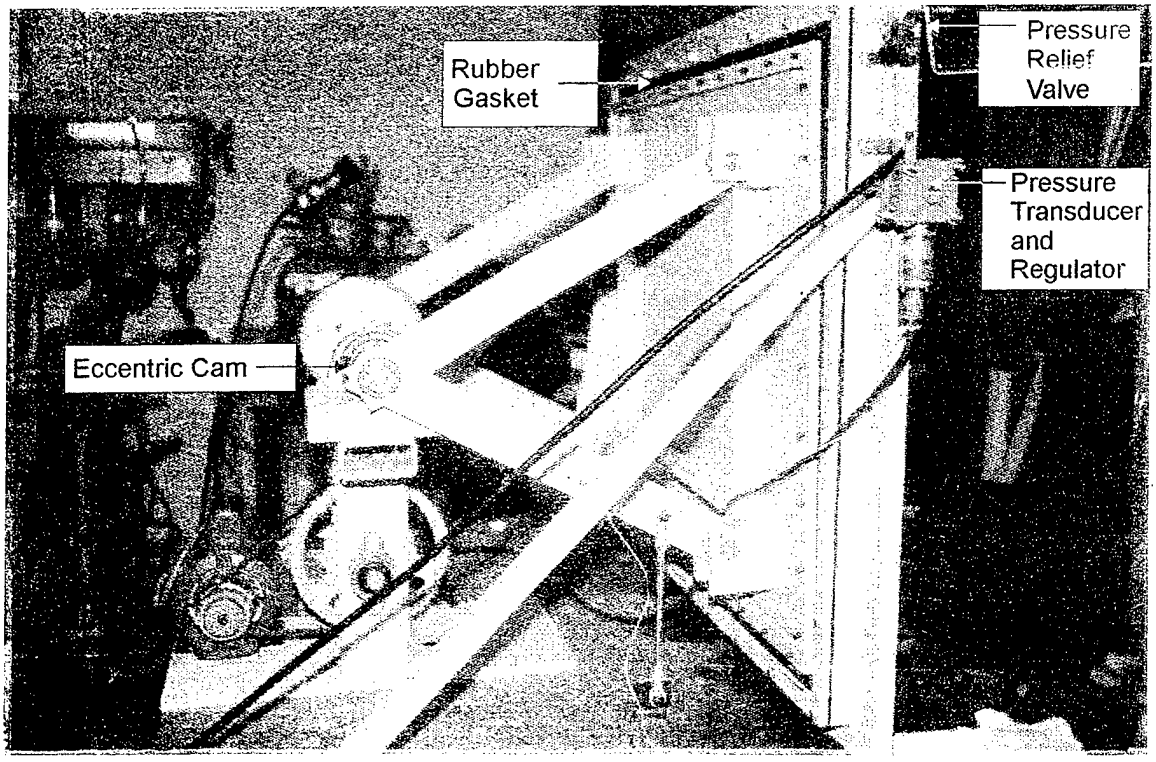

Figure 2-2. Static and Fatigue Test Facility (Rear View).

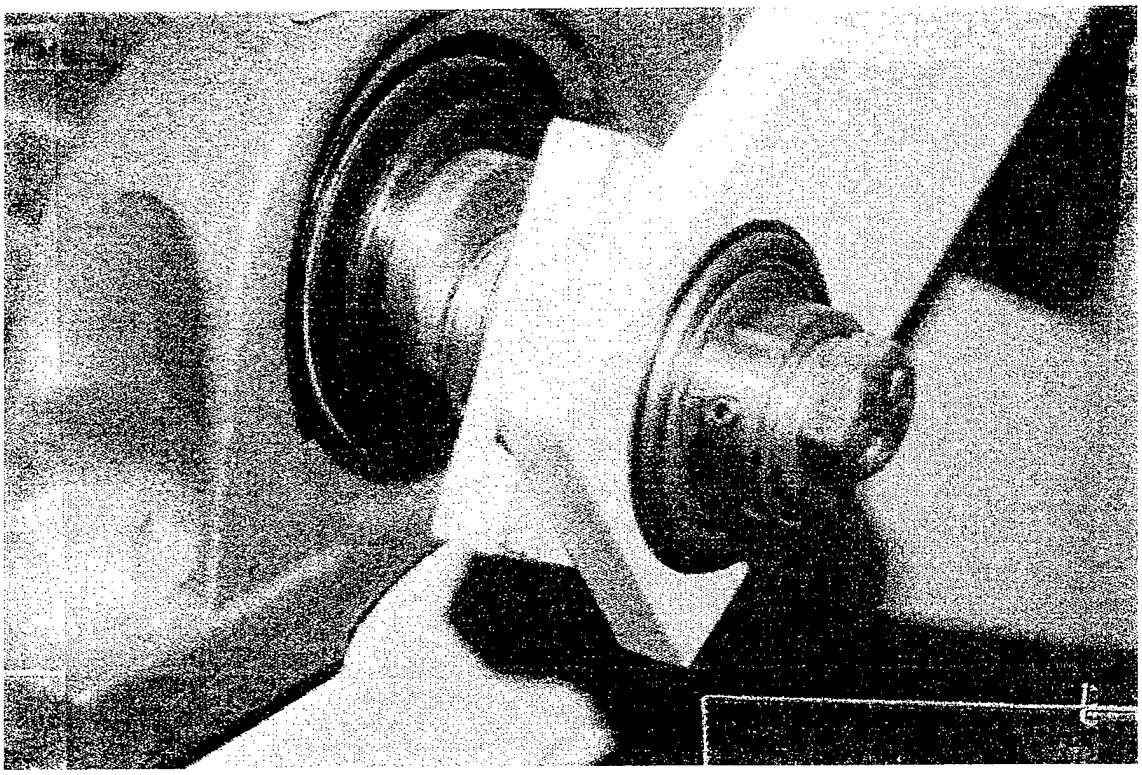

Figure 2-3. Detail of Eccentric Cam.

Operation of an electric motor causes the cam to rotate, which in turn forces the metal plate to move so as to cyclically increase and decrease the chamber volume and pressure. As shown in Figure 2-4, a small rare earth magnet is mounted on the glass pane. A detector near the magnet registers its presence. The duration of the test is measured using a circuit incorporating the magnetic detector. When the pane breaks, the magnet falls away with the broken glass, opening the circuit and stopping the clock. This circuit can be seen in Figure 2-5.

2.1.2 Data Acquisition System and Instrumentation

Several types of data were gathered during the course of the static tests and fatigue tests. Pressure data was obtained using a Viatran 274 pressure transducer. The Viatran 274 pressure transducer has a built-in calibration facility. The transducer is comprised of two units, a sensing head and a control unit. The sensing head has both "zero" and "span" adjustment potentiometers. When a button on the control unit is actuated, the transducer outputs a voltage from an internal calibrated source.

Figure 2-4. Rare Earth Magnet and Magnetic Detector.

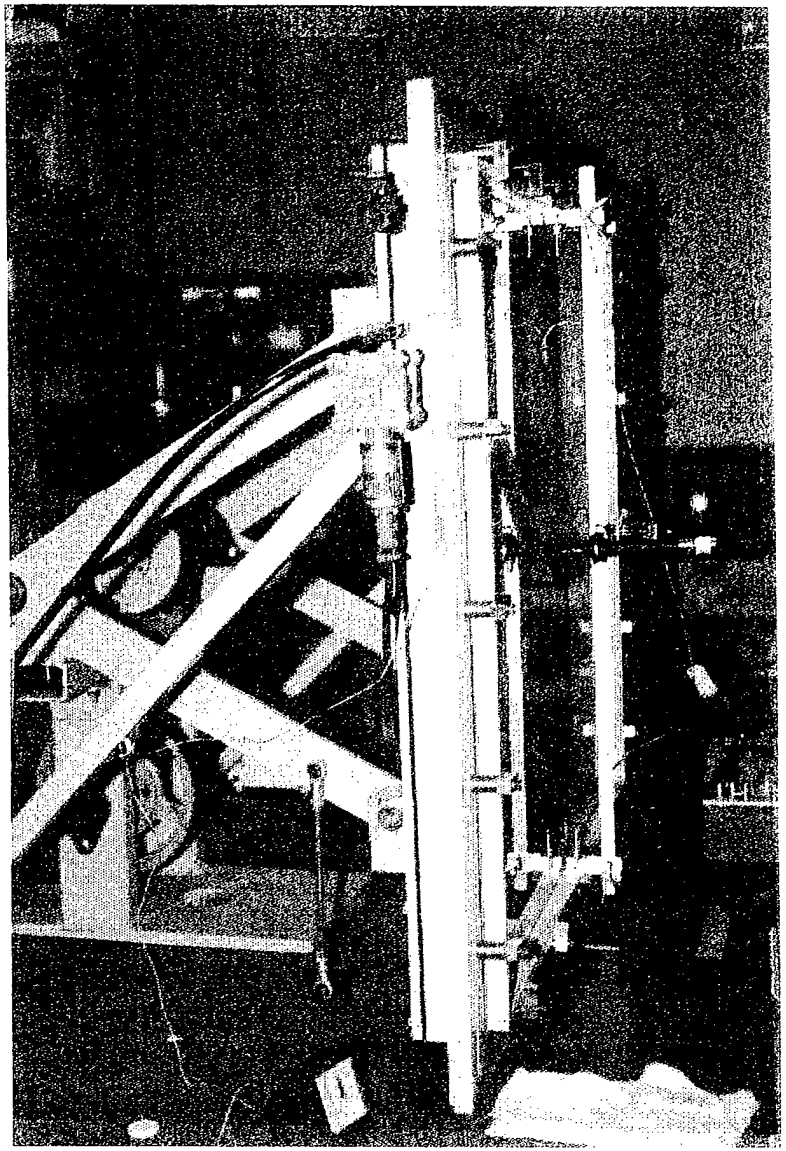

Figure 2-5. Side View of Test Facility Showing Timing Mechanism for Fatigue Tests.

The calibration procedure involves adjusting the zero potentiometer to achieve a zero volt signal and depressing the button on the span potentiometer to achieve a 5 volt signal. These two steps are repeated until both values are achieved. The calibration factor was 52.07 psf per volt.

Displacement data was obtained using a Schaevitz Type 1000 H (S/N 3037) Linear Variable Differential Transformer (LVDT) mounted at the center of the glass pane being tested. The LVDT was calibrated at 0 inches, 0.5 inches, and at 1.0 inches. The calibration factor was 0.1037 inches/volt.

Strain measurements employed a uniaxial strain gage mounted on the unpressurized side of the pane. The gage was mounted midway along the 41.125" edge, one quarter of the way up in the direction parallel to the 35" edge. Its orientation was chosen to allow the maximum strain at that location to be measured.

A WK-06-500AF-350 foil strain gage was selected for these measurements. The gage has a thermal coefficient of expansion close to that of glass. The gage is a 350 ohm (±0.3%) resistance nickel-chromium alloy unit that measures 0.5" by 0.5". The gage has a high fatigue life (10^8 cycles at ±2000 microstrains) and is designed to provide self-temperature compensation.

The manufacturer's application data were used for the strain gages; no separate calibration was performed. It is standard practice in industry to use the manufacturers' published resistance and gage factors for testing calibration and data analysis. These data are supplied by the gage manufacturer with each gage and are intended specifically for this purpose. Strain gages are manufactured under strict quality assurance procedures that verify that the application data supplied with them are correct.

Two gage parameters are used in calibration and data analysis procedures. They are: (1) Resistance—the manufacturer states that it is measured to standards traceable to NBS; and (2) Gage factor—the manufacturer states that their testing method complies with ASTM E-251.

Tables 2-1 and 2-2 list the data acquisition and measurement equipment employed during the tests. Figure 2-6 illustrates the manner in which the equipment was connected for the data acquisition.

System calibration consisted of end-to-end calibration of each channel using a traceable voltage input. Sample data sheets of the Vipac Time Domain and the Anti-aliasing Filter Calibration for the system are presented in Tables 2-3 and 2-4 respectively.

Table 2-1. Data Acquisition Equipment.

QUANTITY	ITEM
1	AT computer system w/monochrome display and printer. Data were acquired and processed with ANCO Vipac software.
1	Vishay Model 2120 Signal Conditioner/Amplifier (2 channel) (S/N 023323, 023338, 023479, 023388)
1	Vishay Model 2110 Power Supply (S/N 23243)
1	ANCO 16-channel Vipac A/D Unit #3
1	Schaevitz LVDT Type 1000 H (S/N 3037)
1	Viatran #274 Pressure Transducer
–	WK-06-500 AF-350 Precision Strain Gages

Table 2-2. Measuring Equipment.

MEASUREMENT	EQUIPMENT	SERIAL NUMBER	CALIBRATION STATUS
Voltage	Fluke 8060A Multimeter	S/N 4495624 ANCO# 88.0601	Calibration Current at Time of Testing
Temperature	Fluke 80TK Thermocouple Module	ANCO# 88.0601X	
Humidity	Oakton Hydrometer/ Thermometer	S/N 91.0008	
Voltage Standard	EDC Model 330	S/N 7712	

Table 2-3. Example of Anti-Aliasing Filter Calibration Sheet.

Filt. No.	dc Voltage Calibration											ac Voltage Calibration					dc Cal.% Error	Poles	PID No.
	− 5.00	− 4.00	− 3.00	− 2.00	− 1.00	0	+ 1.00	+ 2.00	+ 3.00	+ 4.00	+ 5.00	db→F_0 ÷3	dB@2F_0	dB@F_0	ϕ@F_0	F_0			
1	-5.00	-4.00	-3.00	-2.00	-1.01	-.01	0.99	1.99	2.99	3.99	4.98	~~-3~~ 0	-23.9 -23.6	~~-46.6~~ -30.1	-183	10	< 1	8	N/A
2	-5.01	-4.01	-3.01	-2.01	-1.01	-.01	0.99	1.99	2.99	5.99	4.99	0	-23.7	-3.2	-183	10	< 1	↓	↓
3	-4.99	-3.99	-2.99	-1.99	-0.99	.01	1.01	2.00	3.00	4.00	5.00	0.1	-14.2	-3.01	-183	10	< 1		
4	-5.00	-4.00	-3.00	-2.00	-1.00	.00	1.00	2.00	3.00	4.00	5.00	0	-23.7	-3.2	-183	10	< 1		
5	-4.98	-3.98	-2.98	-1.99	-0.99	0.01	1.01	2.01	3.01	4.01	5.01	0.1	-23.7	-2.9	-182	10	< 1		
6	-5.01	-4.01	-3.01	-2.02	-1.02	-.02	0.98	1.98	2.98	3.98	4.98	0	-23.9	-3.2	-183	10	< 2		
7	-5.00	-4.00	-3.00	-2.00	-1.00	.00	1.00	2.00	3.00	4.00	5.00	0.1	-14.1	-3.0	-184	10	< 1	↓	↓
8																			
9	EDC 330 Voltage Source SN 99 1042																		
10	Cal 2/27/92 Due 2/27/93																		
11																			
12	FLUKE 8060A Multimeter 88.0601																		
13	Cal 11/16/91 Due 11/18/92																		
14																			
15																			
16																			
17																			
18																			
19																			
20																			
21																			
22																			
23																			
24																			
25																			
26																			
27																			
28																			
29																			
30																			
31																			
32																			
A																			
B																			

Table 2-4. Example of Vipac Time Domain Calibration Sheet.

Channel No.	DC Voltage Calibration, Volts											Maximum % Deviation	AC Calibration		
	-10	-8	-6	-4	-2	0	2	4	6	8	10		Output Voltage	AC Cal % Deviation	Calculated Frequency
1	-10.00	-8.00	-6.00	-4.01	-2.02	0.02	1.98	3.97	5.97	7.96	9.96	2	1.38	0	~6
2	-10.00	-8.01	-6.02	-4.04	-2.02	0.02	1.98	3.98	5.98	7.98	9.97		1.42	3.0	~6
3	-9.99	-8.00	-5.99	-4.00	-2.01	0.01	1.99	3.99	5.98	7.99	9.98		1.36	1.5	~6
4	-10.00	-8.02	-6.01	-4.01	-2.01	-0.01	1.99	3.99	5.98	7.99	9.98		1.41	2	~6
5	-9.98	-7.99	-5.99	-3.99	-2.00	0.00	1.99	3.99	5.98	7.99	9.98		1.41	2	~6
6	-10.00	-8.02	-6.02	-4.02	-2.02	-.02	1.97	3.97	5.97	7.97	9.97		1.36	1.5	~6
7	-10.00	-8.00	-6.00	-4.01	-2.01	-.01	1.98	3.98	5.98	7.98	9.97		1.38	0	~6
													Wavetek 166 Signal Generator		
													88.12.01	Cald	5/12/92
														Due	5/12/93

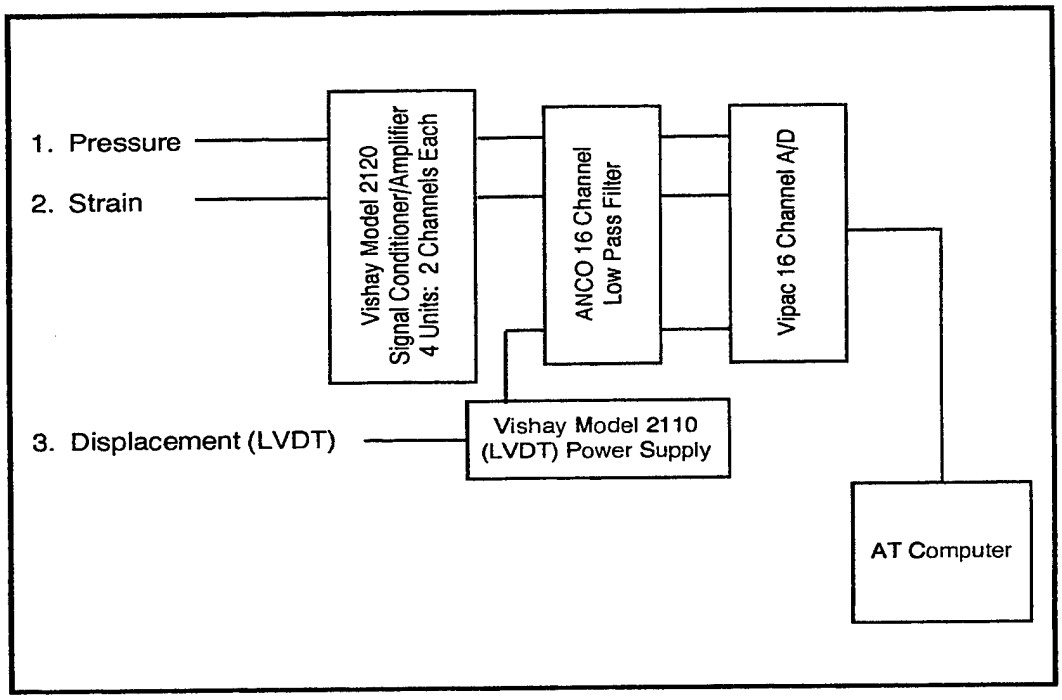

Figure 2-6. Block Diagram of Instrumentation for Static/Fatigue Tests.

2.1.3 Performance of Facility

Static tests were highly repeatable so long as the fixture was used within its design limits. Pressure time histories increased linearly with time as designed, albeit not without slight deviations from linearity, especially toward the end of a test. Abnormal test results were without exception caused by operator error or testing with an edge condition that provided poor air seals around the edges of the glass.

Fatigue facility performance results were substantially more varied. The facility produced a sinusoidal loading waveform as designed. However, the applied load always exhibited some level of asymmetry. Moreover, start-up of the facility produced a transient overshoot in peak pressure which dampened out after a few cycles. Slight variations of the maximum and minimum pressure levels also existed among test trials. Proper air seals were even more important for operation as a fatigue facility than for operation as a static test facility. As a static test facility, pressurization improved the seals on the front segment of the frame. Thus, the only concern was the potential for leaks between the pane and the rear segment of the metal frame. As a fatigue facility, both seals provided a potential path for air leakage. Consequently, clamped edge conditions were used for all fatigue tests. The facility was under-designed for the stresses to which it was subjected. Two tests had to be eliminated because of test fixture failures (tie rods failed once and the rubber gasket failed once). Yet, for those tests when it operated properly, it produced

extremely stable peak stresses in the glass. (For example, in two tests sequences the peak stresses produced had coefficients of variation on the order of 1%.)

2.1.4 Test Procedures

The following procedure was followed in performing static tests:

- Select a pane of the proper type for testing.
- Measure the thickness of the pane with a micrometer.
- Install a strain gage, if required for the test.
- Verify operation of instrumentation and data acquisition system.
- Adjust pressure regulator to produce desired loading rate.
- Install pane in frame with proper edge conditions.
- Check that static test facility pressure relief valve is open and that the gas line valve is closed.
- Install frame in test fixture and secure dogs.
- Install LVDT, if required.
- Close pressure relief valve.
- Begin recording.
- Open gas supply valve.
- Wait until glass breaks.
- After glass breaks, shut gas supply valve and clean up glass fragments.

After some experimentation, the following procedures were adopted for performing the fatigue tests:

- Align piston of motor to reference position.
- Initiate data acquisition.
- Turn on motor driving fatigue fixture.
- Allow to run for 5 to 10 seconds with the pressure relief valve open.
- Close pressure relief valve on a suction stroke.
- Allow test to continue until glass fails or specified test period elapses.
- Shut down data acquisition system.
- Turn off motor.
- Open pressure relief valve.

2.2 SONIC BOOM SIMULATOR TEST FACILITY

Investigation of the possibility of cumulative damage required a method of subjecting test articles to a large number of sonic booms. Field tests were ruled out because of the costs of operating aircraft in the field and of selecting and instrumenting a large representative sample of structures. In addition, field tests

posed challenging problems of experimental control. Thus, the only viable approach was a laboratory sonic boom simulator.

The SBTF consists of a test chamber for simulating sonic booms, stations for mounting articles to be subjected to the simulated booms, and instrumentation for monitoring the applied load, the test article response, and environmental variables.

2.2.1 Test Chamber

The sonic boom simulator is a closed chamber with an exterior height of approximately ten feet and an exterior footprint of approximately fifteen feet by twenty-two feet. The interior volume is divided into three plenum regions: a driver baffle, a pressure plenum, and a test sample room. The chamber has two entrances at opposite ends: an entrance large enough to bring a test article into the chamber and a maintenance entry hatch. The maintenance entry hatch provides access to the driver baffle plenum behind a bank of specially designed speaker modules used to simulate sonic booms. Three pairs of loudspeakers are mounted in each speaker module. Each pair of loudspeakers is mechanically coupled so that they are extended simultaneously. A three-by-four array of speaker modules lines a wall separating the hatch from the test articles. Coupling of speaker action between pairs and among clusters is accomplished electronically.

The simulator can expose a test article surface approximately eight feet by ten feet to a simulated sonic boom. Pressure seals around the test articles allow the air in the plenum between the speakers and the test article to be pressurized and rarefied by the speakers to simulate a sonic boom. The largest compartment is the test sample room between the test article and the chamber entrance. This compartment provides access for introduction of test specimens, observations and maintenance.

The following group of figures clarifies the layout of the simulator. Figure 2-7 presents an artist's rendition of the simulator. Figure 2-8 depicts a photograph of the main entrance to the simulator. Figure 2-9 is a photograph taken inside the simulator showing the speaker modules used to load the test article. Figure 2-10 is a pair of photographs showing the speaker module and the mechanical linkage that drives the speakers inside the speaker module.

Four spare glass panes were installed in the test chamber as part of a pre-test facility check-out. The upper portion of Figure 2-11 depicts the target N-wave and the actual pressure signature produced by the simulator; the lower portion of the figure shows the signal applied to the drivers. The two signals were played through a window breakage model for the window panes to be employed in the glass cumulative damage study. The predicted breakage probabilities for the two signals were significantly different.

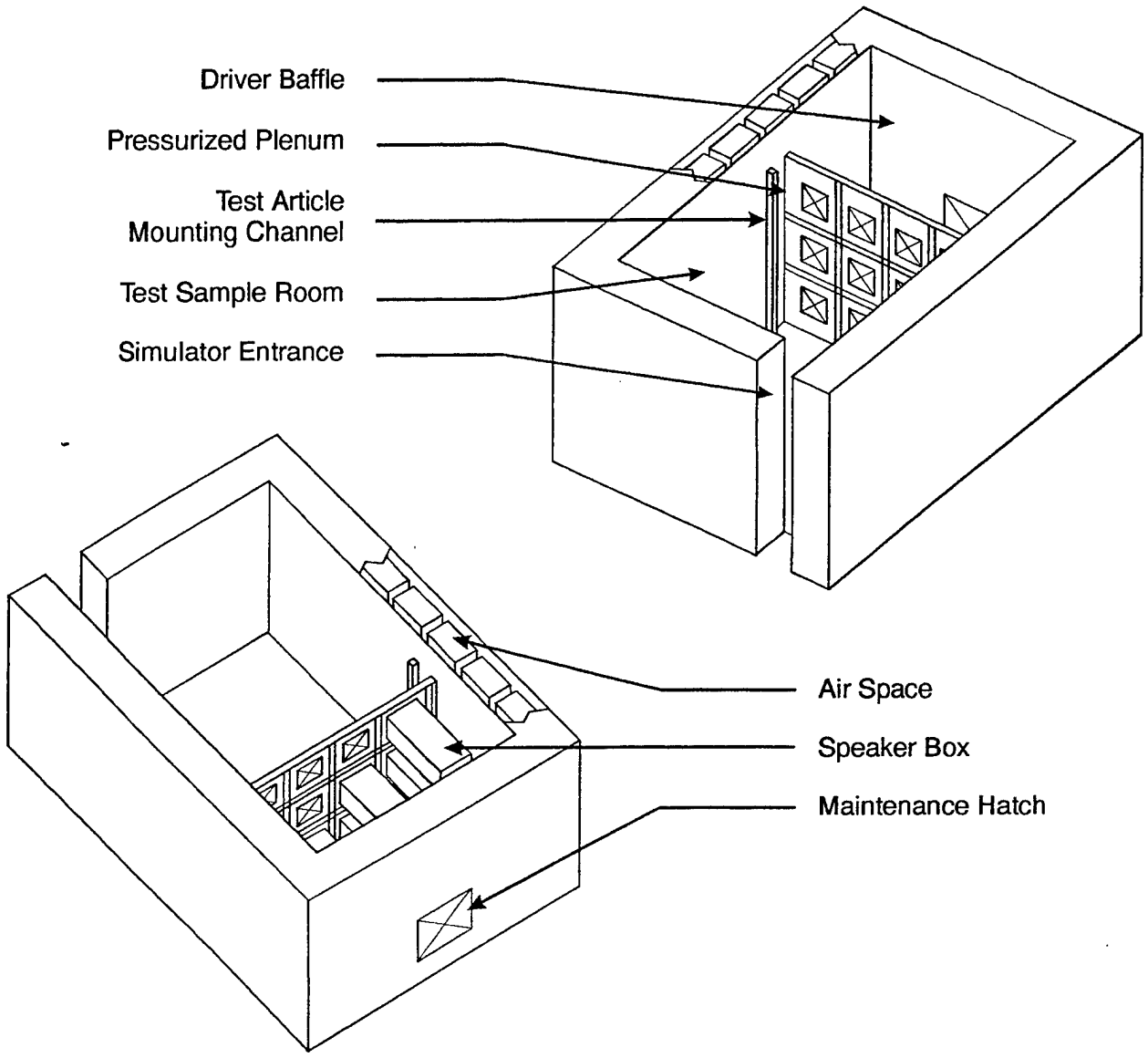

Figure 2-7. Artist's Conception of Sonic Boom Simulator.

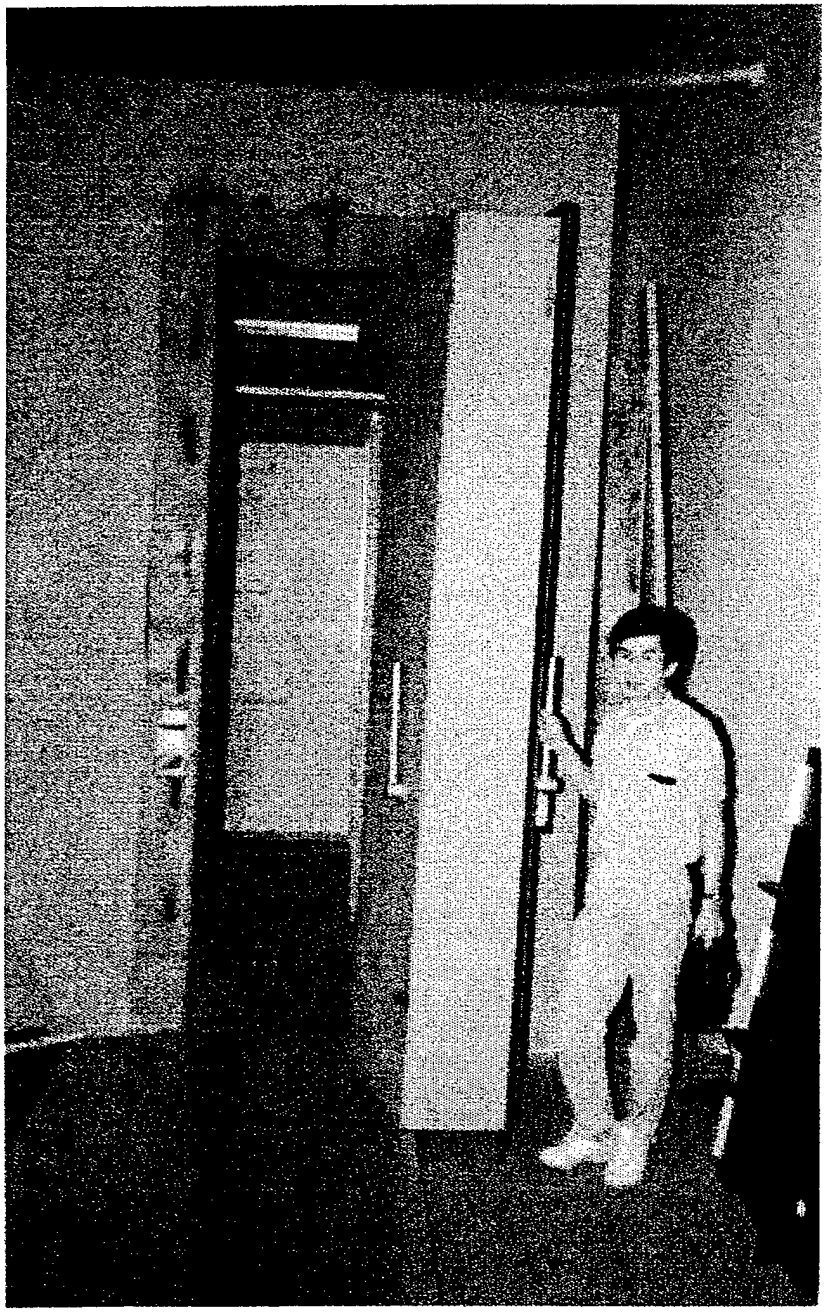

Figure 2-8. Entrance to Sonic Boom Test Facility.

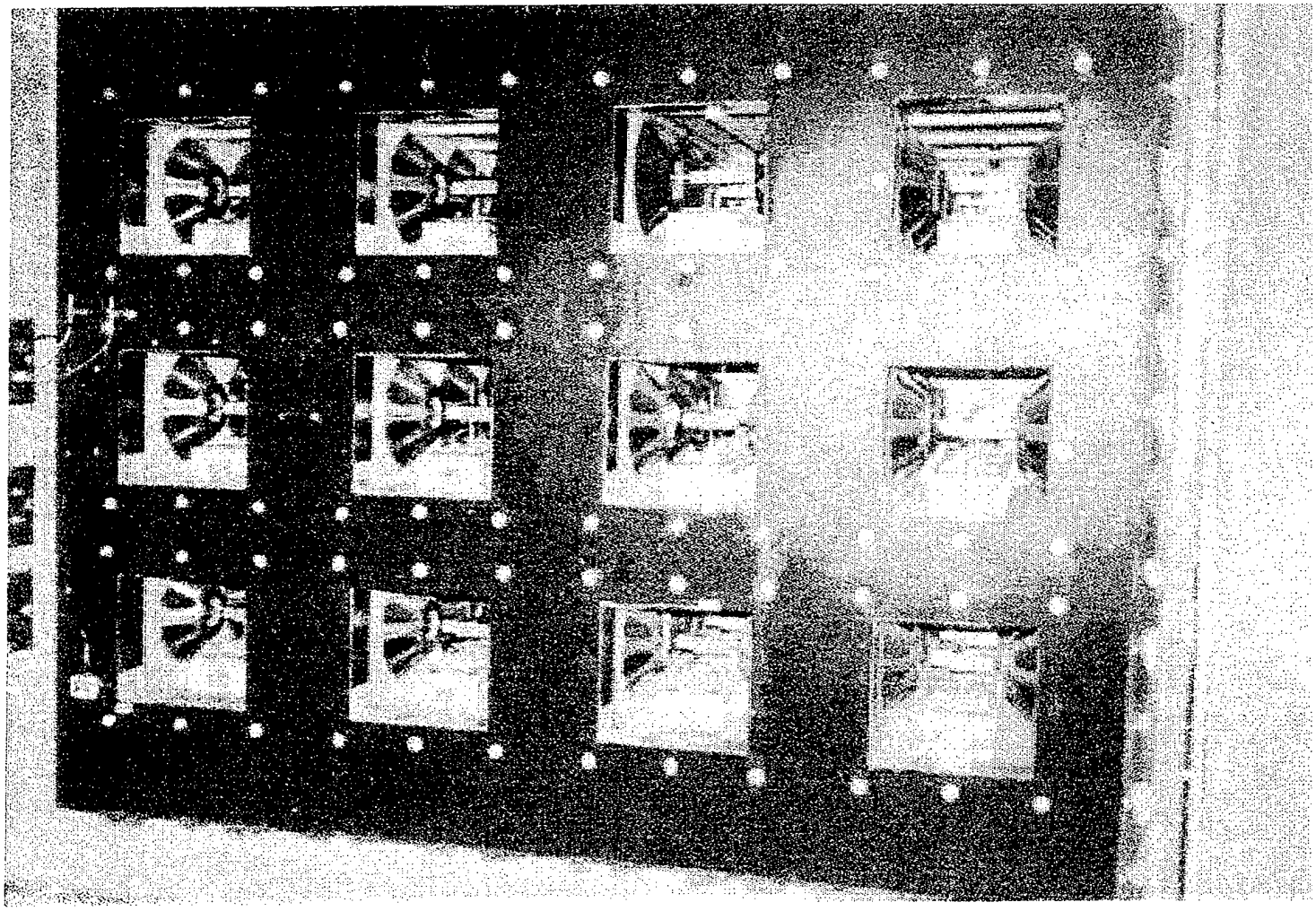

Figure 2-9. Loudspeaker Modules in Test Chamber.

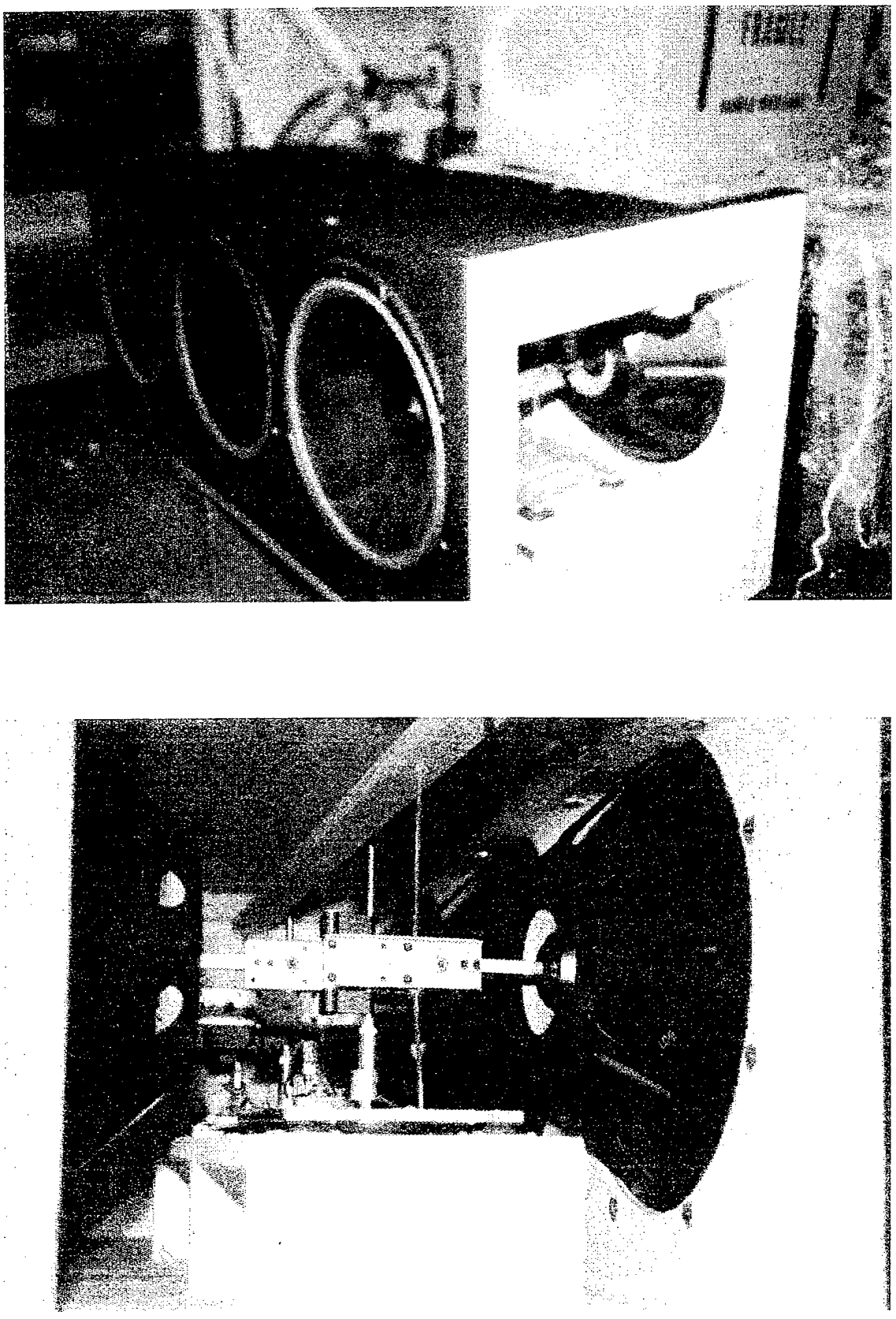

Figure 2-10. View of Speaker Module and Mechanical Linkage.

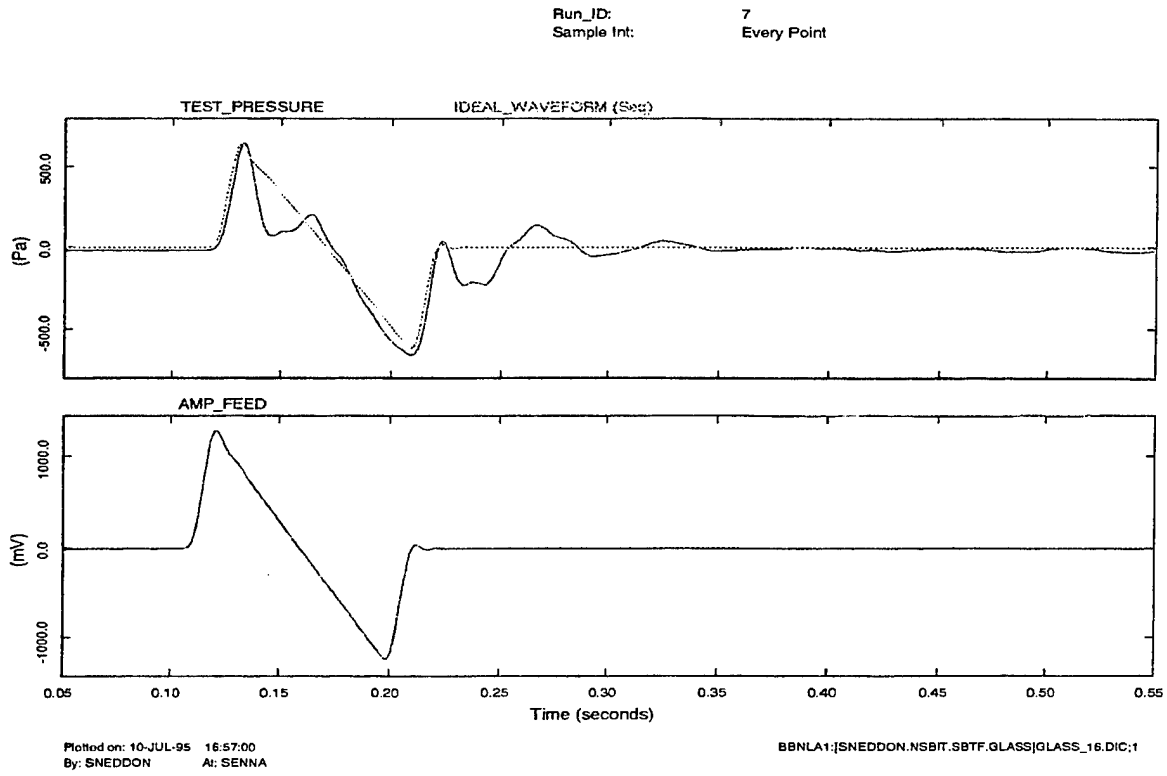

Figure 2-11. Typical SBTF Uncompensated Sonic Boom Waveform.

Section 2.2.3 describes how a pre-distorted input waveform that produces an improved waveform was calculated. The lower trace of Figure 2-12 depicts an example of an input waveform derived by applying the pre-distortion algorithm twice. The upper trace compares the resulting pressure time history with the desired trace. When the time histories were played through the window breakage model, the breakage probabilities fell within 5% of each other. During each test sequence the initial simulated sonic boom was used as a basis for calculating the appropriate "pre-distortion" to produce the desired signal for that particular test article and overpressure level.

2.2.2 Fixture

A steel-braced wooden fixture was built to support the glass panes in their frames for testing in the SBTF. The side facing the pressurized plenum measures approximately 10 feet wide by 8 feet long. As shown in Figure 2-13, the fixture has four openings in a 2-by-2 configuration in its forward facing side to allow four panes to be subjected to a simulated sonic boom at one time. Within each opening is a "backstop" against which the back edge of the metal window frame is supported. Ten toggle clamps are used to secure the front of the glass frames.

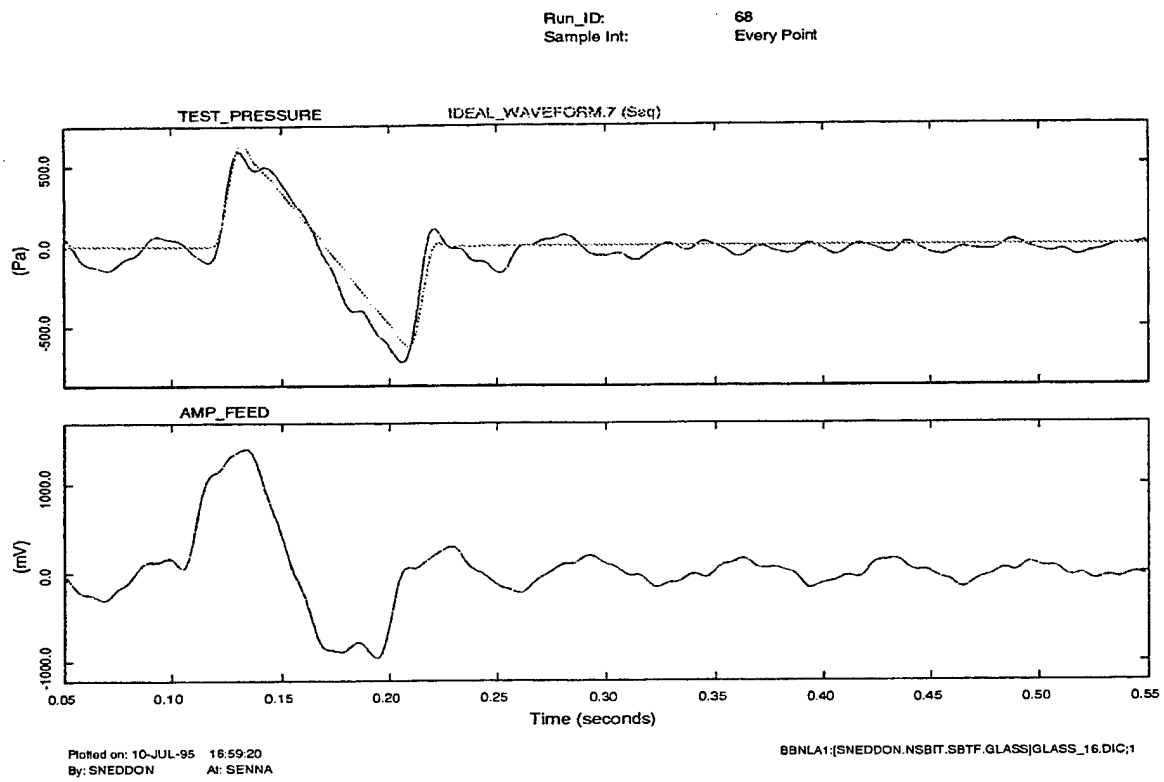

Figure 2-12. SBTF Compensated Sonic Boom Waveform After Two Iterations.

The top and bottom of the depicted face are anchored directly to the SBTF chamber. In addition, support "wings" are provided at each edge to resist the pressure loads. Each wing is approximately 4.5 feet deep. The upper, rear corners of the wings are tied together by a cross-beam and wedges are placed between the wings and the chamber sidewalls to eliminate lateral motion of the wings.

Each window frame (approximately 43.625 inches by 37.5 inches) is made up of a front and back aluminum piece. The frame and glass pane assembly is seated onto the fixture and held in place by the toggle clamps along the four sides for easy installation and replacement. The clamping force can be adjusted so the frame is held tightly or allowed to rattle. Glass panes are sealed between the front and back frames with different insert materials to simulate edge conditions found in real-world environments. Simply supported edge conditions for the panes were achieved in the simulator by using .375 inch wide, .25 inch thick PVC weatherstrip as inserts on both sides of the glass within the metal frames.

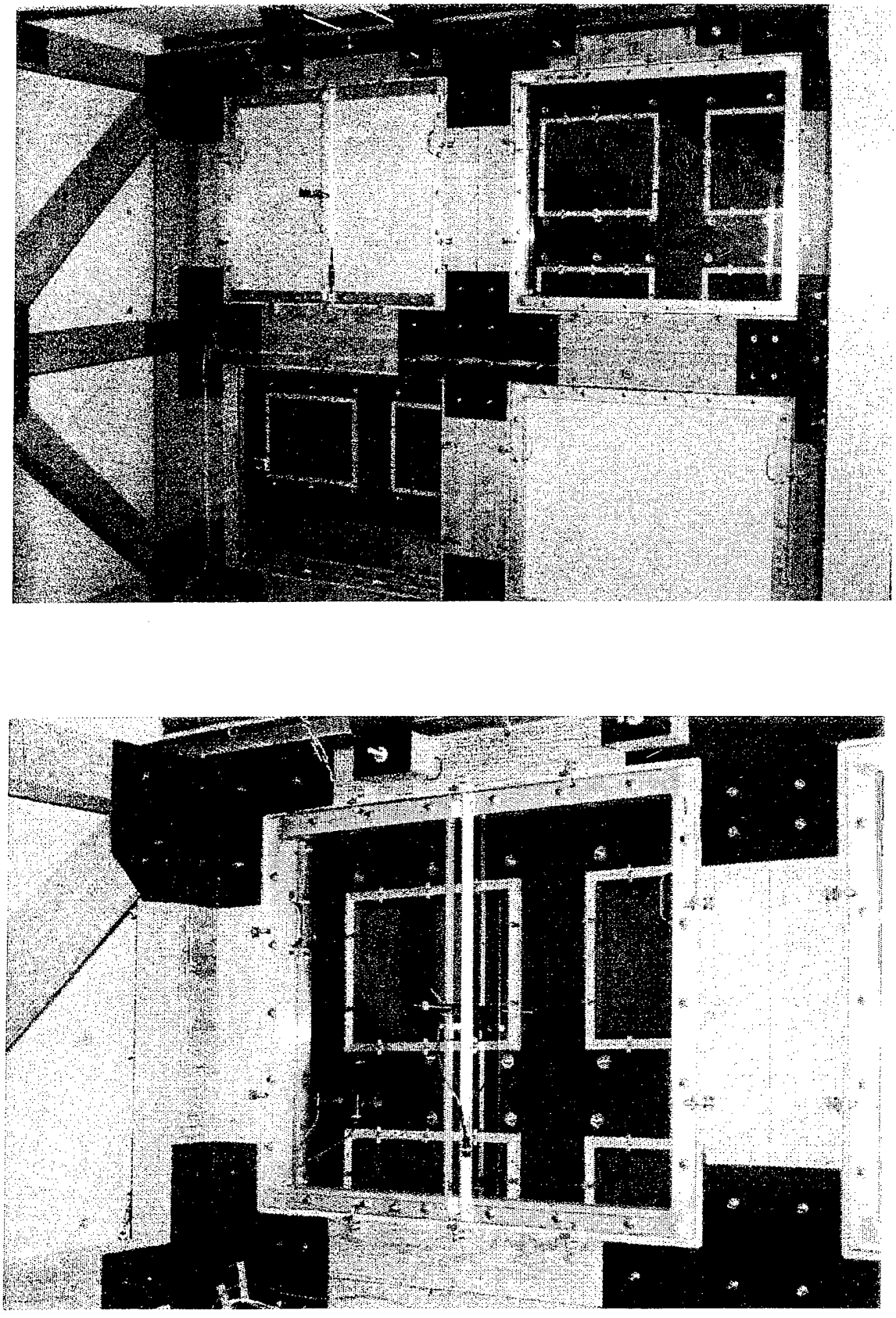

Figure 2-13. Fixture for Glass Tests in SBTF.

2.2.3 Data Acquisition System

As shown schematically in Figure 2-14, the data acquisition system for collecting pressure and other time series test data was based on a DEC VAX 4000/60 computer. (This system was also adapted to perform the data acquisition function during the static tests performed by BBN.) DEC 12-bit A/D and D/A converters were used to generate and digitize the test signals. The data acquisition system can record up to 32 channels of test data at one time. These channels were available for test measurements (pressure, displacement, and acceleration), for measurements of environmental variables (temperature and relative humidity), and for monitoring the health of the sonic boom test facility.

All sound pressure measurements were made using Brüel & Kjær (B&K) condenser microphones, with B&K preamplifiers and power supplies. Acceleration measurements were made using B&K piezoelectric accelerometers and charge amplifiers. Displacement measurements were made using a Schaevitz LVDT. Table 2-5 shows the calibration worksheet for all test instrumentation and lists the specific transducer models and their serial numbers.

The SBTF control software takes commands directly from the user as well as from command files, providing a choice of either interactive or automated operation of the control system. During the SBTF glass tests, the test conductor started each test session interactively. (For additional information regarding test procedures, see Section 2.2.7). For each boom in the test sequence, the control software would start the A/D converter clock (beginning the data acquisition process), and simultaneously buffer sonic boom waveform samples to the D/A converter.

The test plan called for a large amount of raw data to be collected during the testing sequence (typically 32 Kbytes/boom). As with the plaster damage tests, the BBN/Probe™ data analysis package was used for data reduction since it works efficiently with large data sets and provides the required suite of analytical tools. Command files were written to automate the process of analyzing the raw data and generating the required plots and tabulations.

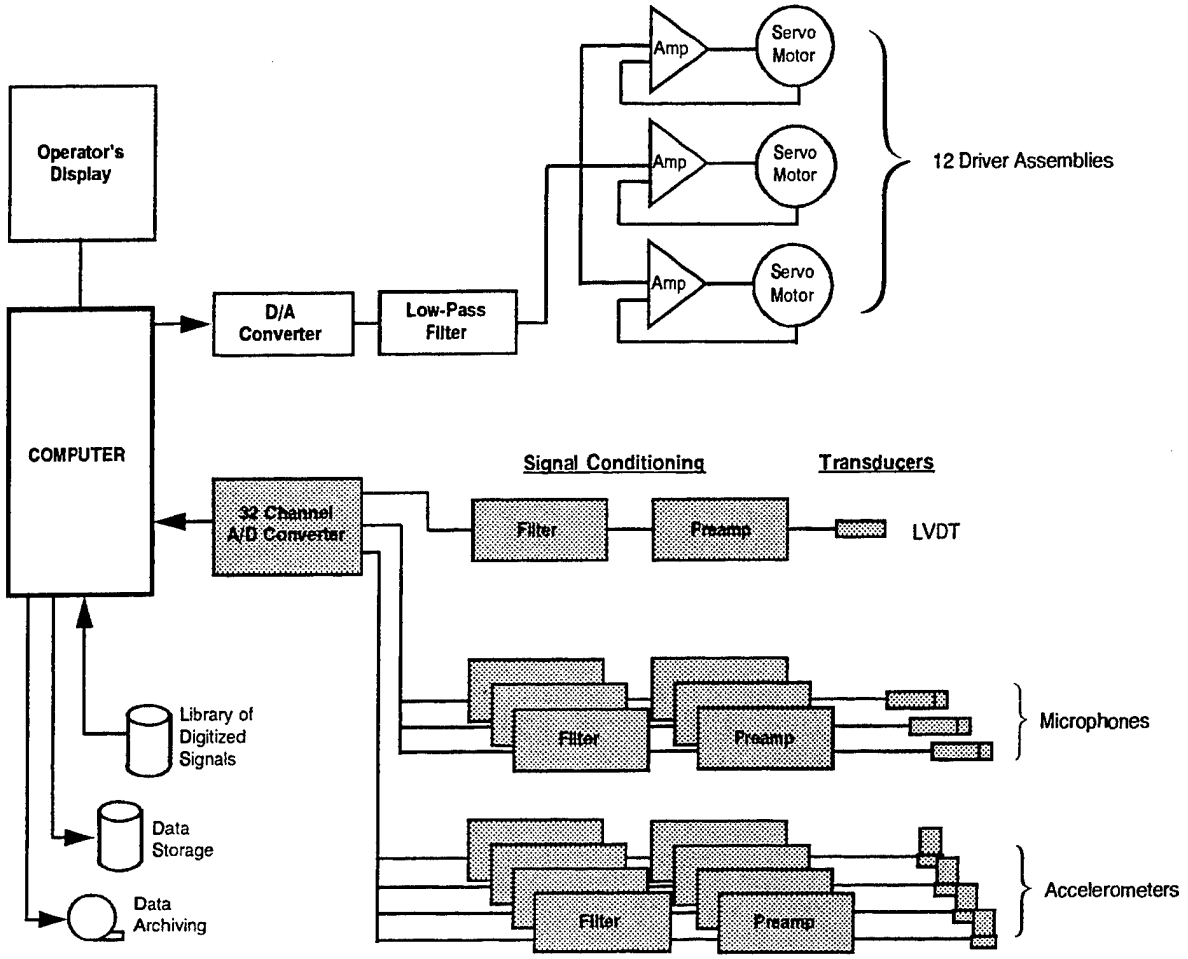

Figure 2-14. Block Diagram of SBTF Instrumentation.

Table 2-5. SBTF Calibration Worksheet.

- - DATA DICTIONARY WORKSHEET - -
A/D CONVERTER CHANNEL ASSIGNMENTS AND GAIN SETTINGS
NSBIT SBTF GLASS EXPERIMENT

Test ID: CALTEST
Description: Window fixture test & instrumentation calibration
Test condition: 15 psf (nominal)
Prepared by: MDS
Date: 9 Jan 95

CHANNEL	DESCRIPTION	TRANSDUCER		PREAMPLIFIER		CALIBRATION	GAINS		
		TYPE	S/N	TYPE	S/N	FACTOR	PREAMP	FILTER	A/D
1	D/A output signal	N/A	N/A	N/A	N/A	$1.000\text{-}10^{3}$ mV/V	N/A	N/A	1
2	Filtered D/A output	N/A	N/A	N/A	N/A	$1.000\text{-}10^{3}$ mV/V	N/A	N/A	1
3	Amplifier feed	N/A	N/A	N/A	N/A	$1.000\text{-}10^{3}$ mV/V	N/A	N/A	4
4	Test plenum pressure	B&K 4147	1543030	B&K 2639	1595845	$6.361\text{-}10^{2}$ Pa/V	1.00	2.00 (A1)	2
5	Back plenum pressure	B&K 4136	1125167	GR P42	3798	$1.375\text{-}10^{3}$ Pa/V	1.00	2.00 (A2)	2
6	Delta-P, microphone A	B&K 4178	1238763	B&K 2633	1259422	$3.129\text{-}10^{2}$ Pa/V	1.00	1.00 (A3)	2
7	Delta-P, microphone B	B&K 4178	1238763	B&K 2633	1259374	$3.112\text{-}10^{2}$ Pa/V	1.00	5.00 (A4)	2
8	Window 1 displacement	Schav 1000	3037	N/A	N/A	$1.000\text{-}10^{2}$ mil/V	N/A	N/A	1
9	Room temperature	Omega HX93	B2092	N/A	N/A	$1.710\text{-}10^{2}$ °F/V **	N/A	N/A	8
10	Humidity	Omega HX93	B2092	N/A	N/A	$1.000\text{-}10^{2}$ %RH/V	N/A	N/A	8
11	Acceleration, Ch 1	B&K 4383	1646109	B&K 2634	1621207	$3.209\text{-}10^{1}$ g/V	1.00	5.00 (A5)	2
12	Acceleration, Ch 2	B&K 4383	1646107	B&K 2634	1621208	$3.251\text{-}10^{1}$ g/V	1.00	5.00 (A6)	2
13	Acceleration, Ch 3	B&K 4383	1646106	B&K 2634	1621209	$3.215\text{-}10^{1}$ g/V	1.00	5.00 (A7)	2
14	Acceleration, Ch 4	B&K 4383	1646105	B&K 2634	1621210	$3.255\text{-}10^{1}$ g/V	1.00	5.00 (A8)	2
15	(Unused)								
16	(Unused)								
17	(Unused)								
18	(Unused)								
19	(Unused)								
20	(Unused)								
21	(Unused)								
22	(Unused)								
23	(Unused)								
24	(Unused)								
25	(Unused)								
26	(Unused)								
27	(Unused)								
28	(Unused)								
29	(Unused)								
30	(Unused)								
31	(Unused)								
32	(Unused)								

NOTES: Calibration factors for each channel are PER VOLT. Final data dictionary scale factors must also take into account preamplifier, anti-aliasing filter, and A/D input gains as appropriate.

Microphone calibration factors are based on pistonphone calibrator, with appropriate atmospheric pressure adjustments.
Accelerometer sensitivities based on 1 g - 9.807 m/s**2

All A/D converter channels set to ±10.00 V (= 4.833 mV/bit)

As discussed in Section 2.2.1, the input waveform to the SBTF amplifiers was modified from the ideal to compensate for the dynamic response of the test article during the actual boom exposure. The goal was to apply a waveform that would, after going through the full electro-mechanical system represented by the SBTF/test article combination, result in the ideal pressure time history. This was achieved as follows: A calibration boom with an idealized N-wave signature was used as the amplifier input. The ideal N-wave and the resulting test chamber pressure were then processed by first calculating the finite Fourier transforms:

$$X_{ideal}(f) = \frac{1}{T}\int_0^T x_{ideal}(t)\, e^{-i2\pi ft}\, dt \tag{2-1}$$

$$X_{meas}(f) = \frac{1}{T}\int_0^T x_{meas}(t)\, e^{-i2\pi ft}\, dt \tag{2-2}$$

where $x_{ideal}(t)$ and $x_{meas}(t)$ are the input (ideal) and pressure (measured) waveforms, respectively. The frequency response function (equation 2-3) for the system was computed from these (equations 2-1 and 2-2). The frequency response function was then inverted and multiplied by the transform of the (ideal) N-wave, to give a frequency domain representation of the corrected signal (equation 2-4). For linear systems, this is the signal that results in the ideal pressure waveform being created after passing through the system ($HX_{corr} = X_{ideal}$).

$$H(f) = \frac{X_{meas}(f)}{X_{ideal}(f)} \tag{2-3}$$

$$X_{corr}(f) = \frac{X_{ideal}(f)}{H(f)} \tag{2-4}$$

An inverse-FFT operation was then performed to arrive at the desired time series:

$$x_{corr}(t) = \frac{1}{T}\int_0^T X_{corr}(f)\, e^{i2\pi ft}\, dt \tag{2-5}$$

The new time series was stored in the waveform library for use by the SBTF control software. This new waveform, when applied to the amplifiers, resulted in a test chamber pressure that more closely approximated the ideal N-wave shape.

This procedure was performed for each design test pressure and for all possible combinations of glass panes and blanks in the test fixture. Because of the response of the test articles, the process is nonlinear. Consequently, a single correction pass did not always produce a suitable waveform. In those instances,

the procedure was iterated and the optimum number of iterations was selected as the basis for inclusion in the waveform library.

2.2.4 Instrumentation

All elements of the SBTF data acquisition system were carefully calibrated to obtain accurate measurement data. This section describes the calibration procedures used.

End-to-end calibration checks were made during each test article change out, using NIST-traceable pistonphone calibrators (for microphones) and calibration shakers (for accelerometers). This was done as a continuing check to verify proper operation of the transducers, signal conditioning electronics and A/D converter.

2.2.4.1 Transducer Calibration

All microphones and accelerometers used in the SBTF glass tests were calibrated using NIST-traceable transfer standards prior to testing.

The LVDT (Linear Variable Differential Transformer, or displacement transducer) was calibrated at displacement strokes of 0, 0.5, and 1.0 inches. The calibration factor was 0.1 inch per volt.

Thermocouples (for temperature measurements) and relative humidity sensors were purchased new and used directly, relying on manufacturer-supplied calibration information. As these were treated as non-critical test parameters, no independent calibration of temperature or humidity sensors was performed.

2.2.4.2 Signal Conditioning Electronics

Prior to the glass tests, all anti-aliasing filters and signal preamplifiers were checked for correct operation, and to assure that gain, input offset, and noise levels were all within acceptable limits. All checks and adjustments were done using precision digital multimeters with current, factory-maintained calibration.

2.2.5 Performance of Test Chamber

Simulated sonic booms were characterized by a high degree of consistency throughout each test sequence. With the notable exception of sonic booms that resulted in pane failures, the waveforms were nearly identical. Figure 2-15 compares the applied pressure waveform for booms 2 and 5,000 for Test Group 1 (tests of aged glass at a nominal applied pressure of 16 psf). Figure 2-16 compares the spectra of these waveforms. Although there was some minor variation in the detail of waveforms among test sequences with different target test pressures, the spectra are quite consistent, as illustrated by Figure 2-17, which compares applied pressure time histories for selected booms at nominal overpressures of 12 and 16 psf.

The following quantities were monitored to track the consistency of the load produce by the sonic boom simulator:

- Peak positive and negative pressures inside the pressurized plenum, and
- Peak positive and negative differential pressures across the test article.

The coefficient of variation (COV) of the peak positive and negative pressures was calculated for each individual test sequence. The values of COV were always less than 1% for all cases. The range and the mean (positive and negative) test pressures and differential pressures during simulated sonic booms are listed in Tables 2-6 and 2-7 respectively.

Table 2-6. Performance of SBTF.

Test Sequence	Peak Positive Pressure (psf)			Peak Negative Pressure (psf)		
	Max.	Average	Min.	Max.	Average	Min.
Aged Glass at 16 psf	16.54	16.12	15.90	-15.75	-15.22	-12.99
Aged Glass at 12 psf	12.68	12.05	11.84	-12.24	-11.71	-11.39
Aged Glass at 14 psf	14.27	14.13	13.70	-14.46	-13.99	-13.77
Flawed Glass at 16 psf	16.15	15.98	15.40	-15.75	-15.54	-15.17
Flawed Glass at 12 psf	12.05	11.95	11.68	-12.16	-11.80	-11.55
Flawed Glass at 14 psf	14.10	13.97	13.72	-14.52	-14.30	-13.93

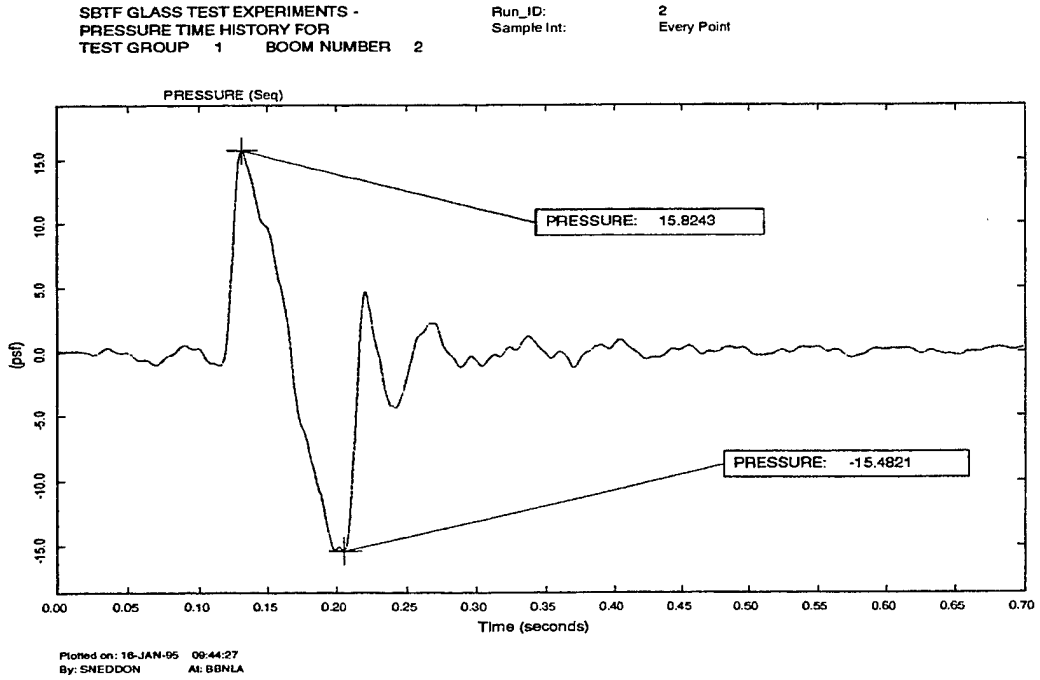

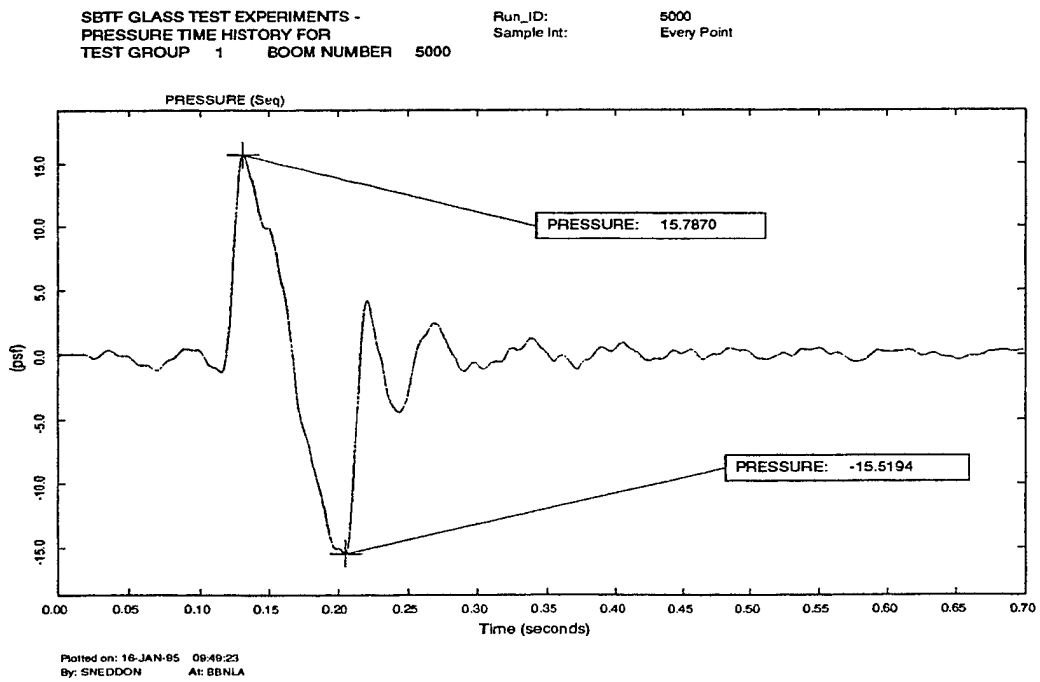

Figure 2-15. Comparison of Test Pressures for Booms 2 and 5,000 from Test Group 1.

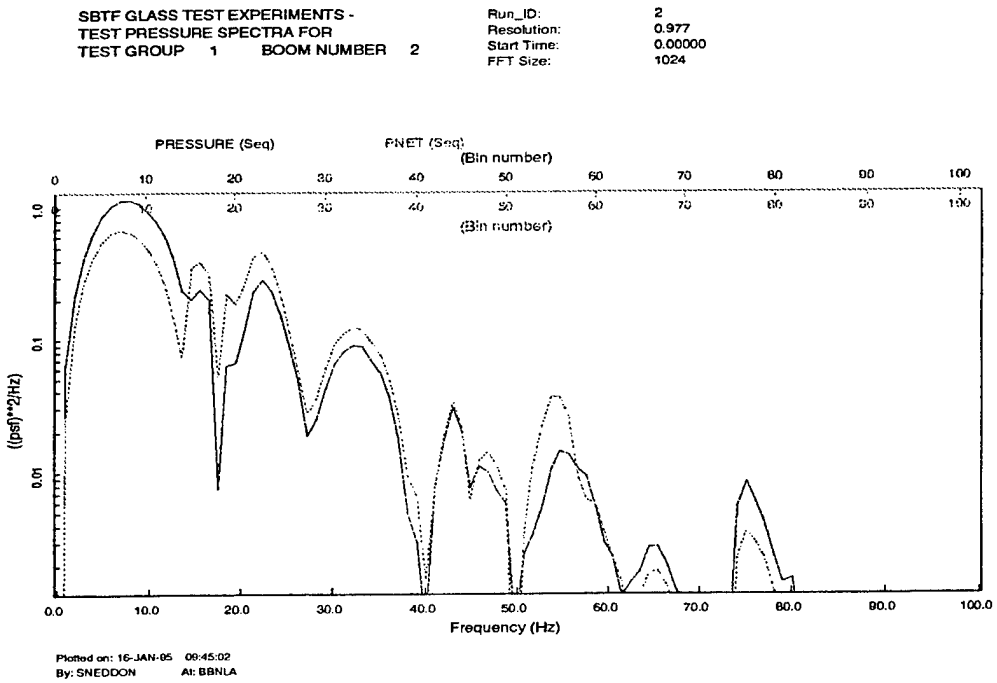

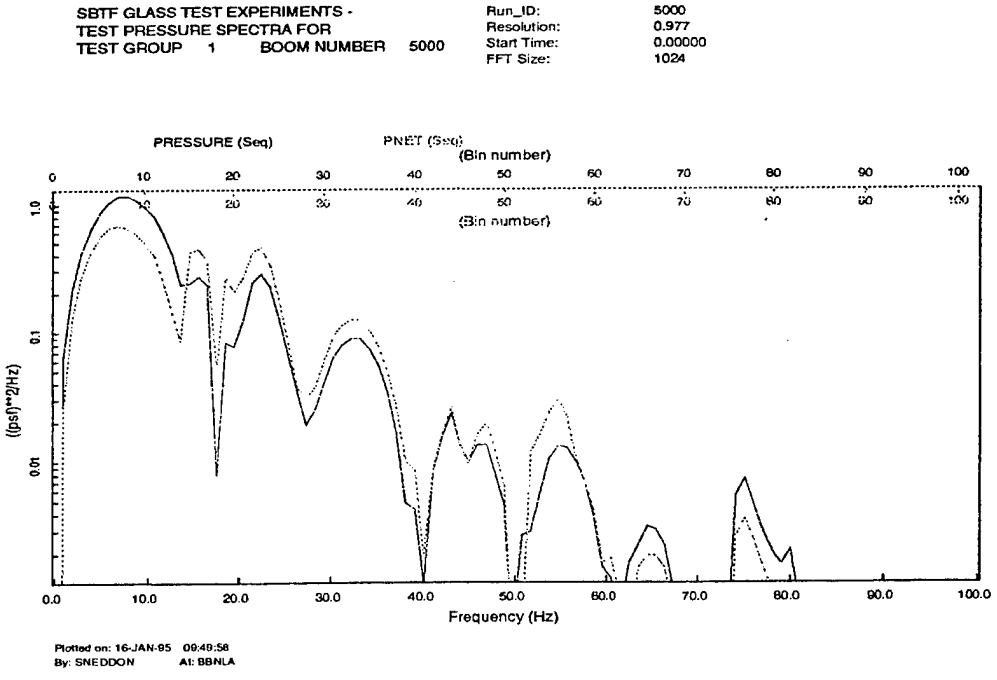

Figure 2-16. Comparison of Spectra of Test Pressures and Net Pressures for Booms 2 and 5,000 of Test Group 1.

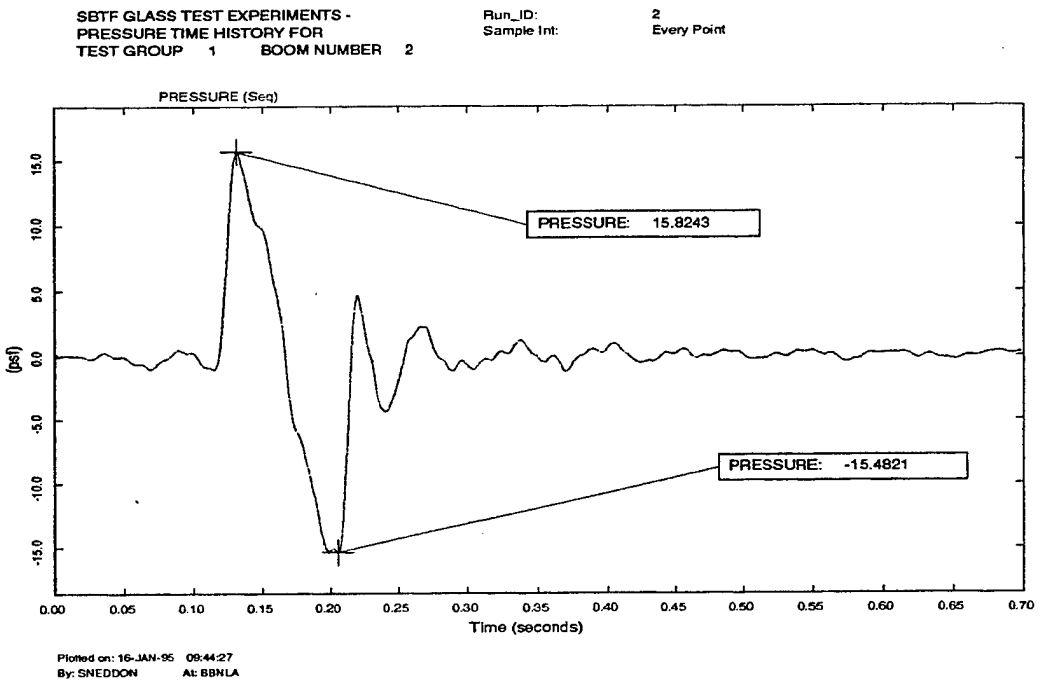

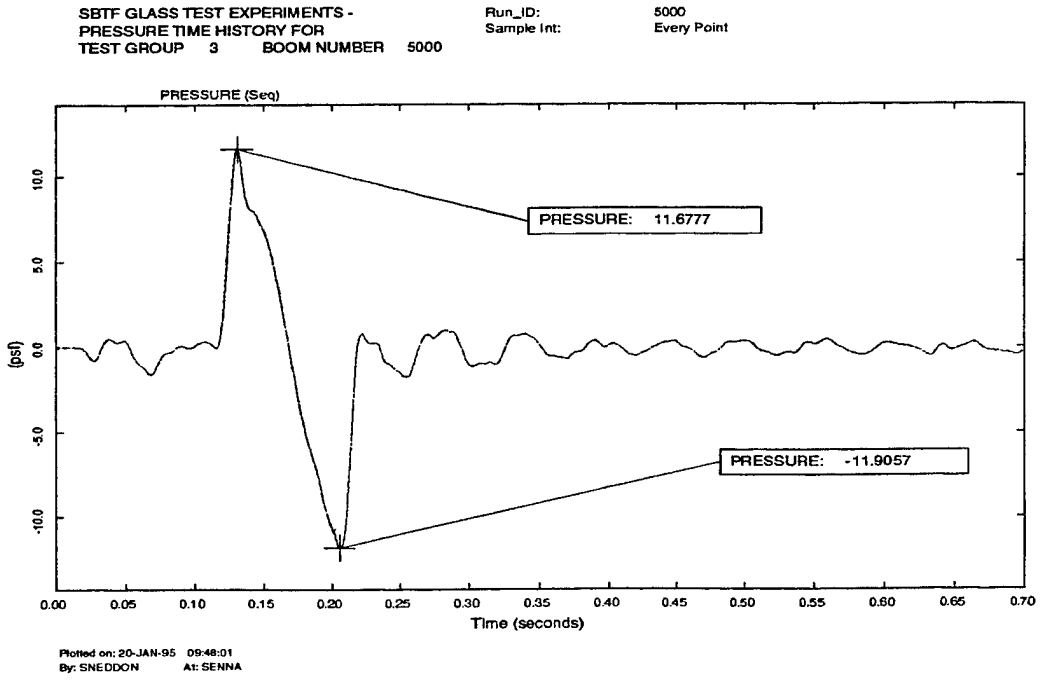

Figure 2-17. Comparison of Pressure Histories for a 16 psf and a 12 psf Simulated Boom.

Table 2-7. Differential Pressure Statistics.

Test Sequence	Peak Positive Pressure (psf)			Peak Negative Pressure (psf)		
	Max.	Average	Min.	Max.	Average	Min.
Aged Glass at 16 psf	15.51	15.16	14.99	-13.97	-13.58	-10.12
Aged Glass at 12 psf	11.05	10.49	10.37	-10.14	-9.82	-9.31
Aged Glass at 14 psf	12.49	12.26	11.99	-12.22	-12.05	-8.85
Flawed Glass at 16 psf	15.13	14.98	14.48	-14.22	-14.01	-13.29
Flawed Glass at 12 psf	10.55	10.41	10.32	-10.14	-10.01	-9.52
Flawed Glass at 14 psf	12.42	12.14	12.03	-12.52	-12.34	-12.01

2.2.6 Test Procedures

The procedures used in performing the SBTF glass tests are specified in the document "Test Plan for Glass and Plaster Tests" (Haber and See, 1991). In most instances, the glass tests followed these procedures directly. However, as with all experiments of this magnitude, there were some exceptions encountered, and these were resolved by the test conductor as they occurred. This section provides an overview of the test procedures, describes exceptions to these procedures when they occurred, and provides additional testing details not included in the formal test plan.

The basic test procedure used for all glass tests consisted of the following major steps:

(1) Mount glass panes in frames with appropriate edge conditions.
(2) Position frames in the sonic boom test facility fixture and secure.
(3) Install accelerometers and LVDT, as required, and connect all instrumentation.
(4) Calibrate all instrumentation channels in the DAS.
(5) Select the appropriate corrected waveform from the library required for the test.
(6) Perform the test sequence by repeating the following steps:
    - expose the panes to sonic booms until a pane breaks or a total exposure of 5,000 booms has been accrued;
    - whenever a pane breaks, clean up the glass and replace the pane with a spare pane; and
    - analyze the collected data.

The SBTF control software was set to automatically halt the testing sequence whenever a test article failed. The time interval between successive booms was 5 seconds, which provided sufficient time for the

disturbance to damp out before the next sonic boom simulation sequence began. For a typical boom, the displacement decayed to 15% of the maximum value in 0.50 seconds.

The original library of sonic boom waveforms was created using the signal generation facility of N!Power, a signal processing software package for Sun and VAX computers. These were stored with a temporal resolution of 1 ms (1 kHz effective sample rate). All signals sent to the SBTF amplifiers were passed through a 100-Hz, 8th-order Butterworth low-pass filter to protect the loudspeaker modules. All sonic boom waveforms employed during the tests included a 100 ms lead-in "delay," meaning that the A/D system collected 100 ms of data before the onset of the actual simulated boom.

The A/D converter was configured to synchronously sample the selected data channels at one thousand samples per second for all test sequences, typically collecting one second of data per boom. Given that the frequency range of interest for this experiment was up to 100 Hz, a sample rate of one thousand samples/second represents considerable over-sampling. However, this sample rate was selected to provide better temporal definition of the pressure waveforms, necessary to estimate pressure maxima and minima accurately. An anti-aliasing cut-off frequency of 250 Hz was used for all data channels throughout the tests. As called for in the test plan, all A/D data was stored to disk for later analysis as well as archived to magnetic tape.

All data reduction for the SBTF glass tests was performed by BBN/Probe™, using automated analysis procedures written for these tests. BBN/Probe™ extracted the required test variables from the data files, performed all necessary engineering units conversions, and computed the quantities called for in the test plan. These results were written to disk as formatted (text) files for subsequent processing and inclusion into reports.

2.2.6.1 Test Plan Deviations

The glass test plan called for calibration booms to be applied to each article at 10% of the target pressure level. As described in Section 2.2.3, these calibration booms were used to calculate the transfer function of the overall system and to make compensating adjustments to the input waveform. Experience with the plaster test program showed that corrections derived from 10% calibration shots did not give an acceptable waveform when extrapolated to the 100% level. As expected, the corrected waveform produced good results when used to create test pressures at or near the calibration level. To overcome this nonlinearity, calibration was performed at full test pressure using spare glass panes.

There were two major deviations from the test plan's data analysis requirements. First, the full time domain analyses called for (all pressure and acceleration channels) were not done for each boom. A much more limited analysis was adopted for every boom, consisting of a record of maximum and minimum test and net pressures, displacement, temperature, and humidity. This decision was made since the simulator had already proved itself to be highly repeatable during the plaster tests making the detailed analyses

largely redundant. The quantity of analyzed test data would have increased substantially while contributing little to the test plan goals. The second major change was that the spectral analyses called for in the test plan were performed only at the beginning and ending of a test sequence and when a pane failed. It was decided that repeating these analyses would not contribute significantly to the test plan goals.

2.3 PREPARATION OF TEST SPECIMENS

Single strength glass panes (0.085 to 0.097 inch thick of dimensions 70 by 41.125 inches were purchased from a single supplier in May 1991. Each piece was cut locally by a professional glass cutter into identical pieces 35 by 41.125 inches. Forty pairs of panes were tagged to identify that they were cut from the same original pane. It was planned that twenty pairs would be required for subsequent matched testing. A set of panes was reserved for static tests to establish the strength of the new glass. The remainder of the glass was placed in wooden racks on the roof of BBN's Canoga Park facility to expose it to atmospheric loads and weathering. (Figure 2-18 illustrates the glass in its storage racks.) The storage of the glass in this manner was intended to simulate the aging process to which window panes are normally subjected. The glass panes were stored for seventeen months in this manner and then removed for testing. During the storage period they were exposed to high winds, rain, smoke from a minor fire at the BBN facility and shaking from earthquakes in the Big Bear and Landers areas.

After the glass was removed from the roof, it was stored on indoor pallets until needed for testing. The first group of tests of aged glass were performed by ANCO Engineers between January 1993 and July 1993. During this period, all of the tests using the fatigue test facility and most of the tests using the static test facility were performed. This included the development of an apparatus for introducing flaws into the surface of the glass in a repeatable manner and verifying that this procedure substantially decreased the stress required to break the panes.

The flawing apparatus consisted of a weighted, diamond-tipped glass cutter at the end of an arm. One end of the arm slid along a metal rod, assuring that the glass cutter moved along a straight line. To introduce a flaw into a glass surface, the entire apparatus was placed on the glass surface. The glass cutter was then moved along the rod to cut a flaw of the desired length.

Three flaw configurations were contemplated: (1) a diagonal flaw running from the center to one corner, (2) a diagonal flaw spanning most of the surface (running corner to corner) and (3) flaws along both diagonals spanning the surface of the glass. When initial experiments suggested that there would be no difference among the strength reduction resulting from these three techniques, the double diagonal flaw was adopted based on the assumption that this would create the most consistent pane strength.

As a result of NSBIT budgetary limitations, activities on this project were suspended after the testing described above, and did not resume until February 1995. During the intervening period, the glass was

subjected to strong shaking during the January 1994 Northridge earthquake. In addition, ANCO Engineers (who had been performing the static and fatigue testing) moved out of the Los Angeles basin during this time period.

All testing performed following the February 1995 program resumption was performed by BBN. Although efforts were made to identify the procedures employed by ANCO Engineers and to obtain the use of as much of the original test equipment as possible, there were significant differences between the static tests performed by BBN and ANCO Engineers. Differences in instrumentation are documented earlier in this section. Differences in testing techniques resulted in significant differences in the displacement of the center of the panes being tested under identical pressures. It is likely that the two sets of tests had slightly different edge conditions for the glass. Consequently, the BBN and ANCO Engineers static tests cannot be compared with each other. Fortunately, all test objectives can be accomplished by evaluations that do not require these comparisons.

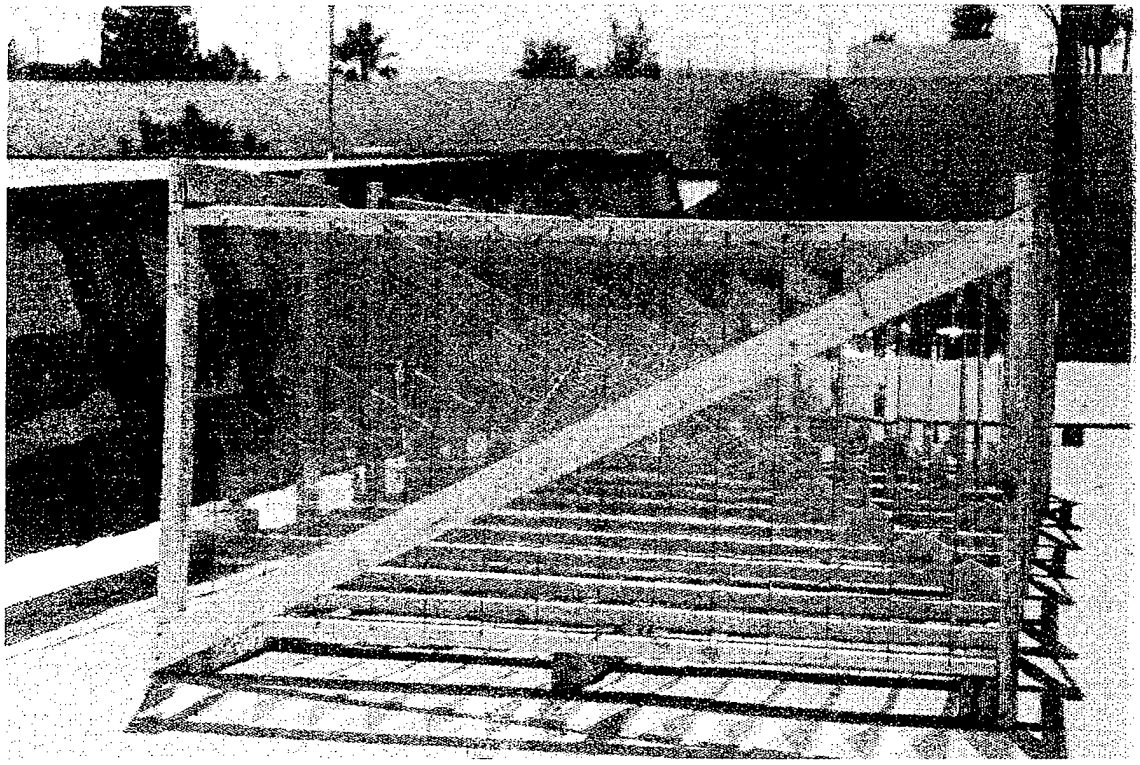

Figure 2-18. Glass Aging In Storage Rack.

This page intentionally left blank.

3 TEST RESULTS

This section presents the results of the cumulative damage glass test program. The first subsection presents a brief review of the literature characterizing glass failure and earlier studies of cumulative damage to glass. This is followed by a section addressing the results of the static and fatigue tests, and tests in the SBTF.

3.1 PREVIOUS INVESTIGATIONS

Glass failure is characterized by the activation of edge flaws and the growth of cracks associated with surface imperfections. Moisture, corrosive chemicals in the atmosphere, and temperature extremes are associated with the growth of microscopic surface imperfections. In his 1980 dissertation (Beason, 1980), Beason summarized the consensus regarding the factors contributing to the growth of flaws to cause glass failure. The maximum local stress, σ_m, associated with an idealized flaw occurring at the flaw tip is given by

$$\sigma_m = \sigma_a K \left(\frac{h}{r}\right)^{1/2} \tag{3-1}$$

where r is the effective radius of the flaw tip, σ_a is the nominal stress, K is the crack geometry factor, and h is the flaw depth. The strength of glass tested in a vacuum is independent of load duration. The strength of glass exposed to water during a test is dependent on load duration and is less than analogous dry strengths. The presence of other polar compounds similarly weaken glass.

It is hypothesized that flaw corrosion occurs because of the action of water on the glass surface. If water is present but no stress is applied, the tip radius of curvature increases and the depth of the crack increases, but the radius of curvature increases faster so that the stress raising potential of the crack is *decreased.* If the flaw is exposed to water and tensile stress, the radius decreases while the flaw depth increases, *increasing* the stress raising potential of the crack.

Beason presents a synthesis of the results of other investigators' work (Brown, 1974; Wiederhorn, 1967; Charles, 1958) with respect to the effects of humidity, temperature and length of exposure to a load. He hypothesizes the following equality:

$$\int_0^{t_f} RH(t)\left[\frac{\sigma(t)}{T(t)}\right]^n \exp\left[\frac{-\gamma_0}{RT(t)}\right] dt = constant \tag{3-2}$$

where γ_0 = 25.0 kcal/mole,
R = 1.986 cal/mole-K,
T(t) = temperature, K
n = 16,
and RH(t) = relative humidity as a decimal fraction

This expression is commonly normalized to a sixty-second load by dividing the quantity by 60. The n^{th} root of the resulting invariant is termed the sixty-second static equivalent stress. Investigation of glass pane failure for several conditions and collections of panes shows that 16 is a representative value of the exponent "n" for most glass (Charles, 1958; Reed and Simiu, 1983).

While repeated loading may be responsible for the growth of flaws, no sonic boom or blast field tests have been found to support the theory of cumulative damage to glass. Previous laboratory tests of repeated simulated sonic boom loads (White, 1972; Kao, 1970) have produced weak, equivocal relationships between final breaking pressures and the number of repetitive loads. White performed regression analyses of the data he and Kao collected to relate breaking pressure to the number of exposures. His computed correlation coefficients were never larger than 0.17 for any of his models.

By contrast, there have been relatively successful fatigue studies of glass using other types of dynamic loads. Levengood (1958) performed one-way cyclic loading tests of pieces of glass 1.5 inches wide by 11 inches long. The beams of glass were supported on knife edges and the load was applied centrally. The applied load caused a maximum deflection of about .125 inch. Samples were cycled for a fixed number of cycles and then tested for failure strength. In the break test, the specimen was supported on knife edges and centrally loaded to failure. Matched control specimens were also tested for breaking strength. These tests were performed at repetition rates of one and two Hz. The change in strength compared with the controls was reported for both loading rates. Short applications of cyclic loading reduced the strength relative to the controls. Progressively longer applications decreased the strength until a minimum was achieved. Cyclic loading for longer periods caused a recovery of strength. Cyclic loading at one Hz for a sufficiently long time eventually produced stronger specimens than the controls. Tests at two Hz were not continued long enough to produce stronger specimens. Levengood interprets his results as healing of minute flaws in the glass surface because of the energy imparted by the cyclic loading.

3.2 STATIC AND FATIGUE TESTS

The same test fixture was used for both the static and the fatigue tests. (See Section 2.1 for a discussion of this apparatus.) The following material presents the results of investigations performed with this facility. In the previous section, we presented a theoretical formulation of the relationship between the strength of glass and the ambient temperature and relative humidity. Effects were minimized by limiting the variation of temperature and relative humidity during the course of the tests. Figures 3-1 and 3-2 plot

the effective stress imposed on the glass relative to conditions of 50% relative humidity and 65°F, respectively, throughout both sets of tests. It is clear from these figures that the overall effect of these variables throughout the testing was minimal. The ranges of relative humidity and temperature during the course of each test are presented as part of the discussion of the individual tests.

Static tests were used throughout the program whenever it was necessary to determine the strength of panes. These tests were used to investigate the effects of aging, the effect of different mounting conditions and to assess whether there was a loss of pane strength induced by the fatigue tests and the SBTF tests.

In the following material most of the edge conditions are described as "clamped." Total fixity of edges is, in practice, almost impossible to achieve. Nevertheless, a comparison of a portion of a measured strain time history with calculated values from a nonlinear finite element model with clamped edges gave consistent results.

Late in the test program, as discussed in Section 2.3, it was necessary for BBN, rather than ANCO, to perform the required static tests. Comparison of plots of measured displacements at the center of the pane versus applied pressure for the two sets of tests showed lesser displacements for the BBN tests than for the tests performed by ANCO. Moreover, both sets of displacements become progressively less than the displacements calculated by the finite element analysis as the load was increased. The most likely explanation for these discrepancies is differences in edge conditions. While the edge conditions near the beginning of the tests may have been close to "clamped," the glass probably began to slip as the load increased.

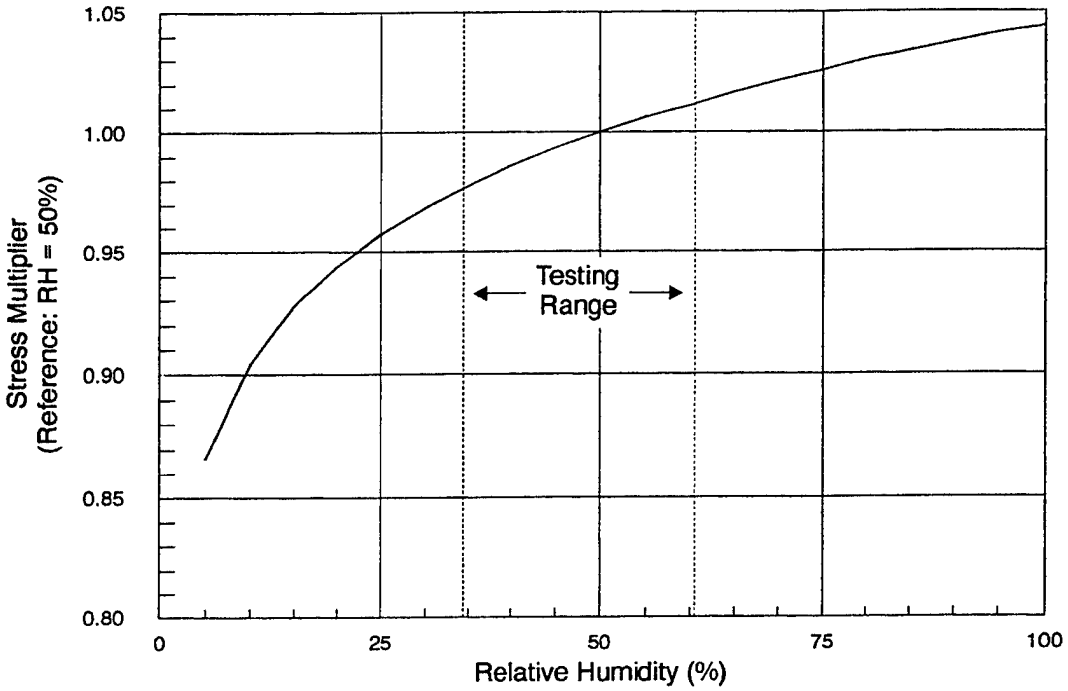

Figure 3-1. Effect of Temperature on Glass Strength During Static and Fatigue Tests.

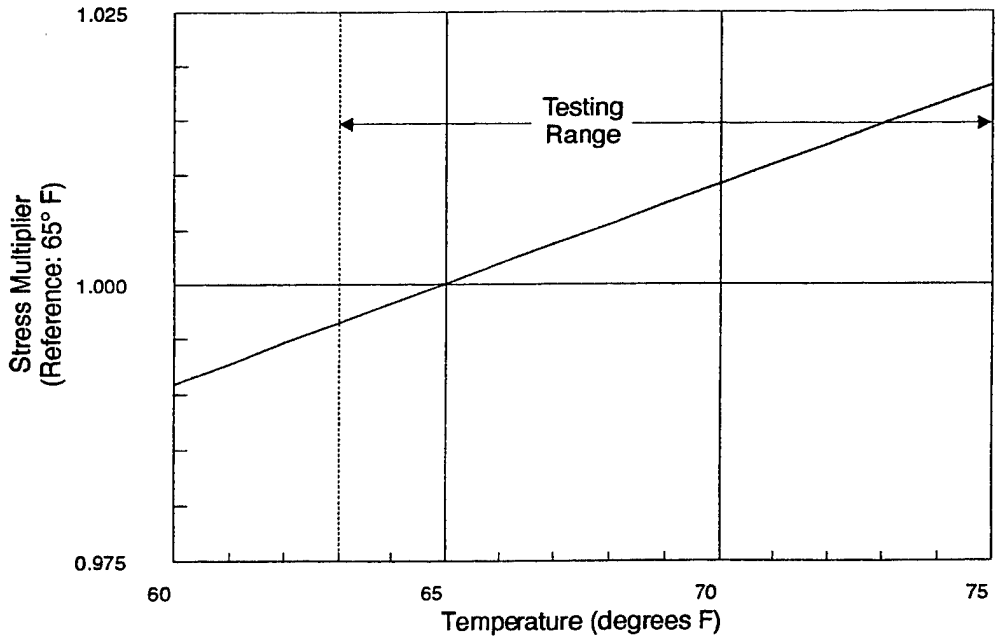

Figure 3-2. Effect of Relative Humidity on Glass Strength During Static and Fatigue Tests.

Consequently, calculations of stresses associated with the tests are not actual stresses but rather the stresses that would have occurred had the edge conditions been fully clamped. Moreover, these values were derived by (1) calculating the stresses based on a nonlinear finite element analysis of a simply support plate and (2) extrapolating relationships between normalized displacements for simply supported and clamped plates and maximum stresses. Thus, the only values of stress in these results that may be directly compared with published strengths are those for simply supported panes.

3.2.1 Static Tests

3.2.1.1 Effect of Aging on Glass Strength

Static tests with clamped edges were run to evaluate the effect of aging glass. Three groups of panes were tested for this purpose: (1) new glass, (2) glass that had "aged" 15 months, and (3) glass that had "aged" 17 months. A clamped edge condition was achieved by using hard nylon (Delrin) inserts on both sides of the panes within the metal frames, as described in the test plan.

Nine panes of new glass were tested in the static test facility shortly after the glass was purchased. The temperature range during these tests was from 66.1°F to 66.9°F. Relative humidity varied from 56% to 64%.

The results of test number 2 were discarded. No catastrophic failure occurred for this pane; instead, the glass cracked at a peak pressure less than one-half the next smallest failure pressure. Test number 1 may also be regarded as questionable. This pane was subjected to several auxiliary tests to measure the resonant frequency of a pane in the test configuration before it was subjected to the static strength test. Table 3-1 depicts the failure statistics for the new glass with and without the results of test number 1. In this and subsequent tables, the strength of glass is characterized by the sixty-second static equivalent breaking pressure, P_{60} (psf), and the sixty-second static equivalent stress to failure, σ_{60} (kpsi).

Table 3-1. Strength of New Glass.

Statistic	All Samples Except Test 2		All Samples Except Tests 1 & 2	
	P_{60} (psf)	σ_{60} (kpsi)	P_{60} (psf)	σ_{60} (kpsi)
Mean	147.83	82.5	156.80	87.5
Standard Deviation	29.85	16.2	16.97	8.58
Coefficient of Variation	0.20	0.20	0.11	0.10
Sample Size	8		7	

At the end of fifteen months, four panes were removed from the BBN roof to determine the effects of aging. Temperature varied from 71.2°F to 71.5°F during these tests. Relative humidity varied from 46% to 48%. Table 3-2 summarizes the results of those tests.

Table 3-2. Glass Strength After Fifteen Months of Aging.

Statistic	All Samples	
	P_{60} (psf)	σ_{60} (kpsi)
Mean	93.96	52.8
Standard Deviation	26.64	14.1
Coefficient of Variation	0.28	0.27
Sample Size	4	

After seventeen months, the remainder of the glass was removed from the roof. Five panes were tested to assess the strength of the panes removed at that time. Temperature varied from 69.5°F to 70.2°F during these tests. Relative humidity varied from 49% to 50%. Table 3-3 summarizes the results of these tests.

Table 3-3. Glass Strength After Seventeen Months of Aging.

Statistic	All Samples	
	P_{60}(psf)	σ_{60}(kpsi)
Mean	69.07	39.4
Standard Deviation	17.39	9.51
Coefficient of Variation	0.25	0.24
Sample Size	5	

The following hypotheses were investigated:

1. Glass aged 15 months is statistically weaker than new glass.

2. Glass aged 17 months is statistically weaker than glass aged 15 months.

These hypotheses were investigated by evaluating the statistic

$$t_{df} = \frac{\bar{x}_1 - \bar{x}_2}{S_o}\sqrt{\frac{n_1 n_2}{n_1 + n_2}} \tag{3-3}$$

where

$$S_o = \sqrt{\frac{(n_1 - 1)s_1^2 + (n_2 - 1)s_2^2}{df}}$$

$$df = n_1 + n_2 - 2$$

$$\bar{x}_j = j^{th} \text{ sample mean}$$

$$s_j^2 = j^{th} \text{ sample variance}$$

and

$$n_j = \text{size of sample } j$$

As characterized by σ_{60}, the 15-month-old glass was found to be weaker than the new glass at a significance level of $\alpha = 0.006$ ($t_{10} = 3.11$). The t statistic based on P_{60} values has the same level of significance and a similar value ($t_{10} = 3.04$). The 17-month-old glass was found to be weaker than the 15-month-old glass at a marginally significant level of $\alpha = 0.07$. The t statistics for σ_{60} and P_{60} are $t_7 = 1.71$ and $t_7 = 1.70$ respectively. Figure 3-3 depicts the decline in glass strength with age.

3.2.1.2 Effect of Edge Conditions on Glass Strength

The effect of edge conditions on breaking strength was investigated using the 17-month-old glass. Six samples were tested in a frame designed to simulate the edge conditions found in a "standard window frame." The edge conditions for a standard window frame were simulated by the selection of inserts holding the glass within the metal frame. Wooden inserts were used to support the glass on all four edges on the low pressure side of the glass; tapered Delrin inserts were used for all edges on the pressurized side. Temperature varied from 67.7°F to 68.8°F during these tests. Relative humidity varied from 40% to 41%. The results of these tests are tabulated in Table 3-4.

Clamped edge conditions were compared with the simulated standard wood frames using a t-test for the σ_{60} and P_{60} values. The result was no statistically significant difference ($t_9 = 0.399$, $\alpha = 0.350$ and $t_9 =$

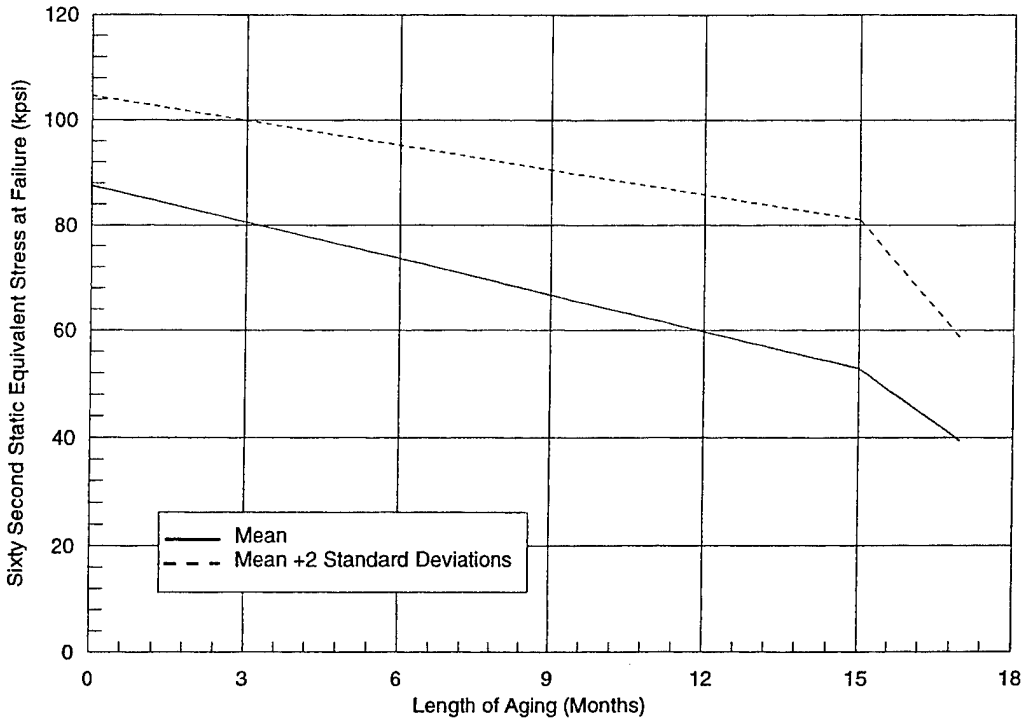

Figure 3-3. Glass Strength *vs.* Age.

Table 3-4. Glass Strength of Panes in Simulated "Standard Wood Frames."

Statistic	All Samples	
	P_{60} (psf)	σ_{60} (kpsi)
Mean	65.8	65.8
Standard Deviation	11.2	11.2
Coefficient of Variation	0.17	0.17
Sample Size	6	

0.378, α = 0.357 respectively).

Anomalous responses were obtained from the panes in the standard wood frames during the calibration effort of the SBTF. The response spectra of the panes were measured as part of the effort to resolve the anomalies. These spectra showed that the tests just described had not achieved their intended purpose because the standard wood frames had produced clamped edge conditions. It was found that the use of

.375 inch wide, .25 inch thick PVC weather-strip as inserts on both sides of the glass produced a simply supported edge condition in response to a simulated sonic boom.

The inserts were modified for use in the static test fixture because of leakage problems. Neoprene inserts were used along all edges on the low pressure side of the glass. Two thicknesses of weather-strip were used along all edges on the high pressure side of the glass. Since the insert on the low pressure side governed whether the glass behaved as if it had clamped or simply supported edges, this treatment produced an edge condition very close to a simply supported condition.

Six panes were tested with these edge conditions. The temperature varied from 68°F to 73.1°F and relative humidity ranged from 47% to 48% during these tests. The pressure loading curve was nearly linear with time for only about five seconds. After that, leakage caused the pressure to grow at a decreasing rate. All of the panes except one failed within a relatively short period of time (approximately 15 seconds). The exceptional pane took approximately forty-five seconds to fail. The sixty-second static equivalent stress for that pane was 10.74 kpsi in comparison to a range of 7.12-9.45 kpsi for the remaining panes. Given the small sample being investigated, calculations were performed with the outlier both included and excluded. The results of these tests are presented in Table 3-5.

Table 3-5. Glass Strength of Panes with Weather Strip Inserts.

Statistic	All Samples		Outlier Omitted	
	P_{60}(psf)	σ_{60}(kpsi)	P_{60}(psf)	σ_{60}(kpsi)
Mean	58.7	8.856	56.0	8.478
Standard Deviation	8.82	1.27	6.55	0.978
Coefficient of Variation	0.15	0.14	0.12	0.12
Sample Size	6		5	

The results of the two sets of tests with weather strip inserts were compared with the results of the tests of glass strength with clamped edges (Table 3-3). The F-test rejected the hypothesis that the σ_{60} variances for the two sets of data were the same at a significance level of $\alpha = 5 \times 10^{-4}$. Consequently, the tests for differences in the mean values of σ_{60} were performed using a t-test for populations with unequal variances as given by equation 3-4 below.

$$t_{df} = \frac{\bar{x}_1 - \bar{x}_2}{\sqrt{S_o}} \qquad (3\text{-}4)$$

where

$$S_o = \frac{s_1^2}{n_1} + \frac{s_2^2}{n_2}$$

$$df = \frac{S_o^2}{\frac{\left(\frac{s_1^2}{n_1}\right)^2}{(n_1+1)} + \frac{\left(\frac{s_2^2}{n_2}\right)^2}{(n_2+1)}} - 2$$

and

$\bar{x}_j$ = j^{th} sample mean

s_j^2 = j^{th} sample variance

n_j = size of sample j

For both the full sample and for the sample with the outlier omitted, the t-statistic supports the alternative hypothesis that a higher level of stress is required to break the glass with clamped edges than with weather strip inserts. In both instances, the level of significance is $\alpha = 9 \times 10^{-4}$ (the respective t-statistics are $t_{4.18} = 7.13$ and $t_{4.13} = 7.23$).

The issue of the relative strength of simply supported and clamped window panes is more commonly interpreted differently than presented above. The usual question is whether it requires a higher pressure to break glass panes with clamped edges or with simply supported edges. When a pressure wave impinges on a glass pane, the resulting pane displacement depends upon both the spectrum of the loading waveform and the response characteristics of the pane. The edge conditions will modify the response characteristics. Thus, for some waveforms and pane sizes a larger peak displacement will occur with clamped edge conditions while with others simply supported edges will produce larger displacements. Generally, a pane with clamped edge conditions will be subjected to a higher maximum stress than a simply supported pane for the same displacement. These stresses will, however, be in different pane locations.

For both the full sample and the sample with the outlier removed, a t-statistic was computed to test the hypothesis that edge conditions did not effect the pressure (P_{60}) required to break the panes, against the alternative hypothesis that the simply supported panes fail at lower overpressures. With the outlier removed, the effect was marginally significant ($\alpha = 0.08$, $t_{5.67} = 1.57$). When the full sample was evaluated, the difference was not statistically significant ($\alpha = 0.12$, $t_s = 1.28$).

3.2.1.3 Effect of Strain Gages on Glass Strength

Another set of panes was tested in "standard wood frames" with strain gages mounted on the panes to test the hypothesis that strain gages caused the panes to fail at lower sixty-second static equivalent stress levels. Two of these tests were regarded as possibly anomalous. Bird droppings were discovered on one pane in the region where the glass failed. Moreover, this pane failed at a substantially lower pressure than the remaining panes. This test was discarded to rule out the possibility that the pane was unrepresentative because of the chemical action of the bird droppings on the glass.

The second potential anomaly was a pane "tested" twice in the static test fixture. The apparatus did not function properly in the first test sequence. A maximum applied pressure of 48 psf was achieved after a period of approximately 200 seconds. This pane was retested and failed at an applied pressure of 67.2 psf after 112 seconds. The concern in retaining this sample was that the initial test might have weakened the pane. The retention of this test in the sample contributes to *raising* the mean failure stress for the sample. Since the purpose of this test sequence was to test the hypothesis that strain gages cause the glass to fail at lower stress levels than otherwise, this test was retained.

Temperature varied from 64.5°F to 66.1°F during these tests. Relative humidity varied from 43% to 46%. Table 3-6 summarizes the results of this test sequence.

Table 3-6. Glass Strength of Panes Instrumented with Strain Gages in Simulated "Standard Wood Frames."

Statistic	Retained Samples	
	P_{60}(psf)	σ_{60}(psf)
Mean	67.8	38.62
Standard Deviation	16.6	8.92
Coefficient of Variation	0.25	0.23
Sample Size	5	

The results for panes tested in standard wood frames with strain gages mounted on the panes (Table 3-6) were compared with those without strain gages (Table 3-3) to test the hypothesis that strain gages caused the panes to fail at lower sixty-second static equivalent stress levels. A t-test rejected the hypothesis that the strain gage weakened the pane ($t_8 = 0.134$, $\alpha = 0.45$). A t-test performed on P_{60} values confirmed this result ($t_8 = 0.118$, $\alpha = 0.45$).

3.2.1.4 Second Baseline for Glass Strength

As a result of budgetary limitations, more than a year elapsed (July 1993 to February 1995) between the time the SBTF was prepared for the planned glass tests and the performance of the first test sequence. During that time period, the BBN facility was subjected to strong ground motion from a nearby earthquake (Northridge Earthquake of January 1994). Although there was considerable damage to other equipment located at the BBN facility, there was no evidence of any damage to the SBTF. Nearly one-third of the panes were broken. Even without the earthquake, the lapse of more than a year since the strength of the glass was measured would have warranted a reevaluation of the strength of the panes.

Although BBN attempted to replicate the test conditions employed by ANCO Engineers in the earlier tests, the BBN tests were characterized by different displacements at the same applied pressures. Consequently, while these tests served their intended function of providing a reference point for all subsequent testing, the static test results from the BBN tests should not be compared with the ANCO Engineers test results.

Twelve panes were tested with clamped edge conditions. The temperature varied between 70°F and 72°F during these tests; the relative humidity range was 46% to 52%. The results of these tests are given in Table 3-7.

3.2.1.5 Sonic Boom Test Facility Survivor Tests

The experimental design was structured so that every pane tested in the SBTF (SBTF) could provide information related to glass fatigue failure. The number of booms to failure and the peak overpressure would characterize those panes that broke during SBTF testing. Residual strength would characterize the survivors.

Table 3-7. Second Baseline for Glass Strength.

Statistic	All Samples	
	P_{60}(psf)	σ_{60}(kpsi)
Mean	62.38	41.81
Standard Deviation	16.07	16.69
Coefficient of Variation	0.26	0.40
Sample Size	12	

Survivors of the simulated sonic boom tests at an applied pressure of 16 psf were tested for residual strength using the same procedures as were applied for the second baseline tests. These tests were

performed at 70°F within a relative humidity range of 48% to 51%. The results of these tests are tabulated in Table 3-8.

Table 3-8. Residual Strength of Panes Surviving SBTF Tests at 16 psf.

Statistic	All Samples	
	P_{60}(psf)	σ_{60}(kpsi)
Mean	66.02	42.82
Standard Deviation	12.31	10.8
Coefficient of Variation	0.19	0.25
Sample Size	6	

A comparison of Tables 3-7 and 3-8 shows that the survivors are characterized by no change in the mean strength but a reduction (not statistically significant) in the standard deviation. An F-test indicates that the reduction in standard deviation is not significant ($\alpha = 0.35$). A t-test confirms that the differences in means is not significant ($t_{16} = 0.133$, $\alpha = 0.45$). The reduction in the standard deviation is probably a result of eliminating the weaker samples by the SBTF tests.

3.2.2 Fatigue Tests

The fatigue tests were designed around the following premises:

- If glass exhibits fatigue characteristics, it should be more evident at stress levels just below the mean failure stress than at lower stress levels.
- A practical evaluation of glass fatigue for application to sonic boom damage assessment should consider a number of load cycles comparable to the largest number of sonic boom load cycles a real window might experience.
- If glass fatigues but a particular pane does not fail during the fatigue test, the residual strength of the pane should be less than it was at pretest.

The White Sands tests (Sutherland *et al.*, 1990) estimated 219 to be the maximum number of booms per year to which a location in a Supersonic Operating Area would be subjected. Over a design life of fifty years, a window in such a structure might be subjected to 10,950 sonic booms. The fatigue tests were designed to apply up to 259,200 load cycles to each pane. The results of the fatigue tests are summarized

in Table 3-9. Notice that this table lists values of peak stress and sixty-second static equivalent stress for both positive and negative displacements. Since these affect opposite surfaces of the pane, the larger stress value will govern failure.

In order to increase the sensitivity of the tests, the strength of each pane subjected to a fatigue test was estimated by performing a static test of a pane cut from the same piece of glass. This procedure was discontinued after test number 40, because it was found that the strength of the matched pane provided no indication of the strength of the pane being used for the fatigue test. This result indicates that the variation in strength of the aged panes was dominated by variations in surface flaws developed during aging rather than flaws introduced during the initial production of the panes.

A total of seventeen panes were tested in the fatigue fixture. The results of two tests (29 and 38) were discarded as unreliable because of test fixture failures during these tests. The last four tests (42, 43, 44 and 45) were performed using a modified test facility. In an effort to overcome difficulties in setting the peak pressure in the chamber to the specified pressure, the AC motor used to drive the movement of the back of the chamber was replaced with a DC motor. This had the effect of eliminating a small initial overshoot in chamber pressure and substantially increasing the time required to increase the chamber pressure to the specified level. The results of these four tests are widely scattered for the same nominal test condition. One pane failed after 169 seconds while another survived 65 hours of testing. As a result of this large data scatter and the changed procedure, these tests were also discarded as not valid. This left eleven valid tests.

Five panes out of the eleven valid fatigue tests survived the test without any apparent damage. Moreover, a review of the residual strength data suggested that the residual strength of the surviving panes was greater than the strength of panes that had not been subjected to fatigue tests. Thus, the statistical evaluation of the data was based on testing the null hypothesis of no difference of the mean strength against an alternative hypothesis that the residual strength of the panes was *greater* than the strength of panes not subjected to fatigue tests.

Two techniques were used to evaluate the effect of the fatigue tests. A t-test for comparing the means of paired samples was performed using the three pairs of panes (fatigue tests 34-36), for which both residual strength data and the strength of the paired pane were available. The following statistic was evaluated

$$t_{df} = \frac{\bar{d}}{S_o / \sqrt{n}} \tag{3-5}$$

where

$$S_o = \sqrt{\sum_{i=1}^{n} \frac{(d_i - \bar{d})^2}{n-1}}$$

$$df = n - 1$$

$$d_i = x_{1_i} - x_{2_1}$$

$$\bar{d} = \frac{1}{n} \sum_i d_i$$

and

$$n = \text{number of pairs}$$

This test is marginally statistically significant. It indicated that the panes subjected to the fatigue tests were stronger than their paired counterparts at a significance level of $\alpha = 0.075$ ($t_2 = 2.281$). Because we had proven that the paired panes strength provided no information regarding the strength of their counterparts, a second test was performed using all of the panes tested as matched panes (eleven panes) as the reference group and all of the panes that survived fatigue testing (five panes) as a second group. This test showed survivors of the fatigue tests were stronger than the reference group at a significant level of $\alpha = 0.017$ ($t_{14} = 2.346$). It is probable that the observed increase in strength resulted from eliminating weaker panes from the sample.

Figure 3-4 depicts a plot of peak stress as a function of the number of cycles to failure. (The larger of the peak positive or peak negative stress is plotted.) The figure depicts both the panes that failed and those that survived 24 hours of testing. The failed panes show a classical fatigue curve with an endurance limit (fatigue limit) of approximately 9.5 kpsi, which occurred at around 2,700 cycles. A regression analysis was performed of peak stress σ_{pk} against the logarithm of the number of cycles, N. The resulting fit was

$$\sigma_{pk} = 63.91 - 15.99 \log N \qquad (3\text{-}6)$$

Table 3-9. Summary of Fatigue Test Results.

Test Number*	Peak Stress		σ_{60}	σ_{60}	Time to First Failure (sec)	Comments	Time to Ultimate Failure (sec)	Static	Tests
	Positive Displacement) (kpsi)	Negative Displacement (kpsi)	(Positive Displacement) (kpsi)	(Negative Displacement) (kpsi)				Matched Pair σ_{60} (kpsi)	Residual Strength σ_{60} (kpsi)
28	13.73	12.75	14.21	11.95	415	Crack between bolts. *OK*	715	41.83	---
29	13.81	12.09	15.38	13.29	3120	Additional cracks: 13920 s, 14160 s, 17520 s, Stopped @ 5h 45m (20700s). Tie down bolts failed. *Bad*	21000	30.26	---
31	18.48	12.52	13.38	11.62	275	*OK*	275	40.42	---
32	16.47	9.96	15.33	9.15	278	*OK*	278	45.00	---
33	3.75	3.46				Survived 24 h *OK*		None	45.29
34	3.61	3.58				Survived 24 h *OK*		40.71	60.13
35	3.39	3.79				Survived 24 h *OK*		44.31	53.31
36	3.01	4.21				Survived 24 h *OK*		44.65	48.16
37	7.53	9.31	7.81	9.42	900	Crack between bolts. *OK*	3862	51.20	---
38					35100	Crack between bolts. Stopped @ 9h 50 m. Gasket *failed* before 8.5 h *Bad*		46.32	36.14
39	9.12	7.40	12.18	9.98	37936	Large fragments at failure, *i.e.*, low stress. *OK*	37936	31.28	---
40	9.77	7.00	11.74	8.46	11020	Large fragments at failure, *i.e.*, low stress. *OK*	11020	51.22	---
41	9.62	7.13				Survived 24 h *OK*		None	47.18
42	11.96	11.98	10.37	10.32	169	Performed With Modified Test Fixture. *Not Valid*	169	None	---
43						Survived 65 h 41 m. Performed with Modified Test Fixture. *Not Valid*		None	Not Evaluated
44						Survived 30 h. Performed with Modified Test Fixture. *Not Valid*		None	Not Evaluated
45	13.41	11.52	15.95	13.71	9330	Performed With Modified Test Fixture. *Not Valid*	9330	None	---

* Pane number 30 was unsuitable for testing because of a crack in the corner of the pane; the matched pane for test 33 was unsuitable for testing as a result of a chipped corner.

The null hypothesis of a zero slope was evaluated using a t-test and rejected at a significance level of $\alpha = 0.03$. This supports the observation that fatigue was observed. Similarly, a regression was performed on the three points along the fatigue limit. The resulting fit was

$$\sigma_{pk} = 9.54 - 0.03 \log N \tag{3-7}$$

As might be expected, in this case the t-test of the null hypothesis of zero slope had a significance level of $\alpha = 0.95$. In other words, it is probable that there is no dependence of peak stress on log N.

An alternative interpretation of the data is given by the sixty-second static equivalent stress, σ_{60}. Assuming that the larger of the values tabulated for positive and negative displacement governs failure, we can calculate the statistics for σ_{60} for the valid fatigue tests. The mean value of σ_{60} is 12.71 kpsi, the standard deviation is 2.08 kpsi, and the coefficient of variation is 0.16. This suggests that σ_{60} is a good characterization of the stress history required to produce failure in these tests.

3.3 SONIC BOOM TEST FACILITY TESTS

Tests in the SBTF were performed between January and June 1995. In contrast to the fatigue test facility, which produced peak test (and net) pressures on the order of 50 psf, the maximum achievable applied peak pressure in the SBTF was 16 psf and the maximum net pressure was 15 psf. (The fatigue facility operated in an open room; thus, the net and applied pressure were the same. The SBTF is a closed chamber. The air behind the window is compressed by the window deflection, resulting in a smaller net pressure than the applied pressure.)

Two sets of tests were performed in the SBTF. In the first set of tests, sets of aged glass panes were subjected to sequences of 5,000 sonic booms at applied pressures of up to 16 psf. Even at 16 psf, no evidence of fatigue was observed. This result was consistent with the observation based on the fatigue tests that, in the absence of surface damage, the fatigue of glass would not be expected at sonic boom test pressures. It was speculated that if the glass could be sufficiently weakened, evidence for fatigue under sonic boom loads would be observed. Specimens for the second set of tests were weakened, as described earlier, by scribing an "X" along the diagonals of the glass panes. As expected, these tests did provide evidence for fatigue under sonic boom loads.

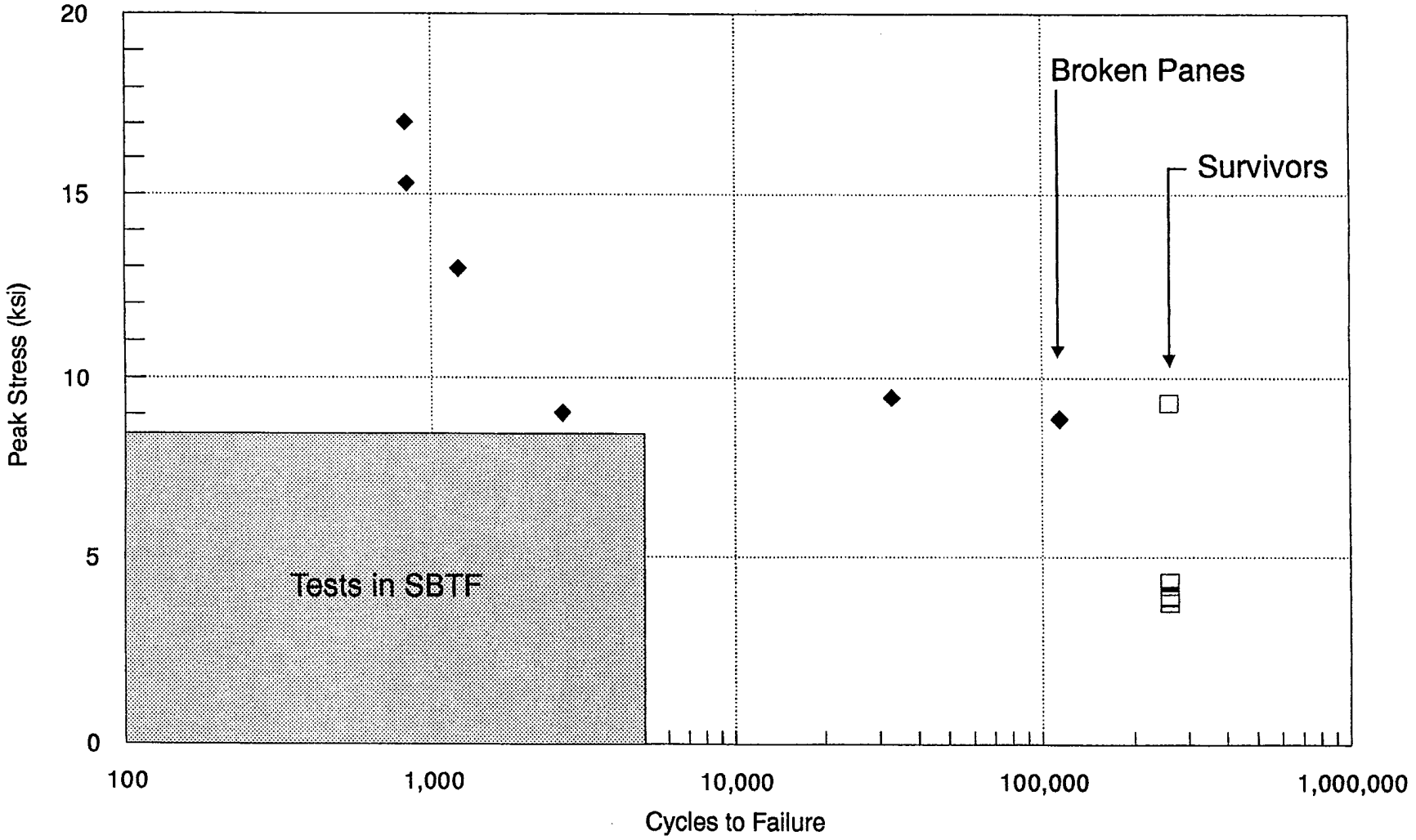

Figure 3-4. Peak Stress *vs.* Time to First Failure.

The results of tests of the scribed glass showed that damaged glass is significantly more vulnerable to fatigue damage and, in particular, to potential for sonic boom contributions to fatigue damage. Thus, while sonic-boom-induced fatigue is not expected to be a problem for glass in good condition, it may increase the probability of sonic boom damage to glass that is precracked, has had its surface abraded by wind-borne sand, or is otherwise significantly weakened.

Temperature and relative humidity inside the SBTF were monitored during all tests since the propagation of surface flaws and failure is affected by temperature and relative humidity settings. Glass strength is less sensitive to changes in relative humidity at high relative humidity than at dry conditions. It is also more vulnerable to damage. To minimize the variation in test results due to relative humidity and to maximize the observable damage, tests were performed at moderately high levels of relative humidity. For all SBTF tests, the temperature changed by no more than 3°F, ranging from 68.79°F to 71.75°F. Relative humidity varied from 59.26% to 59.84%. Table 3-10 summarizes the average values of environmental data for the tests.

Table 3-10. Average Temperature and Relative Humidity During SBTF Testings.

Test Sequence	Temperature (°F)	Relative Humidity (%)
Aged glass at 16 psf	71.09	59.68
Aged glass at 12 psf	71.13	59.46
Aged glass at 14 psf	69.63	59.57
Aged flawed glass at 16 psf	72.07	60.48
Aged flawed glass at 12 psf	71.23	59.95
Aged flawed glass at 14 psf	72.82	59.97

3.3.1 Aged Glass

All tests performed in the SBTF used .375 inch wide, .25 inch thick PVC weather strip inserts on both sides of the glass to produce a simply supported edge condition. Test sequences were performed at three different overpressure levels. During the first sequence, eight panes were tested at an applied pressure of 16 psf. Two panes were broken during this sequence. During the second test sequence, twelve panes were tested at an applied pressure of 12 psf. All twelve panes survived these tests. During the final sequence, twelve panes were tested at an applied pressure of 14 psf. One pane broke during this sequence. Results of these tests are summarized in Table 3-11.

Table 3-11. SBTF Test Results for Aged Good Glass.

Peak Pressure (psf) Applied/Net	Test Groups	Panes Tested	Panes Failed	Test Group in Which Failure Occurred	Booms to Failure
16/15	1 - 4	8	2	1	4850
				2	3638
12/10.5	3 - 5	12	0	N/A	N/A.
14/12	6 - 8	12	1	8	2571

The following hypotheses were evaluated for these tests:

1. Peak overpressure affects the number of sonic boom exposures required to produce a pane failure.

2. Peak overpressure affects the probability of a pane failing.

3. Cumulative damage occurred during the course of the tests.

3.3.1.1 Effect of Peak Overpressure on Number of Booms to Failure

The effect of peak overpressure on the number of booms to failure was evaluated by comparing the test data for the 16 psf tests with those for the 14 psf tests. Since the mean number of booms to failure was *larger* for the 16 psf tests than for the 14 psf tests, it was anticipated that the alternative hypothesis of increased pressure producing decreased number of booms to failure would not be supported. A t-test was performed (assuming unequal variances) to evaluate this hypothesis. As anticipated, the data did not support the alternative hypothesis ($t_{18} = 0.0509$, $\alpha = 0.47997$).

3.3.1.2 Effect of Peak Overpressure on Probability of a Pane Failing

As a second measure of the effect of peak pressure, the null hypothesis that pressure has no effect on the probability of panes breaking was evaluated against the alternative hypothesis that the probability of panes breaking is greater at 16 psf than at 14 psf. Since the point estimate of the glass failure probability at 16 psf was 0.25 while the point estimate at 14 psf was only 0.083, there was some expectation that the data might support the conclusion of a pressure effect.

The Fisher Exact Probability[1] test was performed to evaluate this hypothesis. This test did not support the rejection of the null hypothesis (α = 0.295). A more powerful modification of this test attributed to Tocher was performed. This also failed to reject the null hypothesis that peak pressure does not affect the failure probability.

In summary, the data from the SBTF tests do not statistically support any effect of pressure on failure probability of the panes or the number of sonic booms required to produce failure of a pane.

3.3.1.3 Cumulative Damage

The failure of the three panes late in the testing sequence is consistent with cumulative damage. Three failures, however, is an insufficient sample to develop any statistical inference.

When the frames were opened, it was discovered that there was a large accumulation of glass dust along the lower edge of the glass pane. This suggests the possibility that, during the course of testing, the glass pane shifted so that the lower edge was in contact with the aluminum frame. If this happened, each subsequent sonic boom would cause the edge of the glass to rub against the metal, abrading the glass and introducing edge flaws into the pane. The edge/corner flaws and stresses introduced this way may be the cause of the ultimate failure of these panes.

The surviving panes from the 16 psf tests were tested in the static test facility to determine if the SBTF tests had weakened them. The mean residual strength for surviving panes in the 16 psf test was 42.8 kpsi with a standard deviation of 10.8 kpsi. Only the statistics for this sequence are available. Because these tests did not provide any useful information, no further survivor tests were performed.

3.3.2 Flawed Glass

Eight test groups consisting of four flawed panes each were tested. Flawed surfaces were always placed facing away from the pressurized plenum. The test results are summarized in Table 3-12. The first four groups were tested at applied test pressures of 16 psf. All sixteen panes broke within the first four hundred sonic booms. In test groups 9 and 11, panes failed in pairs. In both cases the pane in the upper right hand corner and the pane in the lower left hand corner broke on the same boom. The remaining two panes also broke together, but tens of booms later. (In test group 9, 27 booms separated the failure of the first and second pairs of panes. In test group 11, 48 booms separated the failures.)

When test group 9 was completed, there was concern that the sets of double failures might indicate that somehow failure of one pane was causing the failure of the second pane. The pressure, displacement, and acceleration time histories were reviewed for evidence of any relationship between the failures. The

[1] Siegel, S., Nonparametric Statistics for the Behavioral Sciences, 1956, pp. 96-104.

interior room pressure time histories for the booms on which the failures occurred (booms 30 and 57) were compared with the time histories for two other booms (booms 29 and 30). The first deviation occurred at approximately 0.15 seconds for both booms 30 and 57. This time was tentatively identified as the time of the failure of the first pane. The time of failure occurred shortly after the peak positive interior room pressure. On boom 57, the second pane to fail was instrumented with the LVDT. At approximately 0.23 seconds, the LVDT trace became irregular, indicating failure of the pane. It was more difficult to identify the time of failure for the second pane on boom 30. The only instrumental data available to support this identification was from the accelerometer mounted in the center of the lower edge of the metal frame. At approximately 0.235 seconds, the accelerometer on the frame of the failed pane began to deviate significantly from its response on other booms, and from the response of the accelerometers on the frames of the other panes on boom 30. This was our best estimate of the time of failure. The time of failure for the second set of panes occurred near the second positive peak of the interior room pressure.

The positive pressure peaks for the interior room corresponded closely to peak displacement in the direction away from the loudspeakers. Thus, the pane failures had the following characteristics:

(1) They occurred when the flawed surface of the pane was in tension.

(2) They occurred close to the time of a maximum level of stress in the flawed surface.

Figure 3-5 compares displacement time histories for typical booms with that of boom 30 (a boom involving failure of panes other than the one instrumented with the LVDT). The displacement time history for the boom involving a failure differed from the other time-history in three notable ways:

(1) The initial peak negative displacement and all subsequent negative displacements were slightly larger than they were for the reference sonic boom.

(2) The second and subsequent positive displacements were somewhat larger than for the reference boom.

(3) Peak pane velocity was somewhat larger than for the reference boom.

Since the second peak positive displacement was less than the initial peak positive displacement, the effect of the greater displacement was, at most, one additional sonic boom. The increase in peak pane velocity, as depicted in this figure, also appears to be a small contributor to the increased accumulated stress to which the panes were subjected. This would suggest that failure of the first pane was not sufficient to cause failure of a second pane on the same boom unless the second pane was on the threshold of failure. Nevertheless, the possibility of the first failure contributing to the second failure cannot be totally ruled out. As a result, analysis of the failure data was based on two alternative assumptions: (1) the second

pane failing in a double failure was a bad data point and must be discarded and (2) the second pane failing was a valid data point.

As for the aged glass, the following hypotheses were evaluated for flawed glass:

1. Peak overpressure affects the number of sonic boom exposures required to produce a pane failure.

2. Peak overpressure affects the probability of a pane failing.

3. Cumulative damage occurred during the course of the tests.

All statistical tests were performed twice—once for the full 16 psf sample and the second time excluding the second panes to fail on booms producing two-pane failure.

3.3.2.1 Effect of Peak Overpressure on Number of Booms to Failure

The effect of peak overpressure on the number of booms to failure was evaluated by comparing the test data for the 16 psf tests with that for the 14 psf tests. These tests were compared using the randomization test for two independent samples.[2] Let n_1 be the number of failures at 16 psf and n_2 be the number of failures at 14 psf. If there is no pressure effect, then the number of outcomes of booms to failure can be assigned to the failures in $\binom{n_1+n_2}{n_1}$ ways. Under the null hypothesis of no effect, there is only one way that the n_2 largest number of booms to failure would occur for the 14 psf tests, and the other n_1 remaining booms would occur at 16 psf. If α is the significance level, then the region of rejection of the null hypothesis consists of the $\alpha \binom{n_1+n_2}{n_1}$ most extreme of the possible occurrences. In other words, if the observed sample is one of the $\alpha \binom{n_1+n_2}{n_1}$ most extreme possible occurrences, then the null hypothesis is rejected at the α significance level.

Using the complete set of tests, the hypothesis of no pressure effect is rejected at the level $\alpha = 0.0065$. With the reduced sample resulting from eliminating the second panes to fail on booms with double failures, the hypothesis of no effect is rejected at the level $\alpha = 0.011$. Thus, both cases support the alternative hypothesis that the number of booms to failure is greater at 14 psf than at 16 psf.

[2] Siegel, S., Nonparametric Statistics for the Behavioral Sciences, 1956, pp. 152-156.

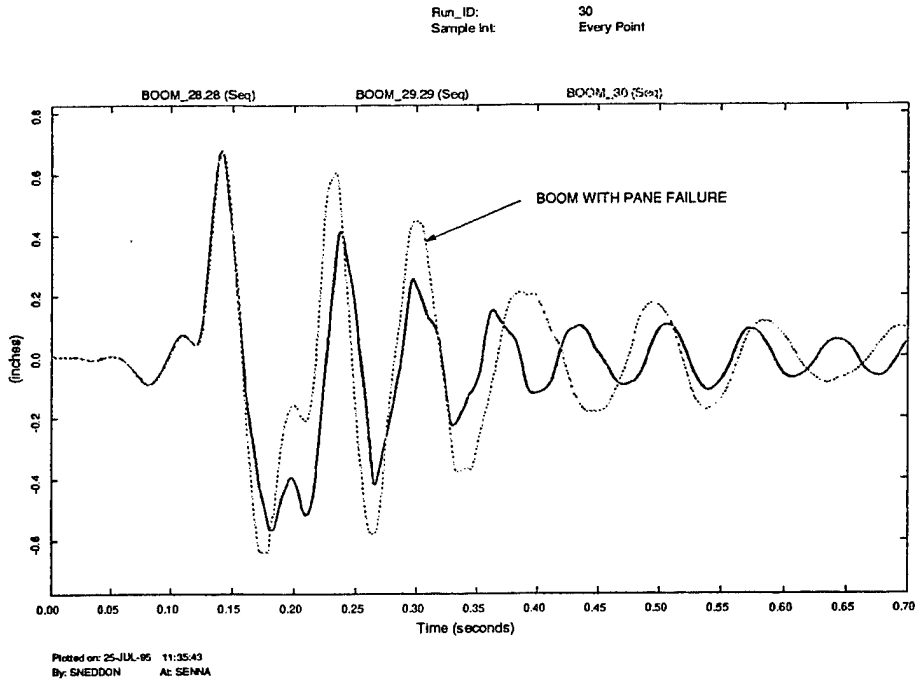

Figure 3-5. Pane Center Deflection Time Histories: Typical Booms *vs.* Boom with Pane Failure.

Table 3-12. SBTF Test Results for Flawed Glass for a Test Sequence of 5,000 Booms.

Peak Pressure (psf) Applied/Net	Test Groups	Panes Tested	Panes Failed	Test Group in Which Failure(s) Occurred	Booms to Failure
16/15	9-12	16	16	9	30*, 57*
				10	49, 126, 200, 232
				11	78*, 126*
				12	115, 154, 201, 371
12/10.5	13	4	0	N/A	N/A.
14/12	14-16	12	2	14	2,018
				16	3,865

*Two panes broke during the same boom

3.3.2.2 Effect of Peak Overpressure on Probability of Pane Failing

As a second measure of the effect of peak pressure, the null hypothesis that pressure has no effect on the probability of pane failure was evaluated against the alternative hypothesis that the probability of panes breaking is greater at 16 psf than at 14 psf.

The Fisher Exact Probability test referenced in the previous section was used for this calculation. For the full sample, the hypothesis of no difference was rejected at a significance level of $\alpha = 5 \times 10^{-6}$. When the second panes to fail on a boom were eliminated from the sample, the significance level "dropped" to $\alpha = 3 \times 10^{-5}$.

In summary, the SBTF test data for flawed panes strongly support the conclusions that (1) the peak pressure increase from 14 to 16 psf reduced the number of booms required to break a pane and (2) the peak pressure increase from 14 to 16 psf increased the probability of a pane breaking in the SBTF tests.

3.3.2.3 Cumulative Damage

Two approaches were used for investigating whether the SBTF tests supported cumulative damage, as described below.

If there had been no cumulative damage effects, all failures during the 5,000 simulated sonic booms would have occurred randomly, and, hence, would have fit a Poisson distribution. Thus, the number of sonic boom events to failure, N, would have had an exponential distribution given by

$$P(N) = 1 - e^{-\frac{N}{N_a}} \tag{3-8}$$

where N_a is the average number of cycles-to-failure for the M sample values, and P(N) is the fractional portion of the items that would fail in N cycles.

The existence of cumulative damage was evaluated using a "goodness-of-fit" test of the cycles-to--failure (N) against the hypothesis that the data had an exponential distribution as defined above. In other words, a rejection of the exponential distribution hypothesis would suggest that a cumulative damage mechanism was involved. This evaluation was accomplished using the Kolmogorov-Smirnov[3] goodness-of-fit test as follows:

1. Calculate the cumulative distribution of observed booms to failure, S(N).

2. Calculate the cumulative distribution under the hypothesis of Poisson distribution, P(N).

[3] Siegel, S., Nonparametric Statistics for the Behavioral Sciences, 1956, pp. 47-52.

3. Determine the maximum value of $D=|P(N) - S(N)|$

4. The full sample consisted of 16 failures at 16 psf. For the full sample, D = 0.88. The critical value of D for a sample size of 16 and a significance level $\alpha = 0.01$ is $D_{0.01} = 0.392$.

Thus, the full sample had less than 1% chance of being from a Poisson distribution. For the reduced sample (12 failures at 16 psf), D = 0.92. The critical value of D for a sample size of 12 and a significance level $\alpha = 0.01$ is $D_{0.01} = 0.490$. This confirmed the conclusion drawn for the larger sample.

The second approach used to demonstrate the occurrence of cumulative damage was to perform a regression of the applied load, P, against the logarithm of the number of booms to failure, N. When the full sample was used, this gave the relationship

$$P = 17.90 - 0.979 \log N \tag{3-9}$$

A t-test was performed to evaluate the null hypothesis of zero slope. This hypothesis was rejected at a significance level of $\alpha = 1 \times 10^{-5}$. A regression performed on the sample remaining after deleting the second panes to fail on a boom gave similar results. The estimated fit is given by

$$P = 18.15 - 1.078 \log N \tag{3-10}$$

The null hypothesis of zero slope was rejected at a significance level of $\alpha = 7 \times 10^{-5}$.

3.4 PRECRACKED PANES

The fatigue tests and the tests in the SBTF suggest that cumulative sonic boom damage to glass is a significant factor only when the sonic boom load is a significant fraction of the load required to damage a pane from a single boom. These conditions might be expected for precracked panes or severely weathered or chemically etched panes.

Appendix B describes in some detail a theoretical investigation of the strength of precracked glass and of its susceptibility to cumulative damage from repetitive sonic booms. The following are the key findings from this investigation:

(1) The assertion by Hershey and Higgins (1973) that precracked glass average strength is one-tenth that of aged glass and that both glass populations have the same variance is a poor description of the strength of precracked glass.

(2) The strength of precracked glass depends on the size, location and orientation of the cracks. Cracks located in high stress regions, normal to the principal stress, have the greatest effect on reducing pane strength.

(3) Cumulative damage from repetitive sonic booms will contribute to the failure of precracked panes. The damage contribution is important for booms with peak overpressures that are a significant fraction of the level required to break the pane on a single boom.

(4) The contribution of wind loads to cumulative damage is significant only for the most vulnerable panes. Statistics for White Sands Missile Range suggest that high wind pressures occur infrequently. Local conditions such as terrain or the presence of other structures may increase the frequency of higher wind overpressures.

3.5 SUMMARY

This study achieved its primary objective of establishing whether or not sonic boom loads can, as a result of a fatigue mechanism, produce cumulative damage to windows. Repetitive sonic booms can produce cumulative damage only when their overpressure levels are a significant fraction of the overpressure required to produce damage from a single sonic boom. Given the range of overpressures typical of a Supersonic Operating Area, these conditions occur only when the windows in question are substantially weaker than ordinary panes. Such conditions would include precracked panes and panes that have been substantially weakened by chemical corrosion or wind-borne abrasive material. The following paragraphs highlight additional findings.

Quantitative results were developed showing that aged glass is weaker than new glass. New glass strength was compared with the strength of panes after fifteen months and after seventeen months of exposure to atmospheric loads and weathering.

No statistically significant differences were observed between the baseline strength of glass panes and that of panes surviving repetitive loading (in either the fatigue tests or the SBTF tests). These tests seem to have eliminated weaker panes, leaving a slightly stronger (not statistically significant) population of survivors.

Other investigators have compared the overpressures required to break glass windows with different edge conditions. A 1962 Canadian study using shock tubes (Murihead *et al.*, 1962) reported that "loosely mounted" glass required substantially higher overpressures to break windows than those required for windows with clamped edges. This contrasts with the earlier, more comprehensive study by Arde Associates (1959) that correctly argued that the sensitivity to shock waves depended on the dynamic response to the particular waveform and the stresses generated by the pane response. As a result, the required failure pressure to break identical panes with different edge conditions depended on the particular waveform and the pane dimensions. In some instances, a pane requires larger applied pressures to break with simply supported edges. Under other conditions, clamped edge conditions require larger applied pressures.

This study evaluated the failure of simply supported and clamped panes under quasi-static (ramp) loading. Calculated sixty-second static equivalent stress failure was greater for panes with clamped edges than for simply supported panes. (The maximum stress in a pane with clamped edge conditions occurs in the middle of the pane edges. When the pane undergoes large deflections, the maximum stress is in the corners of the panes). The sixty-second static equivalent pressure at failure is also smaller for simply supported panes than for panes with clamped edges.

As noted in Appendix A, the SBTF was used to investigate the response of double-glazed windows to sonic booms. The measured displacements were approximately one-half that measured for a single pane. Therefore, damage to double-glazed windows may be expected to require approximately twice the overpressure required to damage single panes (when the total pane thickness of the double-glazed pane is twice the thickness of the single glazed pane).

Current ASAN sonic boom window damage models are dominated by the modeled capacity of precracked glass. Appendix B presents calculations demonstrating that the statistics currently employed in the glass strength model for precracked glass are inadequate.

4 GLOSSARY

Accelerometer	An instrument for measuring acceleration.
A/D Converter	A device for transforming an analog signal (a voltage proportional to a quantity of interest) to a digital signal (a discrete encoded representation of the magnitude of the quantity of interest).
Aliasing	The masquerading of higher frequencies as lower frequencies when a signal is sampled at too low a frequency.
Cumulative Damage	Reduced capacity from multiple sonic booms.
D/A Converter	A device for transforming a digital signal to an analog signal.
Damage	The word damage is used to refer to the fracture failure of glass panes. This includes crack formation, crack extension, shattering, and total breakage.
Fatigue	A progressive weakening of, or damage to a material ultimately resulting in failure.
Finite Element Analysis	A mathematical modeling technique involving the decomposition of the object being studied into a number of convenient geometric shapes, defining known loading, boundary conditions and constraints, and iterating until all conditions are satisfied.
Frequency Response Function	A mathematical relationship that depicts the variation in the ratio of output signal to input signal with frequency.
Low-Pass Filter	An electronic circuit or a mathematical algorithm that eliminates the high frequency content of a signal while allowing the low frequency content to pass undisturbed.
N-Wave	The characteristic waveform for sonic booms generated by an aircraft. The name is derived from the appearance of a time history of the sonic boom overpressure.
Overpressure	Pressure in excess of atmospheric pressure.

Principal Stresses	In a stressed object, one can orient three mutually perpendicular planes so that the stresses on each are either purely normal, tension or compression. The stresses on these planes are the principal stresses. One of the stresses will be the maximum at a point and one will be the minimum at that point.
Radius of Curvature	The radius of a circle that approximates a curve at a point of interest.
Resonance Frequency	The frequency corresponding to the fundamental period of an object. When a periodic disturbing force is applied to an object at its resonance frequency, the response of the object increases substantially relative to its response to a periodic disturbing force at other frequencies.
Shear	Deformation in a manner conducive to tearing.
Sixty-Second Static Equivalent Strength (Overpressure)	Because glass strength varies with the duration of a load, overpressure measurement from each testing sequence is normalized to an equivalent uniform constant stress (pressure) which would cause failure in 60 seconds.
Spectral Analysis	One of several mathematical techniques for representing a time series in terms of periodic function (typically, sines and cosines). As used in this report, the term refers to a determination of the "energy content" by frequency of a time history.
Strain	Forced change in the dimensions of a body typically referring to an elongation per unit length.
Stress	Internal force exerted by two adjacent parts across an imagined plane of separation. Shear stress resists the tendency of the parts to slide past each other, compressive stress resists the tendency of the parts to approach each other, and tensile stress resists the tendency of the parts to separate under the action of an applied load. Frequently, stress will be used to refer to stress-per-unit area.

Sonic Boom Simulators

Devices for replicating the characteristics of sonic booms. Several technologies have been used for this purpose. Loudspeaker systems employ one or more loudspeakers to simulate the sound of a sonic boom. Piston-driven systems compress and rarify the gas within a chamber to simulate a sonic boom. Shock-tube driven systems puncture a diaphragm resulting in the abrupt release of pressurized air to generate shock waves that propagate down a horn to a specimen. Air modulator valve systems are similar to shock-tubes except that the diaphragm is replaced by a high-speed flow valve. Explosive charge systems use (multiple) explosive line charges to simulate a sonic boom N-wave.

This page intentionally left blank.

5 REFERENCES

Arde Associates (1959). "Response of Structures to Aircraft Generated Shock Waves," WADC Technical Report 58-169, Wright-Patterson Air Force Base, Dayton, Ohio.

Beason, W.L. (1980). "A Failure Prediction Model for Window Glass," Texas Tech University College of Engineering Institute for disaster Research Report No. NSF/RAE-800231, Lubbock, Texas.

Brown, W.G. (1974). "A Practical Formulation for the Strength of Glass and Its Special Application to Large Plates," National Research Council of Canada, Publication No. NRC 14372, Ottawa, Canada.

Charles, R.J. (1958). "Dynamic Fatigue of Glass," J. Applied Physics, 29[12], pp. 1657-1662.

Charles, R.J. (1958). "Static Fatigue of Glass," Vol. I, J. Applied Physics, 29[11], pp. 1549-1553.

Charles, R.J. (1958). "Static Fatigue of Glass," Vol. II, J. Applied Physics, 29[11], pp. 1554-1560.

Crandall, S.H., & L. Kurzweil (1968). "On the rattling of windows by sonic booms," J. Acous. Soc. Am., 44[2].

Glass Research Laboratory (1986). "Evaluations of Fracture Patterns, Fallout Patterns, and Lacerative Hazards Presented by Window Glass Broken by Low-Level Blast Waves," Texas Tech University, Lubbock, Texas.

Glass Research Laboratory (1989). "Additional Tasks: Window Glass Subjected to Low-Level Blast Waves," Texas Tech University, Lubbock, Texas.

Haber, J., & D. Nakaki (1985). "Sonic Boom Damage to Conventional Structures," Report No. HSD-TR-89-001, Canoga Park, CA, BBN Systems and Technologies Corporation.

Hershey, R., & T. Higgins (1973). "Statistical Prediction Model for Glass Breakage from Nominal Sonic Boom Loads," Booze, Allen Applied Research, Report No. FAA-RD-73-79, Bethesda, Maryland.

Kao, G., (1970). "An experimental study to determine the effects of repetitive sonic booms on glass breakage," Report No. FAA-NO-70, Huntsville, AL: Wyle Laboratories.

Levengood, W.C. (1958). "Effect of Origin Flaw Characteristics on Glass Strength," J. Applied Physics, 29[5], pp. 820-826.

McLellan, G., & E. Shand (1984). Glass Engineering Handbook, Third Edition, McGraw Hill Book Company.

Michalske, T., & S. Freiman. "A molecular interpretation of stress corrosion in silica," Nature, 295[5849], pp. 511-512.

Michalske, T., & B. Bunker (1984). "Slow fracture model based on strained silicate structures," J. Applied Physics, 56[10], pp. 2686-2693.

Minor, J., W. Beason, & P. Harris, (1978). "Designing for Windborne Missiles in Urban Areas," J. Structural Division, No. 14143, *Am. Soc. Civil Engineers*, pp. 1756-1757.

Murihead, J.C., W.A. Jones, & W.M. McMurty (1962). "On the Hazard of Shock Wave Damage to Window Glass," Suffield Technical Paper No. 268, Suffield Experimental Station, Ralston, Alberta.

Reed, D. A., & E. Simiu (1983). "Wind loading and strength of cladding glass," NBS Building Science Series 154, Washington, D.C.: Center for Building Technology, NBS.

Shand, E.B. (1965). "Strength of Glass—The Griffith Method Revised," J. Am. Ceramic Soc., 48[1], pp. 43-49.

Shand, E. (1954). "Experimental Study of Fracture of Glass," J. Am. Ceramic Soc., 37[12].

Siegel, S. (1956). Nonparametric Statistics for the Behavioral Sciences, McGraw Hill, New York.

Simiu, E., D. Reed, C. Yancey, J. Martin, E. Hendrikson, A. Gonzalez, M. Koike, J. Lechner, & M. Batts (1984). "Ring-on-Ring Tests and Load Capacity of Cladding Glass," NBS Building Science Series 162, U.S. Dept of Commerce, National Bureau of Standards.

Spinner, S. (1956). "Elastic Moduli of Glasses at Elevated Temperatures by a Dynamic Method," J. Am. Ceramic Soc., 39, pp. 113-118.

Sutherland, L.C., R. Brown, & D. Goerner (1990). "Evaluation of potential damage to unconventional structures by sonic booms," Report No. WR 89-14, El Segundo, CA: Wyle Research.

Turner, R., & C. Keley Hill (1982). "Terrestrial Environmental (Climactic) Criteria Guidelines for Use in Aerospace Vehicle Development, 1982 Revision," NASA Technical Memorandum 82473.

White, R.W. (1972). "Effects of repetitive sonic booms on glass breakage," Report No. FAA-RD-72-43, Huntsville, AL: Wyle Laboratories.

Wiederhorn, S.M. (1967). "Influence of Water Vapor on Crack Propagation in Soda-Lime Glass," J. Am. Ceramic Soc., 50[8], pp. 407-414.

Wiggins, J.H. (1988). "Commentary on cumulative damage from repeated sonic booms," Redondo Beach, CA: Crisis Management Corporation.

This page intentionally left blank.

APPENDIX A CHARACTERISTICS OF WINDOW GLASS

Modern window panes commonly employ sheet glass, float glass, or plate glass. Sheet glass is manufactured by pulling a sheet upward from a pool of molten glass, attenuating to the desired thickness, and annealing it. Surface quality of sheet glass is not as good as that of float glass. When high-quality surfaces are required, the glass must be ground and polished. The float process causes molten glass to flow from a melting tank on a bath of molten tin. The glass surfaces flow and smooth themselves while the glass is on the float. The emerging sheet is then annealed. Because the glass is rigid enough to handle without damage by the time it leaves the float, surfaces are of high quality and do not require further finishing. Plate glass is formed using an older process of extruding glass through rollers and finishing it by grinding and polishing. This process is being replaced by the float process.

While annealing is performed to remove residual stress in glass, a number of applications require increasing glass resistance to impact beyond that of annealed glass. Glass is strengthened by heating it to near its softening point and then chilling it rapidly. The surfaces cool and contract while the interior remains relatively warm. As the interior cools and shrinks, the surfaces are rigid and are compressed by the interior. When this results in a surface compression between 3,000 and 10,000 psi, this is called heat strengthened glass. When the surface compression exceeds 10,000 psi, the glass is called fully tempered. The fully tempered glass meets ANSI and federal standards for safety glazing. It is approximately four times as strong as annealed glass. When it does break, the fragments are small pieces. Neither tempered not heat strengthened glass can be cut after the heat treatment.

Insulating glass consists of two or more panes sealed together with an air space between them. Commonly, a desiccant between the panes absorbs any moisture that may have been trapped between the panes at the time of installation. When the exterior pane deflects in response to an applied pressure load, most of the pressure load is transmitted to the interior pane as the small air gap is very stiff and will not significantly compress. Thus, insulating glass requires a more substantial load (approximately twice the load) to produce a given deflection than a single pane. This is supported by Figure A-1, which compares peak deflections under a 16 psf load for a double-glazed window and a single pane.

When selecting glass for structures with normal occupancy, a probable breakage rate of 8 per 1,000 is commonly used. Structural performance will consider wind loads, wind gusting, and wind-borne missiles. Wind loads are developed using fastest mile maps associated with a height of 33 feet above the ground for a specified return period (for example, fifty years). The design wind speeds are modified for the height above the terrain, the upwind ground cover (*e.g.*, urban central core, urban and suburban residential, open country, and coastal areas directly exposed to wind flow over large bodies of water), and effects of local channeling (*e.g.*, canyons and buildings). Gusting is much harder to include in a design because of the small amount of site-specific data available.

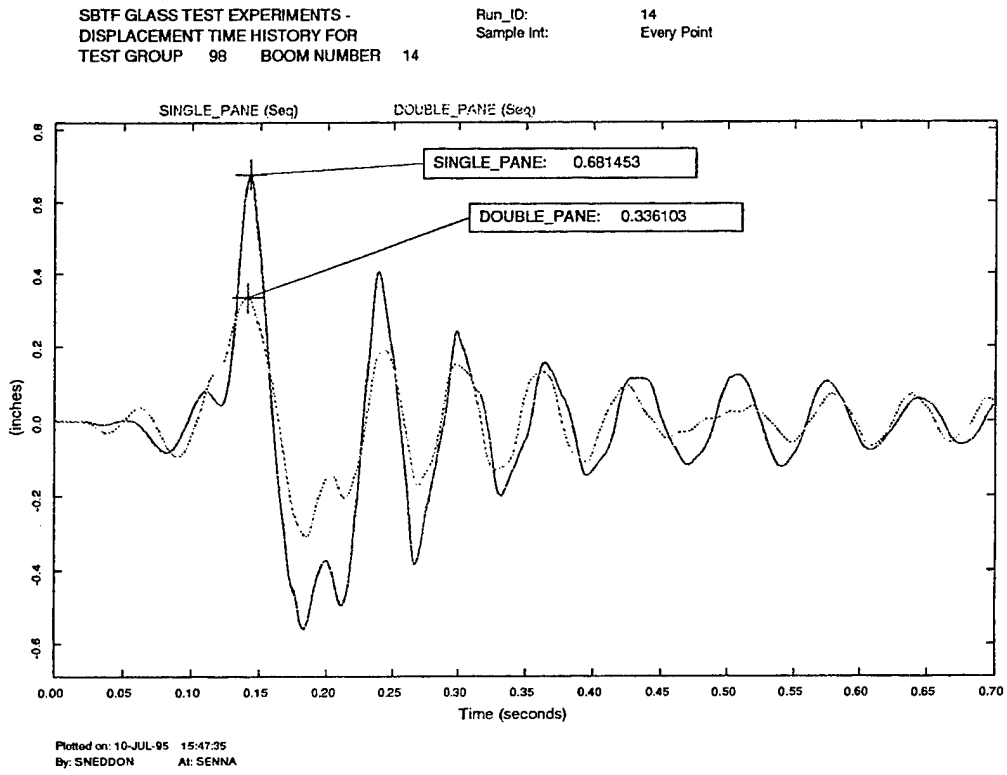

Figure A-1. Comparison of Peak Deflection of a Double Glazed Window and a Single Pane.

Design criteria for wind-borne missiles have been developed at the Institute for Disaster Research, Texas Technical University (Minor *et al.*, 1978). These criteria show that 1/2 inch thick annealed glass is required to resist wind-borne missiles for a design wind speed of 70 miles per hour (most of the country). Needless to say, most installed window glass does not conform to this standard.

Two considerations should be addressed when evaluating the wind load: (1) the required glass strength and (2) the deflection of the glass under the load. Excessive deflection can cause poor performance of glazing gaskets and produce glass-to-metal contact, which can cause breakage. Unfortunately, evaluation of glass deflection is frequently ignored.

A.1 MATERIAL PROPERTIES

The typical chemical composition of window glass is shown in Table A-1.

Table A-2 lists common physical properties of these glasses.

Table A-1. Approximate Chemical Compositions of Commercial Window Glasses, wt%.

TYPE	SiO_2	Al_2O_3	Na_2O	K_2O	MgO	CaO	OTHERS
Float	73-74	0.2-0.3	13.5-15	0.2	3.6-3.8	8.7-8.9	0.07-0.13 Fe_2O_3, 0.2-0.3 SO_3
Sheet	71-73	0.5-1.5	12-15		1.5-3.5	8-10	

Source: McLellan and Shand, 1984

Table A-2. Properties of Selected Commercial Window Glasses.

Type	Viscosity data			Thermal expansion 10^{-7}/°C 0-300°C	Density, g/cm^3	Refractive index	Log of volume resistivity		Dielectric properties at 1 MHz and 20°C	
	Softening point, °C	Annealing point, °C	Strain point, °C				250°C	350°C	Dielectric constant	Loss tangent, %
Float	722	540	510	87.0	2.50	1.518	6.5	5.2	7.0	0.40
Sheet	730	548	505	85.0	2.46	1.510	6.5	5.2	7.0	0.40

Source: McLellan and Shand, 1984

Glass possesses mechanical properties corresponding to those of crystalline solids. It has elastic properties and strength such that it returns to its original shape after deforming forces are removed. Glass does not exhibit plastic flow and consequently has no yield point. Fracture occurs before any permanent deformation; failure is always in tension. For stress calculations, glass may be considered to be homogenous and isotropic without structural discontinuities. The elastic properties of isotropic solids are:

Elastic (Young's) modulus, E
Modulus of rigidity or torsion, G
Bulk modulus, K
Poisson's ratio ν

For isotropic solids, these are related by the following equations

$$G = \frac{E}{2(1 + \nu)}$$

$$K = \frac{E}{3(1 - 2\nu)} \qquad \text{(A-1)}$$

$$\nu = \frac{E}{2G} - 1$$

Representative values for soda-lime sheet glass are E = 10.5 x 10^6 psi and ν = 0.21.

Figure A-2 depicts the temperature dependence of the elastic moduli.

A.2 FRACTURE MECHANICS OF GLASS

Simiu *et al.* (1984) present the development of the relationship between static fatigue and fracture mechanics in glass as follows:

Let K_I be the stress intensity factor and define K_{IC} as the critical value of stress intensity such that failure occurs. K_{IC} is a material property that must be determined experimentally. The stress intensity factor can be related to observable factors as follows:

$$K_I(t) = Y\sigma(t)\sqrt{c(t)} \tag{A-2}$$

where
- Y = geometric shape factor, which is dependent on crack geometry and plate dimensions
- $\sigma(t)$ = nominal stress (stress calculated by assuming the absence of cracks)
- c(t) = length of crack in direction normal to stress
- t = time

Empirically, the following relationship holds for subcritical crack growth (while $K_I < K_{IC}$)

$$\frac{dc}{dt} = A\,K_I^n(t) \tag{A-3}$$

The empirical parameters A and n are dependent on ambient humidity and temperature. Also, it should be noted that the chemical composition of the glass and the type of finishing affect these values. Heat treated glass and tempered glass have similar fatigue properties. They are both quite different from annealed float glass. Rewriting the stress intensity equation gives a relationship predicting the stress level, S_f, at which glass fails as follows:

$$S_f(t) = \frac{K_{IC}}{Y\sqrt{c(t)}} \tag{A-4}$$

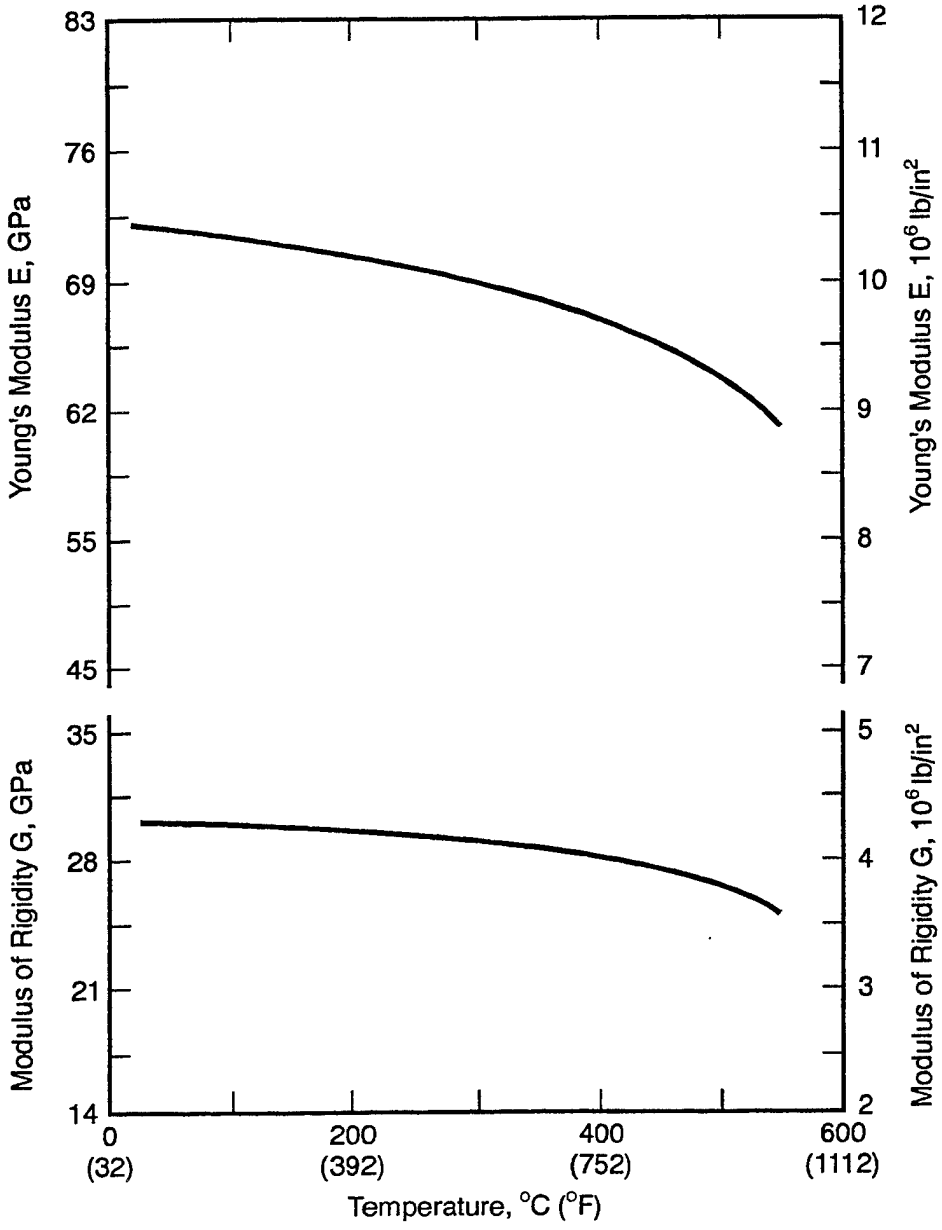

Figure A-2. Elastic Moduli *vs.* Temperature (Spinner, 1956).

From the above equations it may be derived that the strength at time t, S (t), is given by:

$$S(t) = \left[[S(0)]^{n-2} - \frac{1}{B} \int_0^t \sigma^n (T)\, dT \right]^{\frac{1}{n-2}} \tag{A-5}$$

where

$$1/B = \frac{(n-2)\, AY^2}{2} K_{IC}^{n-2} \tag{A-6}$$

Then, for an area over which the tension stress, $\sigma(t)$, is uniform and independent of direction, failure occurs if

$$\sigma(t) \geq S(t) \tag{A-7}$$

Consider the case of a load acting on a panel for a sixty-second time interval. The load introduces a normal stress at a location M parallel to the direction α, denoted by σ_{60} (M, α), which is constant for the duration of the load. Failure initiated by a flaw normal to a radius in direction α occurs at time t=60 seconds if the stress σ_{60} (M, α) is equal to the strength. The failure stress is given by:

$$\sigma_{60}^{n-2}(M,\alpha)\left[\sigma_{60}^2 (M,\alpha) + \frac{B}{60}\right] + \frac{B}{60}[S(0)]^{n-2} \tag{A-8}$$

For typical soda-lime window glasses, σ_{60}^2 is on the order of 1,000 times B/60. Thus,

$$\sigma_{60}(M,\alpha) \approx \frac{[S(0)]^{\frac{n-2}{n}}}{\left(\frac{60}{B}\right)^{1/n}} \tag{A-9}$$

This leads directly to the definitions of sixty-second static equivalent stress used in the main portion of the report

$$\sigma_{60} = \left[\frac{1}{60} \int_0^{t_f} [\sigma(t)]^n\, dt \right]^{1/n} \tag{A-10}$$

The Glass Engineering Handbook (McLellan and Shand, 1984) tabulates the strength of glass with several surface conditions when subjected to a three-second flexural test in air. Freshly drawn glass fibers had the highest strength, ranging from 30 to 400 kpsi. Annealed window glass tested at a strength between 8 and 20 kpsi. At the extreme low end of the tabulated results, sandblasted glass tested at a strength of 1.5 to 4.0 kpsi. It should be noted that when glass has been deliberately weakened by sand blasting, the

surface flaws introduced in this manner dominate the random flaws from manufacturing and handling. As a result, these specimens often have a smaller variability in their strength.

A.3 THE ROLE OF WATER IN FRACTURE MECHANICS

Silica reacts slowly with water in the absence of stress. Yet the application of stress can facilitate a chemical reaction that can cause cracks to grow at speeds greater than one millimeter per second.

The fundamental structure of silica consists of a tetrahedral unit with a central silicon atom surrounded by four oxygen atoms. Corner oxygen atoms are shared by the silicon atoms of two adjacent tetrahedrons. In silica glass, the tetrahedrons form a random network of interconnected rings. Crack growth involves the rupture of individual silicon oxygen bonds.

Water reduces the energy required as follows. Water must enter the crack and absorb to the crack tip. Spare electrons from the oxygen atom in the water molecule begin to form a bond with the unoccupied electron orbitals of a silicon atom. Meanwhile, one of the hydrogen atoms from the water molecule is attracted to an oxygen atom in the silicon-oxygen chain. As these bonds strengthen, the old ones weaken. When the hydrogen transfer to the oxygen in the chain is complete, the silicon-oxygen bond ruptures. Ultimately, the water molecule and original silicon-oxygen bond are replaced by hydroxyl groups attached to silicon (silonal groups).

As noted earlier, the silicon reaction with water is slow in the absence of stress. The effect of stress is to distort the bonds of the silicate tetrahedron making it more likely for the silicon atom to bond with the water.

Wiederhorn (1967) studied crack propagation using microscope slides. Through cracks were introduced in the short end of the slide. Stress was applied by pulling at two points on opposite sides of the crack. Specified loads were applied and a resulting crack length and velocities were measured. Crack velocities were measured at 25°C with relative humidities in a gaseous nitrogen environment ranging from 0.017% to 100%. Figure A-3 depicts the data. Notice that for each level of relative humidity, a crack velocity plateau occurs beyond some level of force. Crack velocities remain stable until a critical force is exceeded. The crack velocity then grows exponentially. Figure A-4 summarizes many experiments relating crack velocity to stress intensity. As in the previous figure, in the presence of moist nitrogen, crack velocity plateaus until a critical value of stress intensity occurs.

Liquid water enhances crack growth over the entire range of crack velocity. This suggests that wet panes, and in particular wet cracked panes, should be highly vulnerable to stress loads.

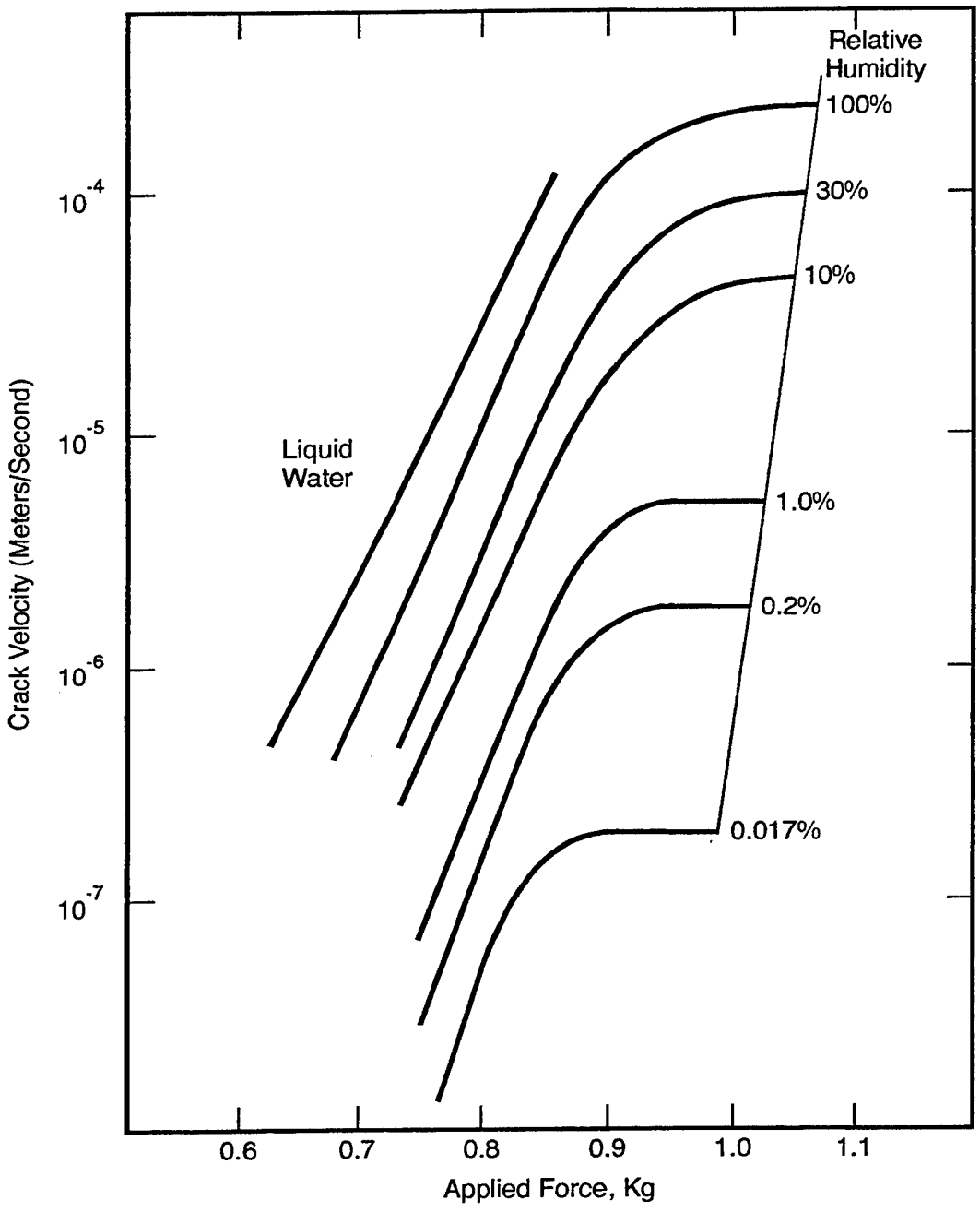

Figure A-3. Dependence of Crack Velocity on Applied Force and Relative Humidity.

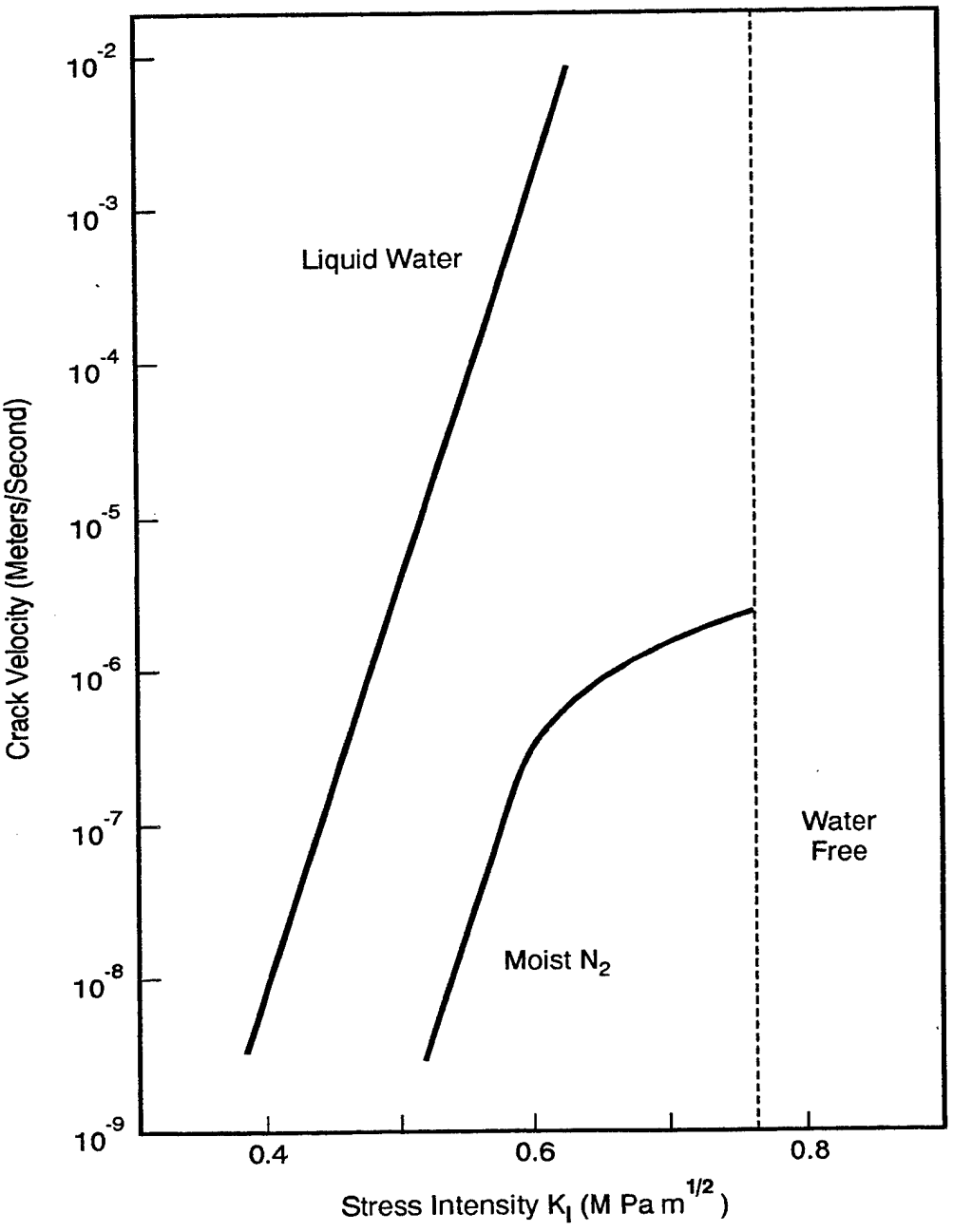

Figure A-4. Effect of Water on Crack Growth in Vitreous Silica (Michalske and Freiman, 1982).

This page intentionally left blank.

APPENDIX B MATHEMATICAL MODEL FOR DAMAGE TO GLASS PANES FROM REPETITIVE SONIC BOOMS

The present ASAN models for sonic boom damage to glass window panes (Haber and Nakaki, 1989) are based on those originally developed for the Federal Aviation Administration (Hershey and Higgins, 1973). In these models, sonic booms impinging on a pane are characterized by a peak overpressure and sonic boom duration. A lognormal probability distribution of applied load is developed based on these parameters.

All window panes are classified into one of ten categories. Five categories are based on window size; each of these has a precracked and normal glass subcategory. A simple linear model is used to develop response statistics for each of the five categories based on window size. The strength of glass in each category is modeled using a lognormal distribution. The probability of a pane breaking is calculated as the probability that the pane response exceeds the pane capacity.

Numerous refinements have been made in modeling the risk of windows breaking from impulsive airloads since development of the ASAN models. Improved submodels have been developed for characterizing the load, predicting the glass response to the loads, and characterizing glass strength. Many of these improvements have been associated with on-going Air Force-sponsored modeling (Bodner *et al.*, 1993) to characterize risk of injuries from shattered window panes resulting from blast overpressures. Although all model elements deserve a review and upgrade, this appendix focuses on issues related to the strength of window panes.

It is important that the following factors be included when the ASAN models are revised:

(1) Refinement of probability distributions. The lognormal distribution is a convenient model, but it is not always a good statistical description.

(2) Interdependence of modeled phenomena. Failure to account for dependencies can grossly distort model predictions. The highest sonic boom overpressures are often associated with caustic waveforms. Nevertheless, for many windows the window response to a caustic waveform will be less than the response to a rounded waveform with the same peak overpressure.

(3) Appropriate incorporation of the findings regarding distributions of sonic booms in Supersonic Operating Areas.

(4) Improved modeling of glass capacity. This appendix addresses a number of the important issues regarding glass strength.

B.1 WINDOW CATEGORIES AND WINDOW STRENGTH

The ASAN window size categories were based on a taxonomy employed by the Air Force for managing risks of injury from window panes shattered by blast overpressures. Since that time, the blast window categories have been replaced with the more realistic categories listed in Table B-1. ASAN models should be updated to reflect the current glass categories.

Table B-1. Revised Window Categories.

CATEGORY	PANE AREA (Sq Ft)	PANE THICKNESS (Inches)	TYPE OF GLASS
I	0 - 2	0.088	Sheet
II	2 - 6	0.088	Sheet
III	6 - 15	0.12	Sheet
IV	15 - 20	0.22	Plate
V	20 - 40	0.22	Plate
VI	40 - 60	0.30	Plate

During the 1980s, Texas Tech University, Glass Research Laboratory (TTU, GRL) performed a large number of glass strength tests characterizing the surface flaw parameters and the sixty-second static equivalent stress to failure. It has been shown that the strength of glass panes can be described probabilistically by a Weibull distribution of the following form

$$Pr\,(x) = 1 - \exp\left[-\left(\frac{X}{S}\right)^{m}\right] \qquad m \geq 1 \tag{B-1}$$

where S = scale parameter or characteristic strength
m = shape or tail length parameter, dependent on glass type

Both the sixty-second static equivalent stress to failure, σ_{60}, and the characteristic strength for two panes of glass from the same strength distribution have been shown to follow a scaling law as shown in the following equation

$$\sigma = \sigma_{ref} \left(\frac{A_{ref}}{A} \right)^{1/m} \qquad \text{(B-2)}$$

Table B-2 lists the strengths from a number of strength tests normalized to a reference area of 3.14 square inches, characteristic of the TTU, GRL ring-on-ring tests. This form of presentation of glass strength has the advantage of including the effects of the loading rate and the type of glass (*e.g.*, sheet glass or plate glass) to allow direct comparisons of the characteristic strengths. It should be noted, however, that for a pane of a specified size and type of glass, the variation in glass strength is much higher than previous sonic boom damage modeling had indicated. The standard deviation of log σ_{60} for panes from real windows is typically 0.33. Earlier studies had used values in the range of 0.2. This strength formulation should be adopted in ASAN for normal window panes.

Table B-2. Normalized Strengths of Glass Panes.

	PANE THICKNESS (Inches)	PANE DIMENSIONS (Inches)	σ_{60} NORMALIZED TO 3.14 Sq In (psi)
Lackland AFB, TX Library (A)	0.25	42 x 29 1/2	11,276
Lackland AFB, TX Library (B)	0.25	37 x 29 1/2	12,342
Lackland AFB, TX Chapel #8	0.25	58 3/4 x 28 3/4	12,800
Kelly AFB, TX	0.121	24 x 34	13,589
Vicinity of Patrick AFB, FL*	0.088 - 0.22	--	10,800
Vicinity of Vandenberg AFB, CA*	0.088 - 0.22	--	12,300

*Panes were collected by TTU, GRL in the vicinity of Patrick AFB, FL and Vandenberg AFB, CA. Panes were cut into small samples suitable for testing in a concentric 2" ring tester. Results shown are for panes at least three years old with at least ten samples.

No special treatment is required for damage to good glass from repetitive sonic booms. As demonstrated in the body of this report, cumulative damage is not significant for good glass.

B.2 STRENGTH OF PRECRACKED PANES

Although it is now generally accepted that the Weibull distribution is a suitable distribution for glass strength, ASAN currently models the strength of panes using a lognormal distribution. Precracked glass is modeled with a mean strength that is one-tenth as large as that of normal glass. The standard deviation of the logarithm of precracked glass is modeled to be the same as that of normal glass. In the ASAN model, precracked glass panes account for 0.61% of the window population, while the remaining 99.39% of the window population is good glass. At typical sonic boom overpressures, damage estimates are dominated by the precracked panes. Despite the importance of the submodel for precracked glass to predicting windows broken, the model has a flimsy foundation. Hershey and Higgins base their estimate of the strength of precracked glass on "a rule of thumb" in the glass industry. Recent conversations with representatives of glass manufacturers' research departments and academic researchers failed to locate anyone familiar with such a rule of thumb or who would agree that it represented a credible judgement. As a result, the fracture mechanics literature was reviewed for an alternative approach.

The fracture mechanics concepts introduced in Appendix A were used to develop an initial characterization of the strength of precracked glass as follows: A nonlinear finite element analysis was performed of a 0.087-inch thick, 41.125-inch by 35.0-inch pane subjected to a ramp pressure loading to 78.5 psf in 42 seconds. This load approximated one of the static tests performed with weatherstrip inserts. The edge conditions for this analysis were: (1) free lateral translation, (2) free rotation and (3) constrained vertical (out-of-plane) translation.

The model was validated by comparing the measured and calculated deflections for the same applied pressure at the center of the pane. Peak stresses initially occur in the center of the plate with these edge conditions. With increased stress, the region of peak stress rapidly moves to the pane corners. Figure B-1 depicts the principal stresses of the upper right hand corner of the pane with a load of 80 psf.

Although the actual stress histories were available from the finite element analysis, these were not used in our analysis. Instead, the simplifying assumption was made that the stresses were linearly related to the pressure. Figure B-2 shows the difference between the stresses resulting from the finite element analysis and this simplifying assumption for the corner element. All elements have dimensions of two inches on each edge. The center of the corner element is located one inch in from each pane edge. In the following material elements will be referred to by the coordinates in inches of their centers. Thus, for example, the second element from the left along the lower edge is the (3, 1) element.

The following analysis makes several simplifying assumptions. The glass pane is treated as sufficiently large so that boundary effects can be ignored. Unless otherwise indicated, stresses are based on calculated values at the center of an element. Unless otherwise noted, cracks are oriented at right angles to the principle stresses so that crack propagation is in Mode I (opening mode). Cracks oriented in other directions will tend to seek an orientation that minimizes the shear loading as they propagate. Additional

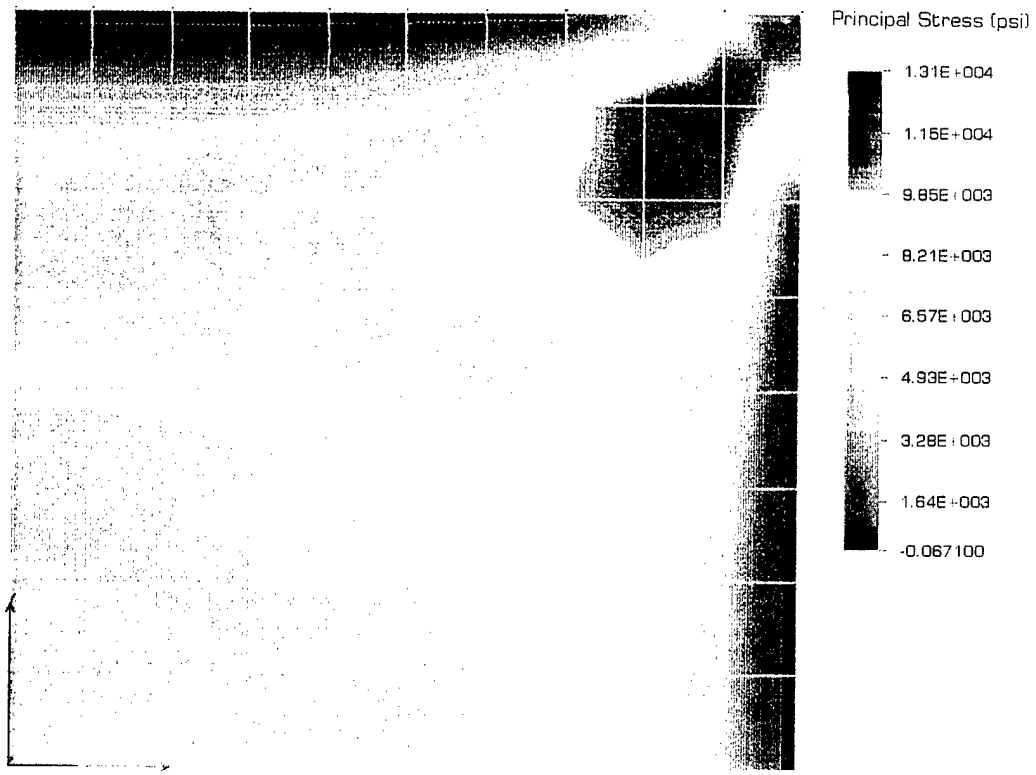

Figure B-1. Principal Stresses in the Upper Right Hand Quadrant of Pane at 80 psf.

energy is required for the initial reorientation of the crack propagation direction. Thus, the values presented below will characterize the minimum pressures required for cracks in a given location to propagate. Modeling the mixed mode crack propagation proved to be too complex to be included at the end of this project.

The following material first derives equations describing the crack propagation, and then presents numerical results for the glass pane modeled.

Combining equations (A-2) and (A-3) gives the following expression

$$\frac{dc}{dt} = AY^n \, c^{n/2} \, \sigma^n \qquad \text{(B-3)}$$

or given an initial crack length, c_o,

$$\int_{c_o}^{c} \frac{dc}{\left(\sqrt{c}\right)^n} = AY^n \int_o^t \sigma(\tau)\, d\tau \qquad \text{(B-4)}$$

or

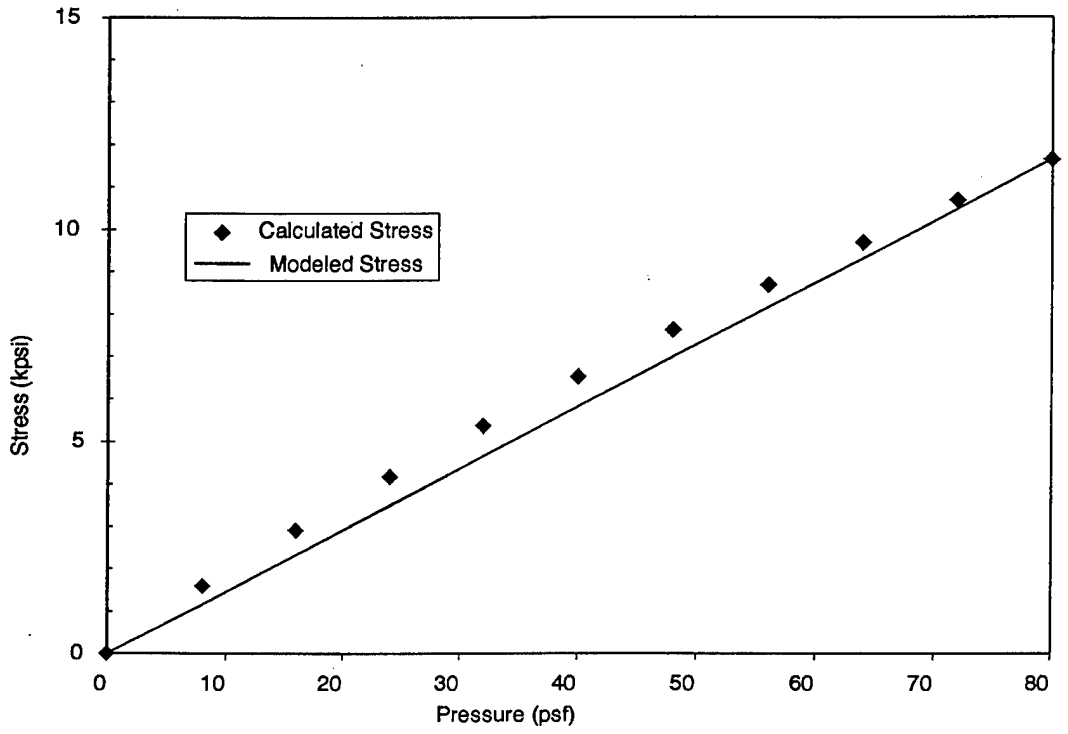

Figure B-2. Comparison of Stress Calculated with Finite Element Analysis and Simplified Model for Corner Element.

$$\left(\frac{1}{\sqrt{c}}\right)^{n-2} = \left(\frac{1}{\sqrt{c_o}}\right)^{n-2} - \left(\frac{n-2}{2}\right) AY^n \int_o^t \sigma^n(\tau)\, d\tau \qquad \text{(B-5)}$$

If the stress is a linear function of time, then stress is given by

$$\sigma(t) = \left(\frac{\sigma_{max}}{t_{max}}\right) t \qquad \text{(B-6)}$$

Equation B-5 then becomes

$$\left(\frac{1}{\sqrt{c}}\right)^{n-2} = \left(\frac{1}{\sqrt{c_o}}\right)^{n-2} - \left(\frac{n-2}{2}\right) \frac{AY^n}{(n+1)} \left(\frac{\sigma_{max}}{t_{max}}\right)^n t^{n+1} \qquad \text{(B-7)}$$

Failure occurs when the crack length, c, grows arbitrarily large, at which time the left hand side of the equation approaches zero. Equating the two terms on the right hand side of the equation gives a time to failure, t_{fail}, as

$$t_{fail} = \left[\frac{2\,(n+1)}{(n-2)} \left(\frac{1}{\sqrt{c_0}} \right)^{n-2} \frac{1}{AY^n} \left(\frac{t_{\max}}{\sigma_{\max}} \right)^n \right]^{\frac{1}{n+1}} \qquad \text{(B-8)}$$

If pressure is a linear function of time

$$p\,(t) = rt \qquad \text{(B-9)}$$

Then, the pressure at failure P_{fail}, will be given by

$$P_{fail} = r\, t_{fail} \qquad \text{(B-10)}$$

The length of glass surface flaws responsible for strength degradation are in the range of 10-100 μM (Wiederhorn and Fuller, 1985). On this basis, the above equations are used to estimate the pressure required to cause a failure in a pane with a 0.001 inch flaw. Using a geometry factor of 1.1 gives an estimated failure pressure of 76.8 psf. This was considered sufficiently close to the observed failure pressure of 78.5 psf to use this simplified model to explore the vulnerability of precracked glass.

Figures B-3, B-4, and B-5 present failure pressure as a function of crack length for three edge elements. Each is based on cracks oriented orthogonally to the principal stresses. In each instance, failure pressures are plotted for loading rates of 1 psf per second, 100 psf per second, and 10,000 psf per second. These figures may be used to determine the conditions required for the strength of a precracked pane to be as low as one-tenth of an uncracked pane. In all cases, a crack will be considered with the orientation that produces the most vulnerable pane. If the tip of the crack is near the center of the (1,1) element the initial crack length must be approximately one-quarter inch to reduce the pane strength by a factor of ten. A favorably oriented crack with its tip near the center of the (3,1) element would have to be approximately one-half inch long to produce the same effect. Finally, a favorably oriented crack with its tip at the center of the (5,1) element would have to be almost two inches long to produce the same effect. The stresses depicted in Figure B-1 show that the crack propagation characterization for element (5,1) is more representative of a large proportion of the plate area (about 80%), while that calculated for elements (1,1) and (3,1) represent portions of the plate (about 20%) about the diagonal near the corner.

These calculations have shown that the Hershey and Higgins "rule of thumb" for precracked glass strength may be a gross distortion of the reduction in strength associated with precracked glass for the following reasons:

- Susceptibility to crack propagation depends on the local stress. As indicated by Figure B-1, this varies significantly with crack location.

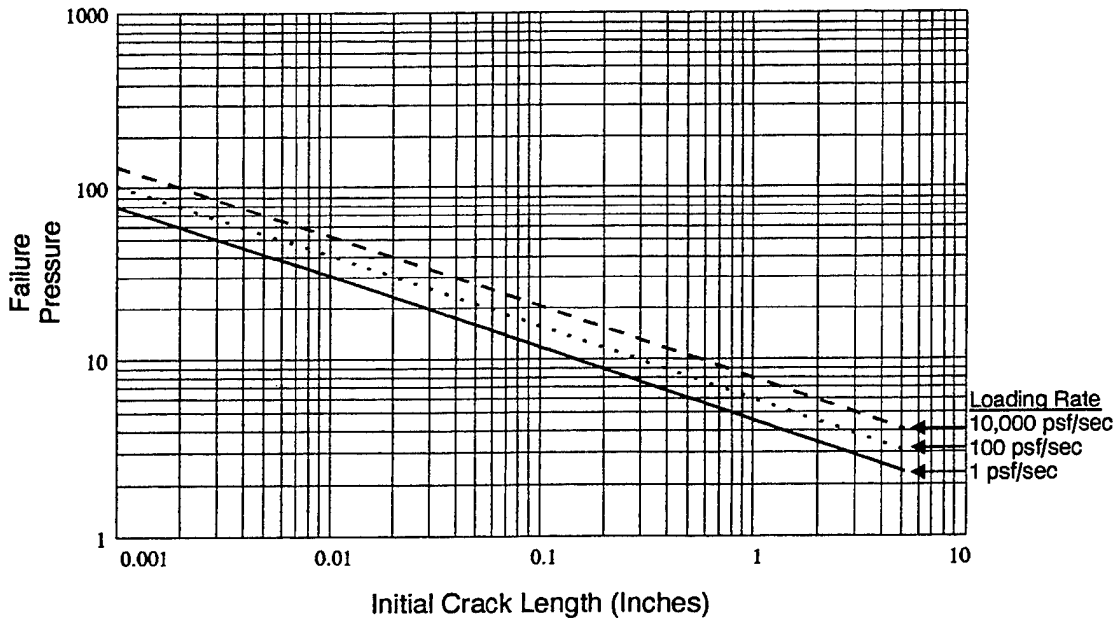

Figure B-3. Minimum Failure Pressure as a Function of Initial Crack Length: Corner - (1,1) Element.

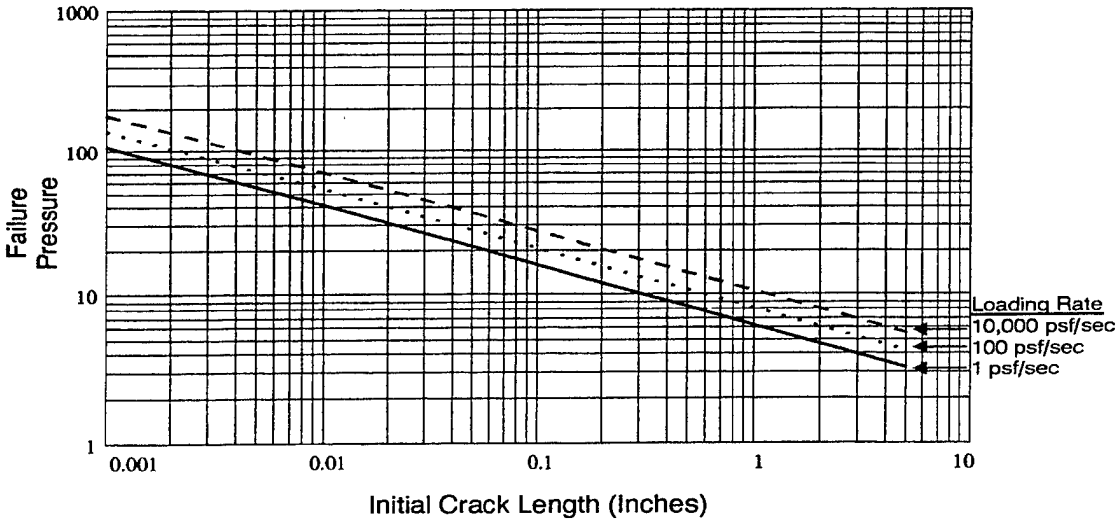

Figure B-4. Minimum Failure Pressure as a Function of Crack Length: (3,1) Element.

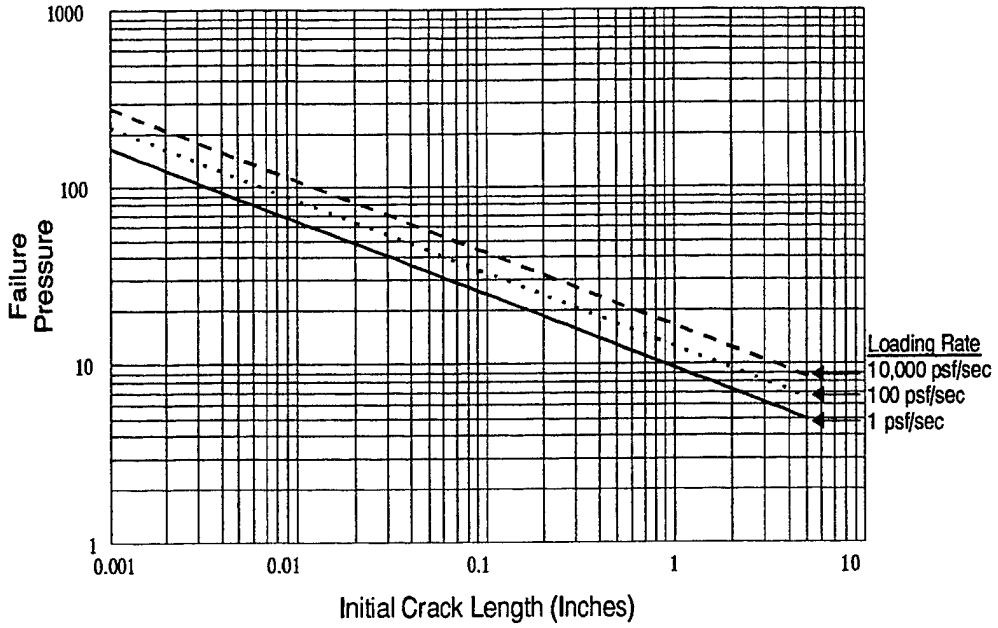

Figure B-5. Minimum Failure Pressure as a Function of Crack Length (5,1) Element.

- Susceptibility to crack propagation depends on crack length as indicated in Figures B-3 to B-5.

- Susceptibility to crack propagation depends on the orientation of the cracks with respect to the principal stresses. All calculations reported here are for the most susceptible orientation.

A more complete evaluation of the vulnerability of precracked glass requires the following:

(1) Development of probability distributions for the size, orientation, and location of cracks in precracked glass.

(2) Evaluating and appropriately addressing the effects of plate boundaries (finite plates) on crack propagation.

(3) Extending the formulation to address arbitrary crack orientations by including a mixed mode crack model.

Figure B-6 presents a conceptual flow diagram for evaluating the effect of glass cracks on the probability of glass failure for single sonic boom exposure.

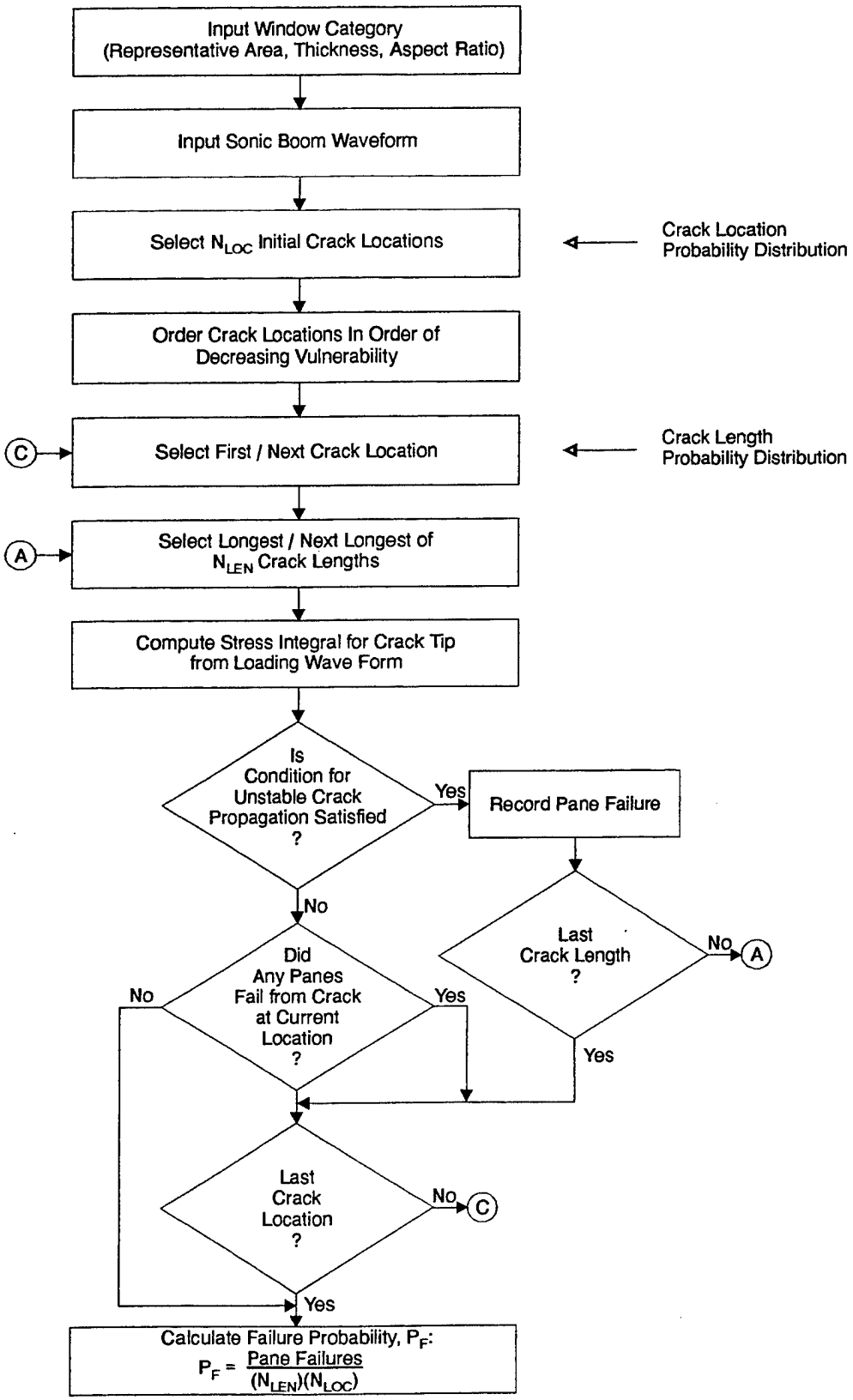

Figure B-6. Probability of Cracked Pane Failure from Single Boom Exposure.

B.3 DAMAGE TO PRECRACKED GLASS FROM REPETITIVE SONIC BOOMS

The effect of repetitive sonic booms can be evaluated using equation (B-7). The following additional assumptions were made for this investigation:

(1) All sonic booms considered have a rise time of 6 ms.

(2) The dynamic amplification factor has a value of two (this allowed the use of the results of the finite element analysis referenced earlier.)

(3) The applied stress occurs during the 6 ms rise time. Subsequent stress cycles for the sonic boom were ignored.

(4) The crack tips advance sufficiently small distances before the crack reaches the critical length so that it is subjected to the same peak stresses from every boom.

The top graph in Figure B-7 shows the number of booms to failure as a function of peak pressure calculated using this approach for three different initial crack locations. The first selected location is the center of the corner (1, 1) element. The initial crack runs from the center of the element to the corner of the pane, a length of $\sqrt{2}$ inches. In the (3, 1) element, the principal stress is oriented at an angle of 38°. The initial crack in this element runs from the edge of the pane to the coordinates (3, 0.87), matching the length of the first crack. In the (5, 1) element, the principal stress is at a 14° angle. The initial crack in this element is of length $\sqrt{2}$ inches with its tip located at (5,0.34).

The bottom graph in Figure B-7 depicts the number of booms to failure *versus* pressure for cracks in the corner element. Three different crack lengths are shown. Figure B-7 shows that cumulative damage is a potential concern for precracked glass. The initial analysis suggests that in order to contribute to cumulative damage, sonic boom peak overpressure must be a substantial fraction of the pressure required to break a pane from a single boom.

One might expect that ambient environmental conditions would contribute to the cumulative damage and thereby significantly reduce the number of sonic booms required to break a cracked window. In an effort to explore this hypothesis, wind statistics for White Sands Missile Range (Turner and Hill, 1982) were reviewed. Pressure loading, P (psf), on a pane, is related to wind speed, V (knots), by the equation

$$P = 2.95 \times 10^{-3} V^2 \qquad \text{(B-11)}$$

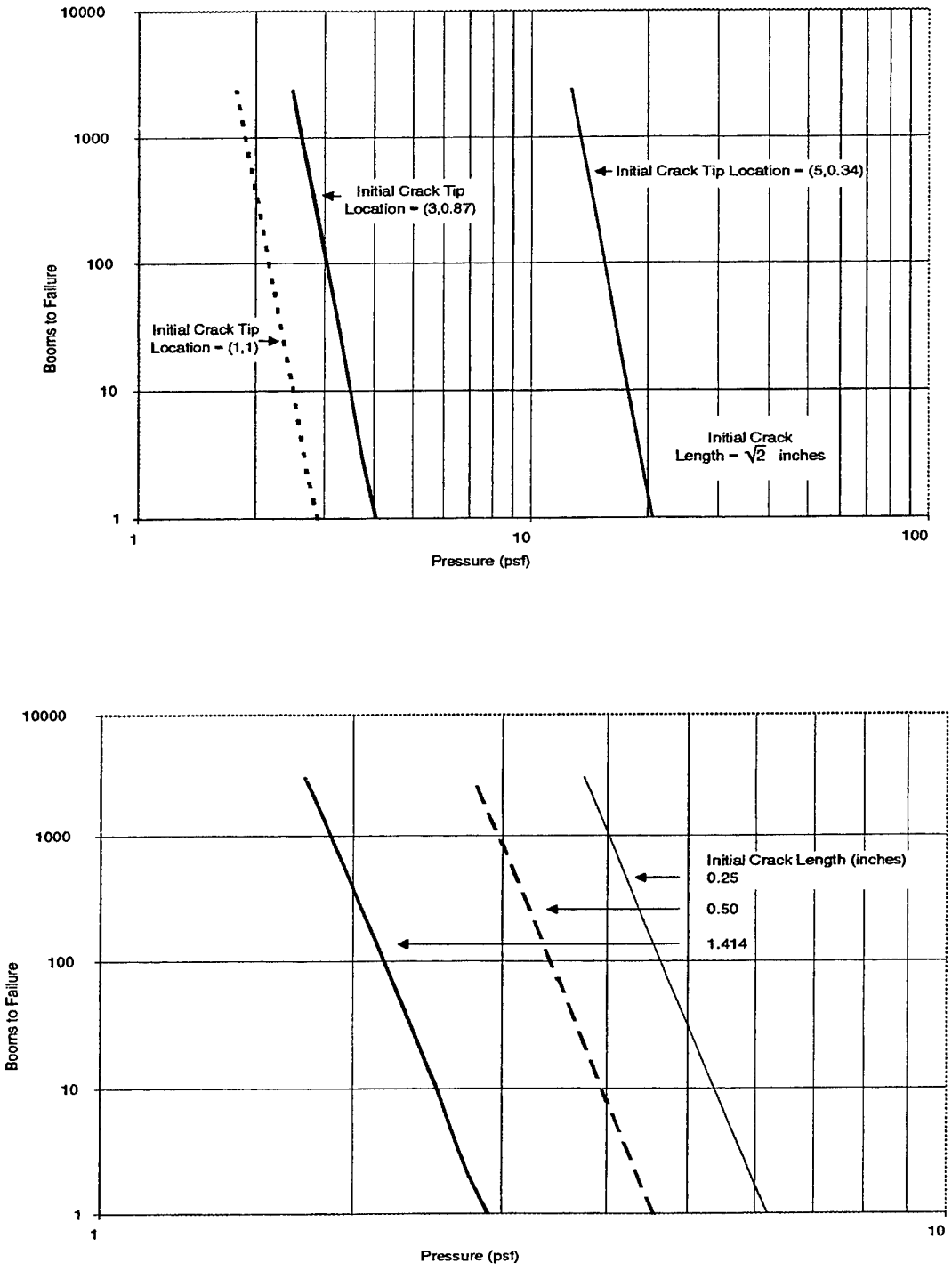

Figure B-7. Booms to Failure *vs.* Pressure for Three Crack Locations (*top graph*) and Three Crack Lengths (*bottom graph*).

Turner and Hill characterize the peak (instantaneous) wind speed, W, at White Sands by a Frechet distribution as follows:

$$F(w \leq W) = \exp\left[-\left(\frac{W}{36.2813}\right)\right]^{(-6.9591)} \qquad \text{(B-12)}$$

Combining equations (B-11) and (B-12) we calculate the annual probability of nonexceedance of wind pressures as shown in Table B-3. These statistics strongly suggest that the wind loading is important only for the most vulnerable precracked panes.

Table B-3. Probability of Nonexceedance of Wind Pressures at WSMR.

PROBABILITY OF NONEXCEEDANCE	PRESSURE (PSF)
0.001	2.08
0.01	2.37
0.1	2.97
0.2	3.33
0.3	3.66
0.4	3.99
0.5	4.37
0.6	4.82
0.7	5.42
0.8	6.30
0.9	8.03
0.95	10.13
0.99	17.14
0.999	36.10

Figure B-8 outlines a procedure for calculating cumulative damage to precracked panes.

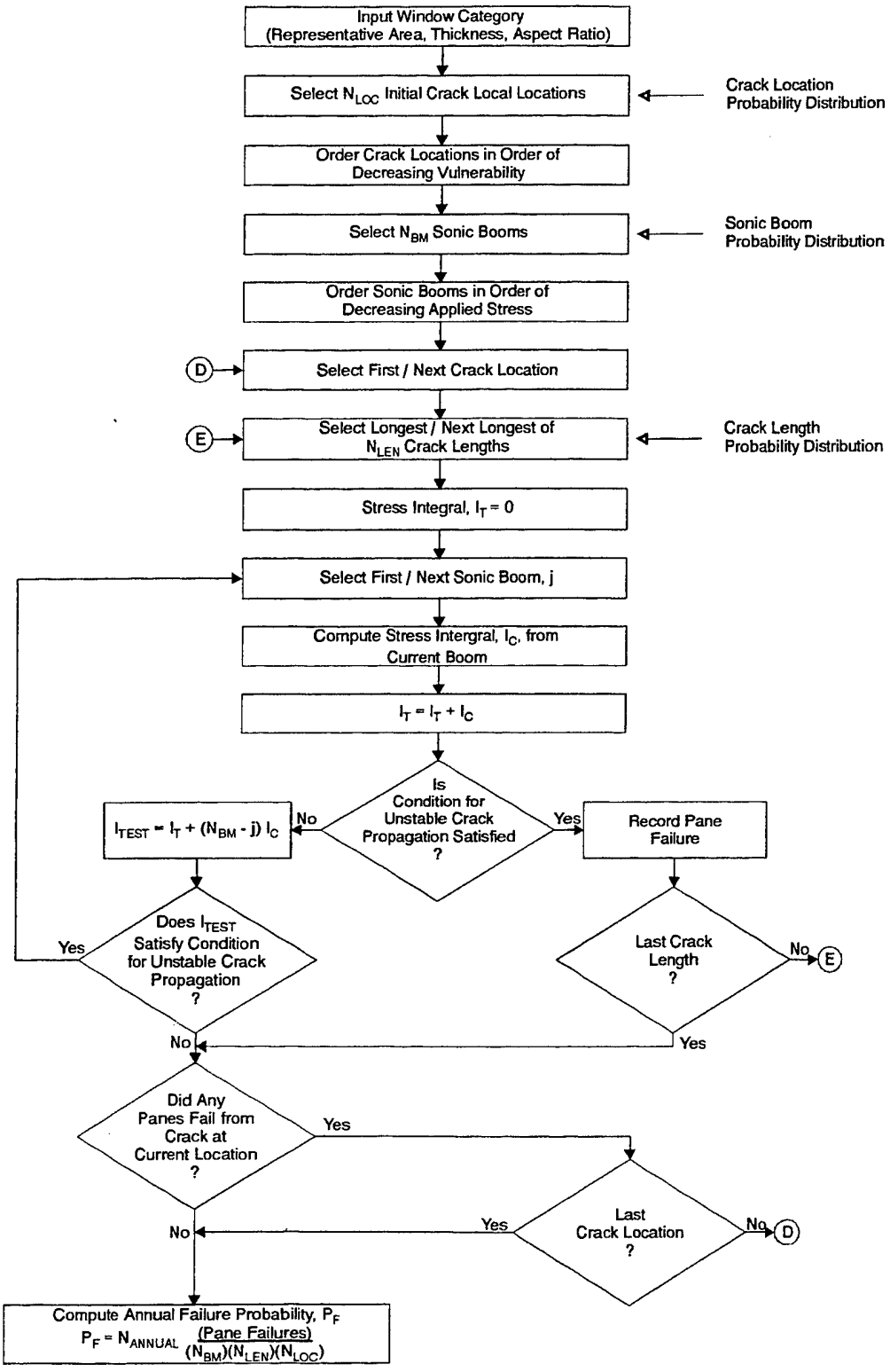

Figure B-8. Cumulative Damage to Cracked Panes.